pharmaceutics

MDPI

Review

Molecularly Aged Protein States as Targets for Drug Design and Delivery in Neurodegenerative Diseases

Reem Alromaihi [1,*], Suleman Abdullah Almerdasi [1], Abdulrahman Abdullah Almusallam [1], Mona Alromaihi [2], Waad A. Aljohani [3], Masood Alam Khan [3], Arif Khan [3] and Khaled S. Allemailem [1,*]

[1] Department of Medical Laboratories, College of Applied Medical Sciences, Qassim University, Buraydah 51452, Saudi Arabia; s.almerdasi@qu.edu.sa (S.A.A.); mslmaa@qu.edu.sa (A.A.A.)
[2] Department of Pediatrics, College of Medicine, Qassim University, Buraydah 51452, Saudi Arabia; mona.alromaihi@qu.edu.sa
[3] Department of Basic Health Sciences, College of Applied Medical Sciences, Qassim University, Buraydah 51452, Saudi Arabia; wa.aljohani@qu.edu.sa (W.A.A.); a_khan@qu.edu.sa (M.A.K.); 4140@qu.edu.sa (A.K.)
* Correspondence: r.alromaihi@qu.edu.sa (R.A.); k.allemailem@qu.edu.sa (K.S.A.)

Abstract

Neurodegenerative drug discovery usually represents a protein target by its gene, canonical sequence, and one or a few structures. That representation can miss the molecular history accumulated by proteins that persist in the brain. Spontaneous chemistry, incomplete repair, altered turnover, proteolysis, phase transitions, and assembly remodeling generate states that may differ from the canonical target in exposure, function, and therapeutic accessibility. We call compositionally resolved species age-generated proteoforms and use molecularly aged protein states when the exact composition remains uncertain. This Review develops a target-state framework for Alzheimer disease, Parkinson disease, amyotrophic lateral sclerosis and frontotemporal dementia, Huntington disease, and multiple sclerosis. It separates detection from age association, causality, brain exposure, proximal target engagement, and clinical evidence. Disease-specific analyses connect tau and amyloid-beta proteoforms, alpha-synuclein and lysosomal or mitochondrial assemblies, TDP-43 loss-of-function states, and persistent myelin or extracellular-matrix states to rational modalities and critical validation experiments. Repair, selective removal, stabilization, state-selective antibodies and small molecules, intrabodies, replacement, and synthesis control are evaluated together with blood–brain barrier transport, cellular and organelle access, pharmacokinetics, and pharmacodynamics. Each class of target state is mapped to the delivery constraint it imposes and the platform for which a precedent exists, and the exposure requirements that state selectivity implies are set out explicitly, including the fraction of a pool that must be engaged, the duration required to move a slowly accumulating state, and the consequences for dosing interval and pharmacodynamic biomarker choice. The aggregate-directed amyloid antibodies are analysed as the existing clinical test of the framework and of its limits. Machine learning remains central to proteoform identification, multimodal prioritization, structure modeling, and molecular design, provided that labels and prospective tests preserve target-state identity. Classical quantum chemistry can address bounded reaction and recognition problems. Quantum computing is treated as an exploratory implementation that requires matched classical baselines and explicit resources. The central requirement is not that an old protein be abnormal, but that a defined disease-relevant state can be selectively engaged while preserving the functional pool.

Check for updates

Academic Editors: Rita Catarino and Francisco A. M. Silva

Received: 2 October 2026
Revised: 13 November 2026
Accepted: 14 November 2026
Published: 18 November 2026

Copyright: © 2026 by the authors. Licensee MDPI, Basel, Switzerland. This article is an open access article distributed under the terms and conditions of the Creative Commons Attribution (CC BY) license.

Keywords: neurodegenerative disease; brain aging; long-lived proteins; proteoforms; drug targeting; blood–brain barrier; target engagement; pharmacokinetics; exposure–response; Huntington disease; machine learning; deep learning; quantum chemistry

1. Introduction

Protein targets are commonly represented as stable biological identities. A gene is linked to a canonical sequence, the sequence is linked to a structure or structural ensemble, and perturbation of that target is evaluated through a biochemical or cellular phenotype. This abstraction has supported much of modern pharmacology, but it omits the chemical history of the protein molecule. The omission is especially consequential in the brain, where many cells are postmitotic, macromolecular assemblies can be maintained for prolonged periods, and local protein renewal varies across regions and subcellular compartments. Savas et al. identified exceptionally persistent nucleoporins and chromatin-associated proteins in the adult rat brain [1]. Toyama et al. later showed that long-term persistence extends to other stable cellular structures and that even nuclear pore subcomplexes undergo slow, incomplete renewal [2]. These observations introduced a target variable that gene-centric models do not encode molecular residence time. Persistence is not confined to one nuclear complex. Fornasiero et al. combined quantitative in vivo labeling with mathematical modeling to measure lifetimes for approximately 3500 proteins in the mouse brain, with pronounced differences among tissues, organelles, synaptic fractions, and individual proteins [3]. Krishna et al. identified long-lived components within mitochondrial respiratory assemblies, where the electron transport chain shows increased stability relative to the surrounding organelle [4]. Bulovaite et al. found that the lifetime of postsynaptic density protein 95 ranged from hours to several months across individual mouse brain synapses [5]. These studies do not support a simple division between short-lived and long-lived proteins. They instead indicate a structured landscape in which lifetime depends on molecular complex, subcellular location, cell type, and physiological context.

Age changes this landscape. Kluever et al. used pulse labeling in young and aged mouse brain to report an average increase of approximately 20% in protein lifetime in aged animals, accompanied by protein-specific and region-specific changes [6]. Rao et al. used continuous labeling across the mouse aging continuum to identify dynamic turnover trajectories, sex-related differences, altered insoluble-proteome behavior, and associations between proteasome activity and the turnover of proteolytic subunits [7]. Li et al. quantified turnover across mouse tissues and brain regions while resolving tens of thousands of phosphosites, which separates protein abundance from protein lifetime and modification state [8]. Guldner et al. used neuron-restricted bioorthogonal labeling to show that average neuronal protein half-life approximately doubled between 4-month-old and 24-month-old mice, and identified 1726 proteins in an aged neuronal aggregome and found that many slow-degrading or aggregating neuronal proteins were detectable in microglia [9]. In the short-lived killifish Nothobranchius furzeri, Kelmer Sacramento et al. attributed more than 40% of age-regulated proteins to post-transcriptional mechanisms, and experimental proteasome suppression reproduced features of age-associated loss of protein-complex stoichiometry [10]. Ding et al. extended the same question across the human lifespan, with proteome profiles spanning 50 years describing organ-resolved aging trajectories [11]. The biological interpretation of these changes remains protein-specific. Longer persistence can preserve an expensive or structurally constrained assembly, reflect adaptive resource allocation, or permit the accumulation of altered molecular states. Conversely, shortened

lifetime can indicate damage recognition, complex instability, or accelerated removal, so lifetime alone does not define dysfunction.

Molecular age emerges from the interaction of residence time with chemical exposure, repair, processing, and clearance. Asparagine deamidation, isoaspartate formation, amino-acid racemization, oxidation, carbonylation, electrophile adduction, glycation, truncation, and crosslinking can change local charge, backbone geometry, stereochemistry, interaction surfaces, or conformational preference [12]. Some changes are spontaneous and irreversible under physiological conditions, whereas others are enzymatically controlled or chemically reversible [13,14]. The distinction matters therapeutically. Qin et al. found that partial loss of protein L-isoaspartyl methyltransferase (PIMT, the product of the PCMT1 gene) activity accelerated isoaspartate accumulation in aging mouse brain and was accompanied by reduced creatine kinase B activity, which connects damage formation, repair capacity, and protein function in one experimental system [15]. Such evidence is stronger than an age-group comparison, but it still does not imply that every isoaspartate-containing protein is a disease target. Smith et al. introduced the term proteoform for the distinct molecular forms produced from a gene through sequence variation, RNA processing, and post-translational change [16]. Estimating how many such forms the human proteome contains remains an open problem in its own right [17]. Proteoform-resolved mass spectrometry can expose molecular identities that are collapsed in gene-level or peptide-level summaries [18], and human brain studies have begun to resolve proteoform families of disease-associated proteins, including intact and truncated tau species [19]. Yet most target-discovery pipelines still use canonical sequences, bulk abundance, or a single reference structure as their starting point. This mismatch can propagate through assay design, structural modeling, virtual screening, biomarker selection, and therapeutic interpretation. A compound tested against a recombinant canonical protein may not recognize an aged proteoform. A reduction in total protein abundance may leave the damaging state unchanged. A degradation strategy may remove both a harmful proteoform and an essential functional pool. Community efforts have proposed building a reference set of human proteoforms, reflecting the need to move beyond gene-level descriptions of the proteome [20]. Artificial intelligence is expanding the scale at which spectra, protein interactions, spatial measurements, perturbation data, and molecular structures can be analyzed [21]. Its value in target discovery nevertheless depends on the identity and quality of the labels supplied to the model [22]. If an age-generated state is absent from the training data, a more expressive model does not correct the target definition. Quantum computation faces a related constraint, in that electronic-structure algorithms may eventually assist selected reaction and binding problems [23], but the calculation must first specify the chemical species, molecular environment, observable, and classical comparator.

This Review places neurodegenerative disease at the centre of the molecular-age framework while keeping normal aging, disease susceptibility, and disease-specific pathology distinct. It first fixes the terms on which the rest depends: protein lifetime as a measured turnover quantity, molecular age as the accumulated chemical and structural history of a protein population, proteoform identity as the target resolution, that is, the molecular level at which a target is specified, and the sequence of evidence required before an age-associated state may be called a therapeutic target. It then turns to the target classes that make the problem hard, where the molecule of interest sits inside an assembly or compartment whose renewal it does not control nuclear scaffolds and transport machinery, respiratory assemblies, myelin and extracellular scaffolds, and synaptic assemblies. Alzheimer disease, Parkinson disease, amyotrophic lateral sclerosis and frontotemporal dementia, Huntington disease, and multiple sclerosis are then compared at the level of the molecular state, the functional pool that must be spared, the modality, and the delivery barrier, with each disease

chosen because it tests a different class of target state. The therapeutic sections integrate state-selective recognition, repair, degradation, replacement, blood–brain barrier transport, cellular and organelle access, pharmacokinetics, and proximal brain target engagement, and they treat the exposure required to move a slowly accumulating state as a quantitative question with consequences for dosing interval and biomarker choice. Machine learning and deep learning are treated as enabling methods across the discovery chain, their value limited by the identity of the labels they are given. Classical quantum chemistry addresses selected chemical mechanisms, while quantum computing remains a bounded option whose value must be established against strong classical baselines.

Scope and Literature Selection

This Review is a narrative synthesis. Literature was identified in PubMed, Scopus, and Web of Science, with searches run to September 2026 and no lower date limit. The cited evidence spans 1983 to 2026. Search terms combined protein lifetime, protein turnover, long-lived protein, proteoform, deamidation, isoaspartate, racemization, oxidation, glycation, crosslinking, and molecular aging with brain, neuron, myelin, Alzheimer disease, Parkinson disease, amyotrophic lateral sclerosis, frontotemporal dementia, multiple sclerosis, Huntington disease, blood–brain barrier, drug delivery, machine learning, and quantum chemistry. Reference lists and forward citations of the retrieved primary studies were screened in addition to the database output. A record was included when it reported a quantitative kinetic or occupancy measurement, a mechanistic perturbation, a defined computational benchmark, or a clinical endpoint attached to a molecular state rather than to a gene-level label. Reviews were used for context and are not the evidence behind any claim to which this Review assigns an evidence level. Records were restricted to peer-reviewed, English-language publications; conference abstracts were excluded, and every 2026 citation used here is a journal article with an assigned volume and digital object identifier, and none is a preprint. Screening was performed independently by three authors, and disagreements were resolved by discussion.

2. Defining a Molecularly Aged Therapeutic Target

2.1. Protein Abundance and Protein Lifetime Describe Different Properties

Protein abundance is a population measurement, while protein lifetime is a dynamic property estimated from synthesis, incorporation, dilution, degradation, and the assumptions of the turnover model [3]. Two samples can contain similar amounts of a protein while differing substantially in the ages of the constituent molecules, and the inverse also holds: a low-abundance population may contain a persistent fraction embedded within a stable complex while the remaining molecules turn over rapidly [2]. Measurements that report one average lifetime can obscure this heterogeneity, which is why the turnover atlas of Li et al. reports lifetime and modification state as separate axes rather than as one summary value [8]. The distinction sets therapeutic direction. Reduced transcription may lower the future supply of a protein but will have little immediate effect on a population that turns over slowly. A short-duration expression assay may fail to detect inhibition of synthesis when the endogenous protein persists beyond the exposure window. Conversely, increasing transcription does not guarantee restoration of an old macromolecular assembly if newly synthesized subunits cannot exchange into it. The nuclear pore work illustrates the problem. Savas et al. found persistent scaffold nucleoporins retained in adult brain [1], but Toyama et al. later showed that stable pore subcomplexes undergo slow exchange rather than absolute permanence [2], and subsequent maintenance studies described how pore composition is renewed and surveyed in postmitotic cells [24]. A useful target model must therefore specify the molecular pool and renewal process rather than assigning one

lifetime to the gene product. Turnover measurements also depend on biological scale, since whole-tissue estimates combine neurons, astrocytes, oligodendrocytes, microglia, vascular cells, and extracellular material, each with its own synthesis and clearance kinetics. Synaptic localization can shift lifetime relative to the corresponding whole-tissue protein [3], and individual synapse types can maintain different residence times for the same scaffold protein [5]. Aging further changes cell composition, metabolic precursor pools, proteasome activity [25], autophagy [26], and intercellular material transfer [9]. Comparisons across age groups therefore require matched labeling designs, explicit kinetic assumptions, region and cell-type resolution, and uncertainty estimates. A reported lifetime is not an intrinsic constant detached from the experiment that produced it. For this Review, protein lifetime denotes a turnover quantity measured under specified experimental and modeling conditions, and residence time is used synonymously with it throughout. The term resolution is used in three distinct senses, each named by its modifier and not interchangeable: target resolution for the molecular level at which a target is specified, running from gene to protein to peptide to modification site to intact proteoform; spatial resolution for anatomical scale, meaning brain region, cell type or subcellular compartment; and optical or imaging resolution for a microscopy or imaging measurement. A fourth quantity that is commonly called resolution in mass spectrometry, the confidence with which a modification is assigned to one particular residue, is called site-localization confidence throughout and is never called resolution. Within the target axis the sense is named either as target resolution or by the molecular level itself, as in gene-level, total-protein, site, proteoform or, generically, molecular resolution; within the spatial axis, either as spatial resolution or by the anatomical scale, as in regional, tissue, cellular or subcellular resolution. The word is not used in any other sense anywhere in this Review. Persistent protein population denotes a molecular pool retained substantially longer than the typical turnover of its biological context. Exceptionally long-lived protein is reserved for proteins supported by direct pulse-chase or comparable evidence of exceptional persistence, as established for nuclear pore scaffolds and other stable cellular structures [1,2].

2.2. Molecular Age Is a Chemical and Structural History

Residence time creates opportunity for change but does not specify what changed. We use molecular age to describe the accumulated chemical, conformational, interaction, localization, and processing history of a protein population, which makes it multidimensional. It cannot be inferred from chronological age alone, and it should not be reduced to a generic damage score, an interpretive problem that has been raised directly in discussions of how complex brain aging actually is [27]. Chemical reactions occur at rates determined by sequence context, conformation, solvent exposure, local metabolites, pH, temperature, metal ions, redox environment, and binding partners. Deamidation can proceed through a succinimide intermediate and produce a mixture of aspartyl stereoisomers [13]. Oxidation can function as regulated signaling at some residues but become irreversible damage at others [28]. Carbonyl species and reactive metabolites can form adducts whose consequences depend on site occupancy and protein context [29]. Proteolysis can remove regulatory or aggregation-limiting regions [30]. Crosslinking can stabilize extracellular structures or restrict their renewal [31]. Treating these outcomes as interchangeable post-translational modifications obscures both mechanism and therapeutic direction [12]. The same caution applies to enzymatic modifications such as O-GlcNAcylation, whose nutrient dependence links metabolic state to proteostasis without implying a single directional effect [32,33]. A causal claim requires more than detecting a modified peptide in old tissue. The apparent age dependence could reflect altered cell composition, postmortem interval, sample oxidation, differential extraction, a change in total protein abundance, or selective survival of

a stable fraction. Site localization can also be ambiguous when several residues yield the same or near-identical mass shift [28]. Orthogonal standards, controlled sample handling, modification-aware false-discovery procedures, and assays that compare modified and unmodified states are needed before assigning function. Isoaspartyl repair provides the mechanistic example. Isoaspartate formation alters the peptide backbone, and Mishra et al. showed that protein L-isoaspartyl methyltransferase initiates a repair cycle rather than simply masking the modified site [34]. In heterozygous Pcmt1 mice, reduced repair capacity was associated with faster accumulation of isoaspartate in the brain during aging and lower activity of an endogenous protein substrate [15]. The same repair activity limits fibril formation from isoaspartate-containing substrates in vitro [35], and isoaspartate has been examined directly as a candidate contributor to neurodegeneration [36] and to Alzheimer disease etiology [37]. This experiment links repair capacity to molecular damage and function, but it does not identify which individual isoaspartyl proteoforms should be therapeutically increased, repaired, or removed. The target remains a state-specific hypothesis until site-resolved perturbation and target-engagement evidence are available.

2.3. Proteoform Identity Sets the Target Resolution

A proteoform is a defined molecular form of a protein arising from a particular combination of sequence and post-translational features [16,17]. Naming a proteoform fixes which molecular entity a therapeutic claim refers to, and therefore fixes what an assay must be able to distinguish. A gene, protein family, peptide, modification site, conformational state, and intact proteoform are related entities, but they are not interchangeable, a point Deol et al. developed for ubiquitin, where the number of chemically distinct forms far exceeds what a gene-level label conveys [38]. The appropriate target resolution, meaning the molecular level at which the target is specified, depends on the biological question. Bottom-up proteomics can localize and quantify many modified peptides at scale, but peptide-level evidence does not always reconstruct the intact combinations present on one protein molecule. Top-down analysis retains the connection among modifications on an intact proteoform [39] while facing limits in coverage, dynamic range, tissue complexity, and identification confidence [18,40]. Immunoassays can quantify predefined epitopes with high throughput but may not distinguish neighboring or combinatorial states, and antibody performance for individual proteoforms varies enough that validated reagent panels have had to be assembled explicitly [41]. Structural methods can resolve selected conformations or assemblies but often favor abundant and stable species [42]. No single measurement provides a complete molecular-age map. Human tau illustrates the gap between gene-level familiarity and proteoform-level knowledge. Tau has been studied for decades, yet intact-protein mass spectrometry by Xu et al. was still required to begin resolving soluble tau proteoforms and truncation products directly from human temporal cortex [19]. Kumar et al. have since shown that molecular features of pathological tau differ among the dementias in which it accumulates [43,44]. Those studies demonstrate analytical feasibility in limited sample contexts. They do not establish population prevalence, causal toxicity, or druggability of every detected form. Detection expands the candidate target space, while causal and pharmacological experiments determine which candidates deserve intervention. We use age-generated proteoform only when a molecular form is sufficiently resolved and its relationship to molecular residence time or organismal aging is supported. When composition is unresolved, we use molecularly aged protein state. This broader term can include a persistent conformational ensemble, interaction state, insoluble fraction, or assembly whose exact proteoform composition remains uncertain [45]. Proteoform is defined by composition and carries no statement about residence time. Damaged proteome and molecular aging describe a condition of a tissue rather than a therapeutic unit, and a

modification-defined species excludes truncation, crosslinking, and assembly state. Table 1 sets out the terminology used here against established usage.

Table 1. Terminology used in this Review reconciled with established usage. For each term the table states the use adopted here, the existing vocabulary it overlaps, and the claim it does not make.

Term	Use in This Review	Established Terms It Overlaps	What It Does Not Assert
Protein lifetime (residence time)	Kinetic property of a measured protein population, estimated from labeling and a stated kinetic model	Half-life, turnover rate, protein age	That the persistent molecules are chemically altered, or that the estimate transfers to another compartment or cell type
Molecular age	The accumulated chemical, conformational, interaction, localization, and processing history of a protein population	Molecular aging, protein damage, damaged proteome	A single scalar damage score, and no equivalence with chronological age
Age-generated proteoform	A compositionally resolved molecular form whose relationship to residence time or organismal aging is supported by evidence	Proteoform, post-translationally modified species, intact proteoform	That the form is pathogenic, or that it is the only form present
Molecularly aged protein state	A persistent conformational, interaction, insoluble, or assembly state whose exact composition is unresolved	Conformer, strain, aggregate, insoluble fraction, damaged proteome	A defined chemical composition, and therefore no claim of proteoform-level selectivity
Target state	The molecular unit that a therapeutic is required to engage, which may be a proteoform, a conformer, an assembly, or a depleted functional pool	Drug target, druggable target	Druggability, and no implication that the gene product as a whole is the target
Functional pool	The population of the same gene product that must be preserved during intervention	Physiological pool, wild-type protein	That the pool is chemically homogeneous or kinetically uniform

2.4. An Evidence Ladder for Therapeutic Promotion

An age-associated molecular state becomes a credible therapeutic target through sequential evidence. First, the state must be detected reproducibly with an explicit analytical confidence model. Second, its association with age must survive control for abundance, sampling, cell composition, and technical artifacts. Third, the state should be localized to the relevant brain region, cell type, compartment, and disease stage. Fourth, it should be connected quantitatively to a molecular, cellular, or physiological phenotype. Fifth, a controlled perturbation should test whether the state is required for, sufficient for, or contributory to that phenotype. Sixth, an intervention must engage the specified state rather than only altering a downstream readout. Translational interpretation requires evidence in human tissue, human experimental systems, or an appropriate in vivo context, together with delivery, exposure, and safety measurements. Failure at one level cannot be repaired by computational sophistication at a later level. A machine-learning model can prioritize an age-associated proteoform [22], but that output remains a prediction until the state

is perturbed. Docking can propose a binding geometry, but a score is not a measured affinity [46]. Molecular dynamics can describe behavior within a simulated ensemble, but it does not establish activity in a cell. A quantum calculation can estimate an electronic energy for a defined chemical model, but it cannot validate the biological relevance of that model. The ladder is therefore a standard for the evidence and for the claims drawn from it. This framework also accommodates protective and adaptive states. The aging brain does not undergo uniform proteome deterioration. Some proteins persist longer, others turn over faster, and turnover changes differ among regions and compartments [6–8]. Aggregation or transfer to microglia may represent failed clearance, active disposal, a protective sequestration process, or a mixture of these mechanisms [9,47]. A therapeutic program that removes an accumulated state without resolving its function could eliminate a buffer against more toxic species. The direction of intervention must be demonstrated rather than inferred from accumulation. Promotion therefore depends on evidence accumulating in a fixed order, and a candidate may stall at any rung without ceasing to be useful biology. Figure 1 contrasts the canonical description of a brain protein, a gene with a sequence and a representative structure, with the ensemble of time-dependent states that the same gene product can occupy in a persistent cellular compartment.

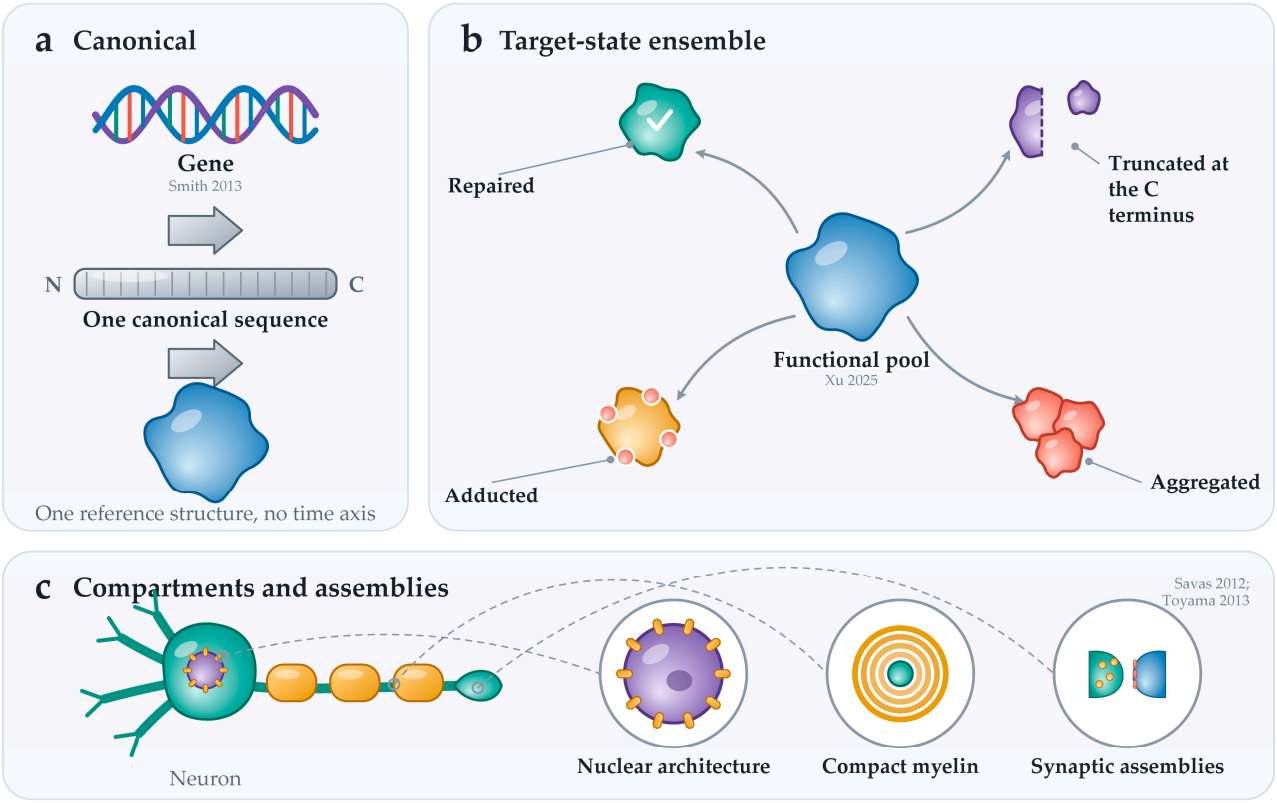


Figure 1. Molecular time creates hidden therapeutic targets. (**a**) A canonical sequence and a representative folded structure provide only the leftmost description of a brain protein [16]. (**b**) Persistence, spontaneous chemistry, incomplete repair, processing, complex exchange, and altered clearance create a heterogeneous target-state ensemble [19]. Panel (**c**) shows a neuron with callouts to nuclear architecture, compact myelin and a synapse, indicating that these states occupy distinct compartments and assemblies [1,2]. Blue states represent preserved functional populations, while teal, violet, amber, and coral states denote chemically or structurally distinct populations without assigning toxicity. The figure is conceptual and not quantitative.

3. How Persistent Proteins Acquire Molecular Age

3.1. Persistence Changes the Reaction Window

Residence time is only the opportunity for chemistry; what that opportunity produces is the subject of this section. The chemical history of a protein is governed by exposure time as well as by reaction rate, so a residue that reacts slowly may remain essentially unchanged in a protein replaced every few hours and become measurably heterogeneous in a population that persists for months. The relationship is not linear in a living brain. Conformation can bury or expose a susceptible site, assembly partners alter local solvent and electrostatics, and repair or selective clearance can remove one product faster than another, so two proteins with the same measured lifetime can carry quite different chemical burdens. A lifetime estimate therefore defines an opportunity window and not a damage measurement, and the two must be measured separately before either is used to define a target. Turnover studies across brain regions [8], synapses [5], mitochondria [4], and aging vertebrate models [47] show that persistence is structured by compartment and complex membership and is not a property assigned uniformly to a gene product, which is why the chemistry that follows has to be described per compartment as well as per residue. Table 2 collects the principal quantitative measurements on which this argument relies, and the subsections below take the chemical routes in turn: backbone rearrangement and stereochemical drift, then oxidation, carbonyl chemistry, glycation, truncation and crosslinking, and finally the one tissue in which the whole chain from zero turnover to clinical phenotype has already been measured.

Table 2. Quantitative measurements of brain protein lifetime and turnover cited in this Review. Each entry lists the biological system, the labeling or profiling approach, and the reported result that constrains the molecular-age framework.

System	Approach	Reported Result	Reference
Adult rat brain	15N pulse-chase with mass spectrometry	Nucleoporins and histones identified as exceptionally long-lived, persisting for the measured lifespan of the animal	[1]
Adult rat brain and cultured cells	Metabolic pulse-chase, system-wide screen	Long-lived proteins extend beyond the nuclear pore to other stable cellular structures; pore subcomplexes show slow, incomplete renewal	[2]
Mouse brain, tissues and subcellular fractions	In vivo 13C6-lysine labeling with kinetic modeling	Lifetimes measured for approximately 3500 proteins, differing across tissues, organelles and synaptic fractions	[3]
Mouse mitochondria	Long-term isotope labeling with electron microscopy	Electron transport chain subunits retained longer than the surrounding organelle, indicating heterogeneous renewal within one assembly	[4]
Mouse brain, single synapses	PSD95 lifetime imaging across the lifespan	Postsynaptic density protein 95 lifetime ranged from hours to several months across synapse types	[5]
Young and aged mouse brain	Pulse labeling with regional resolution	Mean protein lifetime increased by approximately 20% in aged animals, with protein-specific and region-specific deviations	[6]

Table 2. *Cont.*

System	Approach	Reported Result	Reference
Mouse aging continuum	Continuous labeling, soluble and insoluble fractions	Dynamic turnover trajectories with sex differences, altered insoluble-proteome behavior, and proteasome-linked changes in proteolytic subunit turnover	[7]
Mouse tissues and brain regions	Turnover atlas of proteome and phosphoproteome	Turnover quantified across regions with tens of thousands of phosphosites resolved, separating abundance from lifetime and modification state	[8]
Mouse neurons, 4 and 24 months	Neuron-restricted bioorthogonal labeling	Average neuronal protein half-life approximately doubled with age; 1726 proteins identified in the aged neuronal aggregome, many detectable in microglia	[9]
Killifish Nothobranchius furzeri brain	Proteome and transcriptome profiling with proteasome suppression	More than 40% of age-regulated proteins attributed to post-transcriptional mechanisms; proteasome suppression reproduced loss of complex stoichiometry	[10]
Killifish, multiple tissues	Aggregation and quality-control profiling across age	Tissue-specific landscape of protein aggregation and quality control during vertebrate aging	[47]
Human plasma and tissues, 50-year span	Population proteome profiling	Organ-resolved aging trajectories and signatures across the adult lifespan	[11,48]

Figure 2 formalizes this point as a competition among synthesis and assembly, subunit exchange, spontaneous chemical conversion, chaperone and enzymatic repair, unfolding and aggregation, clearance, and intercellular disposal. The central protein in the figure is shown in a functional state, because longevity can be adaptive. Long residence times may preserve costly macromolecular assemblies, reduce the energetic burden of replacement, or maintain structural continuity [4]. The same persistence can become a liability when repair capacity falls, damaged subunits cannot exchange, or a slow conversion creates a state with higher aggregation or interaction propensity [10]. Interpretation requires at least two measurements that cannot substitute for each other, a kinetic estimate of persistence and a molecular measurement of the state that accumulated. Aging also changes the rates around this system. Proteasomal capacity declines early in Alzheimer disease tissue and in cellular models [25], chaperone availability is regulated locally within dendrites [49], translation elongation slows in the aging killifish brain [50,51], ribosome-associated quality control counteracts age-associated pathology across species [52], and neuronal autophagy is required for normal synaptic function [26,53]. Chaperone-mediated autophagy prevents collapse of the neuronal metastable proteome [54], and mitochondrial dynamics and quality control shape proteostasis under metabolic stress [55]. Metabolic transitions in human brain aging are not gradual, and a midlife window has been proposed on the basis of nonlinear metabolic change [56]. A mean increase in lifetime may therefore reflect slower degradation, lower synthesis, altered precursor labeling, or a change in cellular composition. The most defensible experiments fit explicit kinetic models, report uncertainty, assess precursor-pool behavior, and compare more than one peptide per protein. They also distinguish an old molecular fraction from a tissue collected from an old organism. These distinctions explain why apparently conflicting reports of increased and decreased turnover can both be biologically correct [7,11]. Proteostasis failure has been described in

overlapping but non-identical forms across neurodegenerative and systemic conditions, including Alzheimer disease [57,58], transdifferentiated Alzheimer neurons with lysosomal repair deficits [59], tau-directed CRISPR screens in induced neurons [60], diabetic brain proteotoxicity [61], age-related HIV neurodegeneration [62], and gut-linked ageing phenotypes [63]. Regulatory pathways that modify this landscape include REST-dependent stress resistance and neural excitation [64,65], NAD+-dependent autophagy [66], nutrient-driven O-GlcNAc signaling [32], and microglial lipid handling through CLN3 [67]. Each of these connects a proteostatic mechanism to an age-related phenotype without establishing that any individual persistent molecule is a drug target.

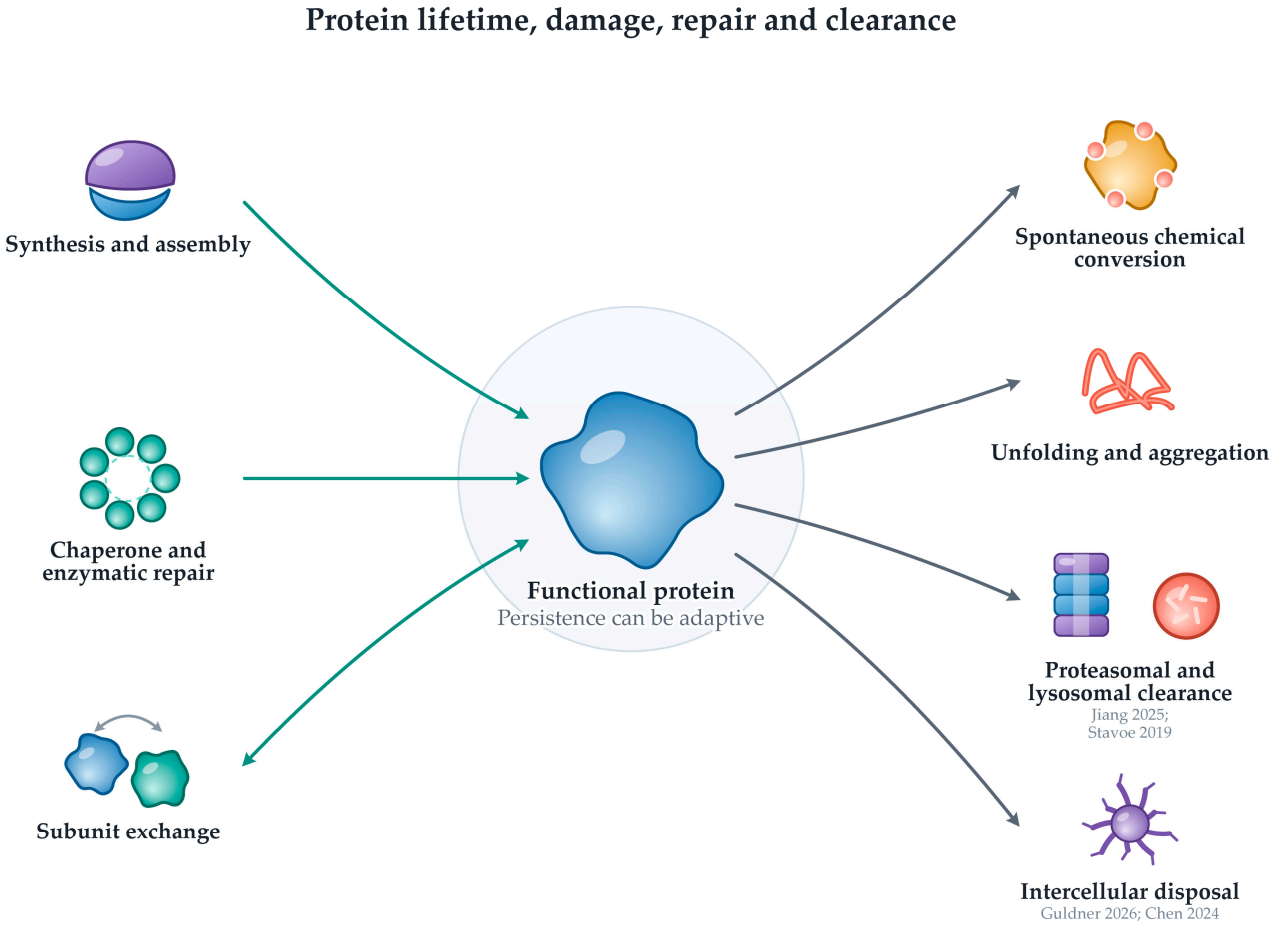


Figure 2. Protein lifetime, damage, repair, and clearance. Molecular age emerges from competing rates of synthesis and assembly, subunit exchange, spontaneous chemical conversion, chaperone or enzymatic repair, unfolding and aggregation, proteasomal or lysosomal clearance [25,26], and intercellular disposal [9,47]. Neuronal material transferred to microglia is shown as one possible route and not as proof of toxicity. The central protein remains functional to emphasize that persistence can be adaptive. An altered rate on any branch can change the age distribution without changing total protein abundance [8].

3.2. Backbone Rearrangement and Stereochemical Drift

Spontaneous deamidation of asparagine and isomerization of aspartate can proceed through a cyclic succinimide intermediate [13]. Hydrolysis yields conventional aspartate as well as isoaspartate, which inserts an additional methylene group into the peptide backbone. The products can include different stereoisomers, and the change is not cosmetic. A backbone rearrangement changes local geometry, protease susceptibility, hydrogen-bonding opportunities, and the relationship between side chains at an interface, and it can pro-

mote fibril formation from substrates that are otherwise stable [35]. Reaction rate depends strongly on neighboring residues, conformational flexibility, pH, and solvent access [14]. Site occupancy is consequently more informative than a generic statement that a protein is deamidated, and isoaspartate has been evaluated as a candidate contributor to neurodegeneration on exactly those terms [36,37]. Protein L-isoaspartyl methyltransferase initiates a repair cycle by methylating abnormal isoaspartyl residues [34]. The cycle can return part of the population toward conventional aspartate, but it consumes S-adenosylmethionine and is neither perfectly efficient nor equivalent to restoring the original asparagine [14]. Experimental reduction in this repair capacity accelerates isoaspartate accumulation in brain and can reduce endogenous protein activity [15]. That result supports a mechanistic connection among spontaneous chemistry, repair, and function. It does not establish that globally increasing repair will be beneficial, because repair direction, compartment access, substrate competition, and methylation burden remain relevant. A target program should identify the site, quantify its occupancy, establish its functional direction, and then decide whether repair, replacement, or selective removal is rational. Racemization presents a still harder analytical problem because D and L residues can be isobaric. Conventional bottom-up workflows may not separate them, and database searches cannot infer stereochemistry from mass alone. Chiral chromatography, tailored enzymatic digestion, ion-mobility behavior, synthetic standards, or orthogonal structural measurements may be required. Claims about age-dependent racemization should therefore state what was directly resolved. The therapeutic implication is substantial, because a stereochemical change can create a state-specific epitope or alter a binding pocket without changing elemental composition. It can also invalidate a canonical structural model whose residue chirality is fixed by construction.

3.3. Oxidation, Carbonyl Chemistry, Glycation, Truncation, and Crosslinking

Oxidation spans regulated signaling, reversible chemistry, and irreversible damage [68,69]. Methionine sulfoxide can be reduced enzymatically in a stereospecific manner, and site-resolved profiling of mouse hippocampus showed that methionine sulfoxide speciation changes with age and with Alzheimer disease pathology, concentrating in mitochondrial and glycolytic pathways [70]. Cysteine oxidation can encode signaling or indicate loss of redox control, and glutathione status shifts across brain disorders and aging [71]. Tyrosine nitration and other tyrosine modifications accumulate in aged tissue [72], while metal-catalyzed reactions can alter activity or promote fragmentation, with zinc proposed as one link between metal handling and oxidative brain aging [73]. Redox proteomics has mapped these changes across the aging brain [74] and in Alzheimer disease tissue specifically [75], and inflammatory activation can drive them further, as shown for microglial nitric oxide production after TNF-alpha and IFN-gamma exposure [76]. Sample preparation itself can generate oxidation, so age comparisons require matched handling, antioxidants where justified, procedural blanks, and evidence that the measured product existed before extraction [28]. Oxidative regulation also intersects with amyloid catabolism, since several amyloid-degrading enzymes are themselves redox-sensitive [77], and selenoprotein systems contribute to antioxidant capacity in brain [78]. Reactive carbonyl species arise from lipid peroxidation, carbohydrate metabolism, and oxidative fragmentation. Their adducts can alter charge and steric environment, create electrophile-specific interaction surfaces, or crosslink proteins [31]. Glycation and advanced glycation end products are especially relevant to long-lived extracellular and vascular proteins, where replacement is slow and accessibility differs from intracellular targets [29,79]. Glycation also modifies the aggregation behavior of amyloidogenic proteins directly [80], and DJ-1, a Parkinson-associated protein once proposed to reverse glycation, acts as an antagonist of adduct formation rather than an eraser of existing adducts [81]. The same chemical class can have different consequences

in a soluble enzyme, a membrane protein, and an extracellular scaffold. Bulk carbonyl or fluorescence measurements are useful for burden but insufficient for target definition. Site-resolved measurements, intact-state reconstruction, and functional perturbation are needed to determine whether an adduct is causal, compensatory, or simply a record of exposure. Proteolytic truncation can generate a stable fragment with localization, assembly behavior, or toxicity that differs from the precursor, and calpain and cathepsin activity has been proposed as one route to such fragments in neuronal death [30]. Crosslinking can stabilize a useful extracellular structure or trap an intracellular complex in a nonrenewable state, with transglutaminases providing an enzymatic route in addition to spontaneous oxidative crosslinks [31,82]. Figure 3 maps these chemical routes to their molecular consequences and does not treat all changes as one post-translational-modification category. The six branches represent charge and backbone changes, stereochemical changes, oxidation, carbonyl and glycation adduction, truncation, and crosslinking, and their endpoints include altered folding, interaction, solubility, and assembly. Each route must be demonstrated with chemistry-specific evidence before it is assigned to an individual target, and Table 3 pairs each route with the human or animal evidence currently available for it.

Table 3. Chemical routes to age-generated protein states and the evidence supporting each. Reported observations are separated from the analytical risk that limits their interpretation and from the therapeutic question that remains open.

Chemistry	Reported Evidence in Brain or Disease Tissue	Principal Artifact Risk	Open Therapeutic Question	Reference
Deamidation and isoaspartate formation	Reduced PIMT activity in Pcmt1 heterozygous mice accelerated brain isoaspartate accumulation and lowered creatine kinase B activity [15]; the succinimide route and its aspartyl products are chemically defined [13,14]; PIMT initiates a repair cycle rather than masking the site [34] and limits fibril formation from isoaspartate-containing substrates in vitro [35]; isoaspartate examined as a contributor to neurodegeneration [36] and to Alzheimer disease etiology [37]	Ex vivo deamidation during extraction and storage	Should the site be repaired, removed, or tolerated	[13–15,34–37]
Racemization	Stereochemical change without change in mass; D and L residues are isobaric, so chiral separation, selective digestion, ion mobility, or synthetic standards are required to resolve them [15]	Stereochemistry inferred from mass alone	Can stereoselective recognition be achieved at a defined residue	[15]
Oxidation	Methionine sulfoxide speciation in mouse hippocampus changed with age and with Alzheimer pathology, concentrating in mitochondrial and glycolytic pathways [70]; redox proteomic maps of the aging brain [74] and of Alzheimer disease brain [68]; tyrosine modification accumulates with age [72]; oxidation spans regulated signaling and irreversible damage [68,69]	Preparation-induced oxidation during extraction and handling [28]	Is the state reversible, and is it causal or adaptive	[28,68–70,72,74,75]
Carbonyl adduction	Advanced glycation end products alter cellular signaling [29]; oxidative crosslinking generates defined peptide and protein adducts [31]	Nonspecific derivatization during enrichment	Does adduction create a unique reactive or antigenic surface	[29,31]
Glycation	Glycation modifies the aggregation behavior of amyloidogenic proteins [80]; DJ-1 antagonizes glycation rather than erasing existing adducts [81]; long-lived extracellular and vascular proteins accumulate adducts and crosslinks [29,79]	Bulk fluorescence signal assigned to one target protein	Can matrix remodeling preserve tissue mechanics while reducing adduct burden	[29,79–81]

Table 3. *Cont.*

Chemistry	Reported Evidence in Brain or Disease Tissue	Principal Artifact Risk	Open Therapeutic Question	Reference
Truncation	Truncated and highly resistant amyloid-beta proteoforms detected in human astrocytes [83]; intact and truncated tau proteoforms resolved from human temporal cortex [19]; top-down characterization of truncated proteoforms established as a method [84]; calpain-cathepsin route proposed for neuronal fragment generation [30]	Proteolysis during tissue handling	Remove the fragment, block its generation, or replace the pool	[19,30,83,84]
Crosslinking	Oxidative crosslinking mechanisms characterized in peptides and proteins [31]; transglutaminases provide an enzymatic crosslinking route [82]	Crosslink formation or loss during extraction	Is controlled remodeling safer than maximal removal	[31,82]

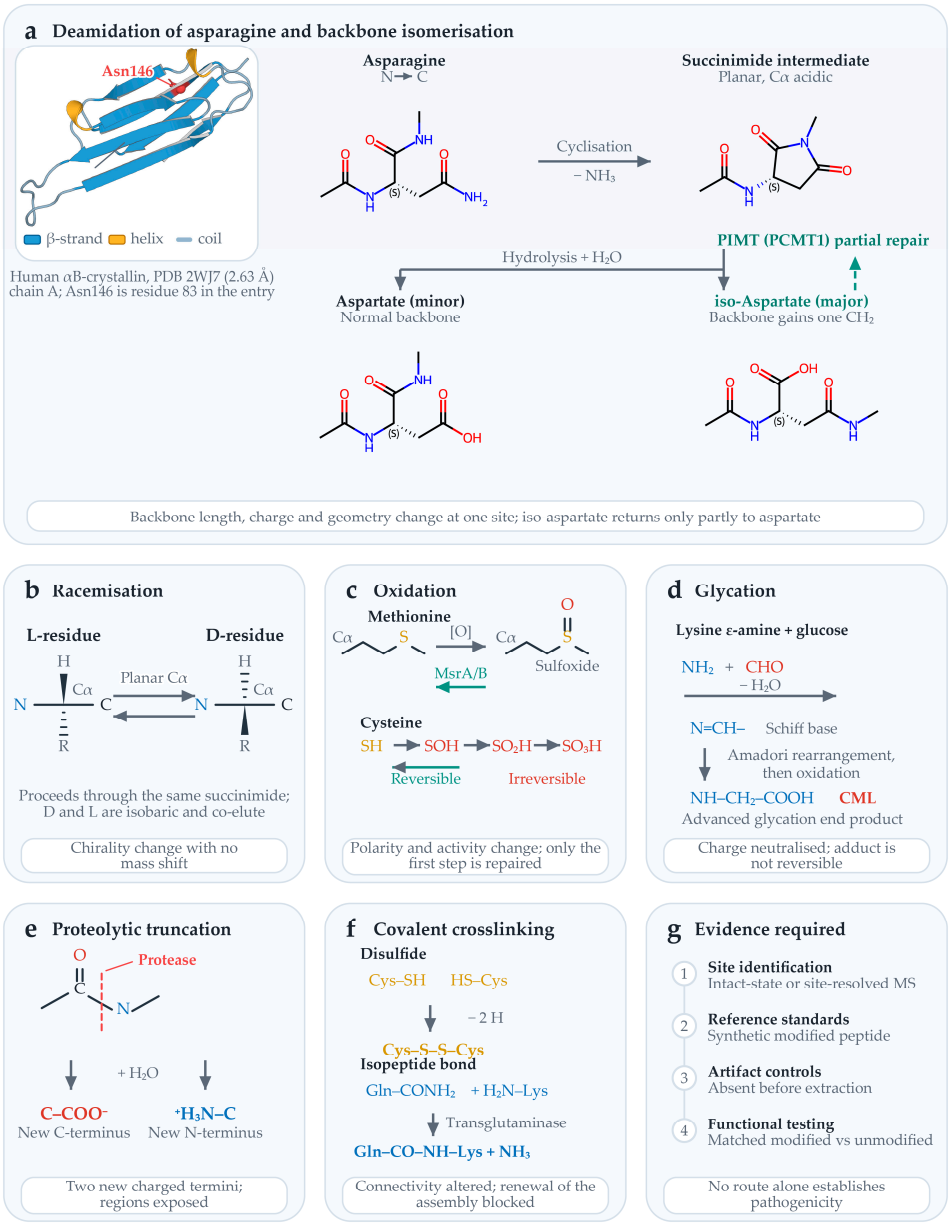


Figure 3. Chemical routes to age-generated proteoforms. Six chemical routes are drawn as explicit structures, with backbone direction running from the amino to the carboxy terminus throughout. In

panel (**a**) each species is drawn as a residue within a peptide chain, with the preceding residue represented by an acetyl group and the following one by an N-methylamide, and the alpha carbon carries the (S) configuration of the parent L-amino acid in every structure. Those four structures were generated with RDKit and checked against the PubChem records for L-asparagine (CID 6267), L-aspartic acid (CID 5960) and succinimide (CID 11439). (**a**) Deamidation of asparagine proceeds through a cyclic succinimide intermediate with loss of ammonia, and hydrolysis of either ring carbonyl gives iso-aspartate, in which the backbone gains one methylene group, or aspartate, in which the backbone is unchanged; protein L-isoaspartyl methyltransferase (PIMT, encoded by PCMT1) returns part of the iso-aspartate pool through the succinimide and so repairs it only partly [13,34], (**b**) racemisation proceeds through the same planar succinimide and inverts the alpha carbon with no change in mass [14], (**c**) methionine is oxidised to the sulfoxide and reduced back by methionine sulfoxide reductases, whereas cysteine oxidation is reversible only at the sulfenic stage [28], (**d**) the lysine epsilon-amine condenses with glucose to a Schiff base, rearranges to the Amadori product and oxidises to carboxymethyl-lysine [29], (**e**) peptide-bond hydrolysis generates a new carboxy terminus and a new amino terminus, both charged and both labelled [30], and (**f**) crosslinking is shown as a cysteine disulfide and as a transglutaminase-catalysed isopeptide bond between glutamine and lysine [31]. Panel (**g**) sets out the evidence required before any route is assigned to a particular site. The inset in panel (**a**) shows the alpha-crystallin domain of human alphaB-crystallin, chain A of PDB 2WJ7 determined at 2.63 A, rendered in PyMOL (version 3; Schrödinger, New York, NY, USA) from the deposited coordinates as a secondary-structure cartoon, with beta-strands as arrows and helices as ribbons and with the deamidation-prone Asn146 marked. That entry numbers its own residues 3 to 87, so Asn146 of the mature protein is residue 83 in the coordinate file. The structures in panel (**a**) are vector output from RDKit and the remaining chemical structures were drawn as vector artwork by the authors; the inset is a render of deposited atomic coordinates.

3.4. The Ocular Lens as a Validated Reference Case

One tissue provides a complete chain from zero turnover through spontaneous chemistry to a clinical phenotype. Lens fibre cells degrade their organelles during differentiation and retain the crystallins synthesized before that point, so the protein present in the centre of an adult human lens was made in early life and is never replaced [85]. Residence time in the lens is consequently not estimated from a labeling model; it is set by anatomy and has been measured directly by radiocarbon dating [86] and by aspartate racemization [87]. Against that fixed clock, the same chemistry has been mapped at site resolution. Asparagine and glutamine deamidation accumulates across alpha-, beta-, and gamma-crystallins with age and is enriched in the water-insoluble fraction [88], and racemization, truncation, glycation, and disulfide and non-disulfide crosslinking follow the same age dependence and are implicated in nuclear cataract [89]. The functional consequences were established biophysically. Deamidation at specific interface residues lowers solubility and promotes high-molecular-weight aggregate formation [90], and modification of alphaB-crystallin reduces the chaperone activity that keeps the remaining crystallins soluble [91]. Loss of that solubility produces the refractive-index fluctuations that scatter light, which is the physical definition of the clinical lesion [92]. In the lens, molecular age, defined chemistry, loss of a specific molecular function, and a clinical phenotype have been measured in one tissue, through a fixed residence time, site-resolved modification mapping, solubility fractionation, and a functional readout taken on the same preparation. Two differences limit how far this extends to brain. The mature lens fibre cell has no proteasomal, autophagic, or cellular clearance capacity and no repair enzymes acting on the persistent pool, so damage there is cumulative by construction, whereas brain cells retain partial renewal, isoaspartyl repair, and selective degradation [15,34], and an observed brain state is always the product of damage and of the processes competing with it. The lens also contains one dominant and functionally homogeneous protein class whose endpoint is optical, while the brain states considered here involve heterogeneous assemblies with electrophysiological, metabolic,

and transport functions. The chemistry is known in brain; the direct measurement of human residence time is not. Causal interpretation in the lens is itself not complete: the evidence is biophysical and genetic rather than interventional, since no treatment reverses the accumulated chemistry in a human lens.

4. Measuring Molecular Age at the Required Molecular and Spatial Resolution

4.1. Turnover Experiments and Their Assumptions

A target state can only be dated as well as the kinetic experiment behind it allows, and that experiment carries assumptions worth stating. Stable-isotope labeling can estimate synthesis and disappearance over time, but the result depends on the biological model and the mathematical assumptions applied to it. Pulse labeling can identify molecules retained from an earlier interval [1]. Continuous labeling can resolve incorporation trajectories across an aging cohort [7]. Dynamic labeling in adult animals can compare tissues and subcellular fractions [3], while cell-selective bioorthogonal labeling can restrict the observable pool to neurons or another engineered population [9], and these designs answer related but nonidentical questions. Label recycling, incomplete precursor equilibration, growth dilution, changing cell composition, peptide-specific detectability, and model misspecification can bias an apparent half-life, and an aging study adds further constraints. Young and old groups may differ in food intake, amino-acid metabolism, body composition, activity, or disease burden, and each of these changes the enrichment and the time course of the free amino-acid precursor pool that the kinetic model treats as known [3], so an apparent difference in protein lifetime can arise with no change in the chemistry or the degradation of the protein itself [7]. A further constraint is one of identifiability rather than of practice. Time-course designs are standard in this literature, and the studies cited above sample multiple intervals across labeling and chase periods [3,6,8,9]; the problem arises when a labeled fraction is read at a single terminal time, because synthesis and degradation then enter the fitted curve only through their combination. At steady state the size of a labeled pool is set by the ratio of the two rates, so one measurement of that pool has one equation and two unknowns, and a given enrichment is equally consistent with slower degradation, reduced synthesis, and incomplete precursor labeling. Separating the terms requires at least two post-label intervals, an independent measurement of precursor enrichment, or a pulse-chase design in which the labeled population is followed after label withdrawal, which is why the designs listed above are not interchangeable [1]. Region-level tissue contains multiple cell types with distinct kinetics, which is why regional and phosphosite-resolved atlases report turnover separately for each unit rather than pooling them [8]. Insoluble extraction can enrich persistent assemblies while losing other fractions, and aggregation profiling across tissues shows how strongly recovery depends on that choice [47]. Strong studies therefore report the labeling protocol, precursor measurements, kinetic equation, inclusion criteria, peptide-level observations, uncertainty intervals, and sensitivity analyses. Lifetime should be attributed to the measured population, not promoted to an immutable property of the protein. Interpretation also depends on what the degradation machinery is doing during the labeling window. Proteasome activity falls early in Alzheimer disease brain and cellular models [25], chaperone-mediated autophagy protects a metastable neuronal proteome that collapses when the pathway is lost [54], macroautophagy operates under distinct constraints in axons and dendrites [26,93], and localized chaperone synthesis maintains dendritic proteostasis independently of the soma [49]. A change in any of these processes alters an apparent lifetime without any change in the chemistry of the protein itself. Reports of altered turnover should therefore state which arm of the system was measured. Table 4 lists these constraints with the design or reporting that resolves each.

Table 4. Interpretive limits of molecular-age evidence and the designs that resolve them. The table collects the constraints discussed in Sections 4 and 5 so that each can be checked against an individual study rather than read as a general caution.

Inferential Step	Limitation	Why It Arises	Design or Reporting That Resolves It
Lifetime estimation	Synthesis and degradation are not separable from one terminal measurement	At steady state the labeled fraction depends on the ratio of the two rates, giving one equation and two unknowns	Two or more post-label intervals, measured precursor enrichment, or a pulse-chase design with label withdrawal
Lifetime estimation	Apparent half-life is biased by label recycling, precursor equilibration, and growth dilution	Released labeled amino acids re-enter synthesis, and the free pool equilibrates more slowly than the model assumes	Explicit kinetic equation, precursor measurement, sensitivity analysis, and more than one peptide per protein
Age comparison	Cohort differences in intake, metabolism, body composition, and disease burden mimic a lifetime difference	These variables alter precursor enrichment and its time course rather than protein chemistry	Matched feeding and husbandry, measured precursor enrichment in both groups, and reporting of cohort covariates
Attribution of age	Tissue taken from an old animal is not the same as an old molecular fraction	Bulk tissue mixes molecules of all ages, and composition itself changes with age	Report the measured population, resolve cell type or compartment, and avoid promoting lifetime to a property of the gene product
Spatial resolution	Region-level values average cell types with different kinetics	A region contains neurons and glia whose turnover differs for the same protein	Cell-selective labeling, regional and phosphosite-resolved reporting, or single-cell-resolved measurement
Fractionation	Recovery depends on the extraction chosen	Insoluble extraction enriches persistent assemblies and discards other fractions	Report extraction protocol and recovery with standards, and compare fractions rather than one
Chemical identity	A detected mass shift does not fix the site or the chemistry	Several residues can give near-identical shifts, and search-space expansion weakens localization control	Modification-aware false-discovery control, orthogonal standards, and intact-state confirmation
Age association	Enrichment in old or diseased tissue is not pathogenicity	Cell composition, agonal state, postmortem interval, extraction, and selective survival all covary with age	Covariate control, balanced batches, controlled sample handling, and comparison of modified with unmodified pools
Causal perturbation	A tool that changes a molecular state usually changes something else as well	Residue substitution alters folding, overexpression alters stoichiometry, and global proteostasis inhibition creates secondary damage	Convergent designs, site-specific installation or repair-enzyme manipulation, matched structural controls, and rescue

Table 4. *Cont.*

Inferential Step	Limitation	Why It Arises	Design or Reporting That Resolves It
State detection in situ	Conformation-selective reagents may not discriminate the proposed state	Antibody performance across nominally equivalent reagents varies more than the states being compared	Validated reagent panels, testing against related assemblies and chemical states, and orthogonal mass-spectrometric confirmation
Direction of effect	Accumulation does not indicate whether the state should be removed	The same accumulated material can be toxic, a protective sink, a disposal intermediate, or an inert record	Test both directions of intervention and measure the functional pool alongside the proposed harmful state
Human evidence	Cross-sectional postmortem data cannot order cause and consequence	Sampling occurs once, at the end of a disease course, under selective survival	Triangulation with longitudinal models, staged cohorts, and ex vivo engagement measurement
Pharmacology	Total exposure is not engagement of the state	Compartment access, target-mediated disposition, and membrane partitioning intervene between dose and target	Unbound and compartment-resolved exposure with a proximal, state-resolved pharmacodynamic readout

4.2. Bottom-Up, Top-Down, Native, and Spatial Measurements

Bottom-up proteomics offers depth and throughput, since proteolysis produces peptides that can localize many modifications and support turnover estimation. Its central limitation for this Review is loss of connectivity. Two modified peptides may come from the same intact molecule or from different members of the population. Open searches enlarge the detectable chemical space but also enlarge the hypothesis space, increasing the burden on false-discovery control and localization [28]. Synthetic standards, site-determining fragment ions, retention behavior, isotopic patterns, and orthogonal enrichment can improve confidence, and deep-learning predictors of precursor and fragment behavior are now part of that toolkit [94,95]. Top-down mass spectrometry preserves the intact molecular form and can reveal combinations of truncation and modification [39,84]. Sample handling before analysis remains a limiting step, and dedicated processing workflows have been developed for it [96]. Quantitative throughput has improved but still lags bottom-up methods [97], and the practical decision of when top-down analysis is warranted has been set out explicitly [40]. Middle-down strategies occupy an intermediate scale, as shown for alpha-synuclein glycoforms [98]. Native mass spectrometry can uncover modifications that are lost or unassignable in denaturing workflows [99], crosslinking and structural mass spectrometry add information about assemblies and conformations [100], and single-cell proteoform analysis is beginning to resolve intact forms at cellular resolution [101]. These gains come with reduced depth, dynamic-range limits, difficult fragmentation, and complex inference. No method should be described as proteoform-resolved unless the combination of mass, fragmentation, localization, and uncertainty supports that level of molecular assignment [18]. A family of unresolved intact masses is valuable evidence, but it is not a complete structural identity [19]. Intact-proteome measurements from human tissue, including pediatric brain tumors, illustrate both the information gained and the coverage still missing [102]. Spatial proteomics and imaging place a state within a region, cell type, or subcellular compartment [103]. Single-cell and single-nucleus measurements

can reduce composition confounding [104], although current depth may be insufficient for rare modified forms. Microfluidic workflows combined with transfer learning have raised the spatial resolution achievable in complex tissue [105], three-dimensional intact-specimen methods retain anatomical context that sectioning destroys [106], proteoform-selective imaging links intact molecular identity to tissue position [107], and deep visual proteomics has mapped proteotoxicity within histologically defined cells in human disease [108]. Laser-capture microdissection, proximity labeling, organelle purification, and synaptic fractionation increase anatomical specificity while introducing isolation biases. Human postmortem tissue adds agonal state, postmortem interval, fixation, storage, comorbidity, medication, and terminal disease as covariates. These variables belong in the design and in the reported metadata. One further complication concerns what the reference sequence itself contains. Alternate RNA decoding can produce stable and abundant protein species that a canonical database does not predict [109]. A molecular-age pipeline that searches only canonical sequences will therefore misassign or discard part of the very heterogeneity it is designed to detect. Figure 4 shows the measurement stack that follows from these constraints. Isotope labeling supplies kinetic information, regional and cell-type sampling supplies biological localization, and bottom-up, intact-protein, native-complex, spatial, and structural branches supply complementary molecular observables. The branches converge only after orthogonal biochemical validation. A mass-spectrometric match, an image, or a predicted structure alone cannot establish a time-dependent therapeutic target, so the target resolution a programme needs is set by the claim it intends to make, and no single platform supplies it. Table 5 compares what each platform actually delivers and what it cannot resolve.

Table 5. Analytical platforms for molecular-age targets. Each platform is paired with a reported application relevant to persistent or modified brain proteins, the limitation that constrains its use, and the orthogonal evidence required before a state is declared resolved.

Platform	Principal Observable	Reported Application Relevant to Molecular Age	Limitation	Required Orthogonal Evidence	Reference
Bottom-up LC-MS	Peptide abundance, modification site, isotope incorporation	Lifetimes measured for approximately 3500 mouse brain proteins [3]; regional turnover and phosphosite atlas across mouse tissues [8]; site-resolved detection and quantification of oxidative modifications [28]	Loses connectivity between modifications carried on one molecule	Synthetic peptide standards and targeted fragmentation	[3,8,28]
Middle-down MS	Large fragments with linked modifications	Alpha-synuclein glycoforms characterized at intermediate fragment size by middle-down analysis [98]	Digestion control and spectral interpretation complexity	Intact mass and site-specific standards	[98]

Table 5. *Cont.*

Platform	Principal Observable	Reported Application Relevant to Molecular Age	Limitation	Required Orthogonal Evidence	Reference
Top-down MS	Intact proteoforms and truncation products	Soluble and truncated tau proteoforms resolved from human temporal cortex [19]; truncated proteoforms characterized directly [84]; quantitative throughput improved but still limited [97]; sample processing identified as the rate-limiting step [96]; criteria for when top-down analysis is warranted set out explicitly [39,40]	Dynamic range, fragmentation efficiency, and sample preparation	Orthogonal intact mass and validated immunochemistry	[19,39,40,84,96,97]
Native and crosslinking MS	Complex composition, conformation, and proximity	Native top-down analysis uncovered modifications not assignable under denaturing conditions [99]; structural mass spectrometry applied to the assembled proteome [100]	Gas-phase behavior and crosslink inference	Structural and biochemical restraints	[99,100]
Spatial and single-cell proteomics	Region, cell type, or compartment localization	Deep visual proteomics mapped proteotoxicity in histologically defined cells [108]; microfluidics with transfer learning raised tissue resolution [105]; three-dimensional intact-specimen analysis preserved anatomy [106]; proteoform-selective tissue imaging linked intact identity to position [107]; single-cell proteoform analysis demonstrated [101]; single-cell and spatial workflows reduce composition confounding [103,104]	Depth and spatial resolution trade-off; isolation bias	Independent imaging or microdissection replication	[101,103–108]

Table 5. *Cont.*

Platform	Principal Observable	Reported Application Relevant to Molecular Age	Limitation	Required Orthogonal Evidence	Reference
Structural methods	Conformation and assembly architecture	Cryogenic electron microscopy resolved tau filament folds from Alzheimer brain [110] and alpha-synuclein fibril polymorphs from distinct synucleinopathies [111]; applications and limits in drug discovery reviewed [42]	Favors abundant and conformationally ordered species	Biochemical and cellular confirmation of the modeled state	[42,110,111]
Chiral analysis	Residue stereochemistry	Required to distinguish isobaric D and L residues that mass alone cannot separate [12]	Low throughput and high demand for synthetic standards	Synthetic stereoisomers	[12]

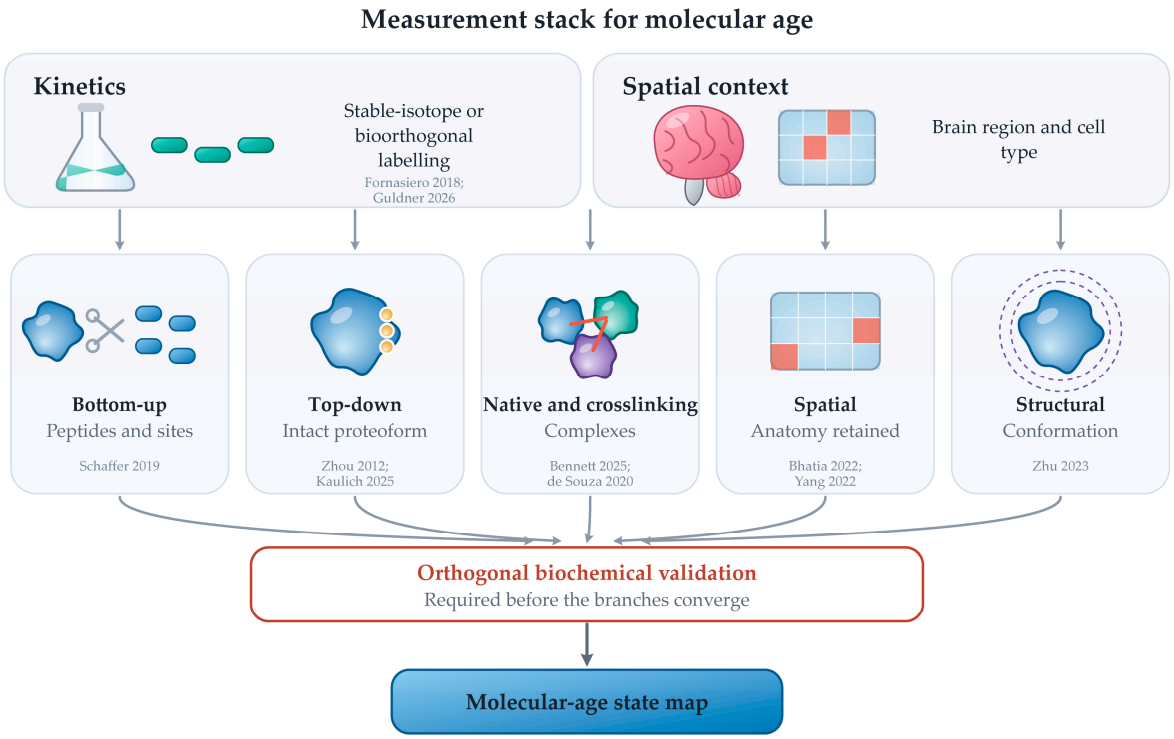


Figure 4. Measurement stack for molecular age. Stable-isotope or bioorthogonal labeling provides kinetic information [3,9]. Brain-region and cell-type sampling provides spatial context. Bottom-up analysis resolves peptides and sites [18], top-down analysis preserves intact proteoform connectivity [39,40], native and crosslinking approaches interrogate complexes [99,100], spatial measurements retain anatomy [106,107], and structural methods constrain conformation [42]. Convergence on a state map requires orthogonal biochemical validation. Instrument drawings are generic and do not represent a manufacturer or a specific dataset.

5. From Association to a Causal Target

Detection and dating establish that a molecular state exists, and neither establishes that changing it would help a patient; Figure 5 sets out the seven stages that separate the two. Detection establishes that a state was measured with a defined error model, and replicated age association shows that its abundance or occupancy changes with age once relevant covariates are addressed. Spatial localization assigns the state to a brain region, cell type, compartment, or assembly, and functional association connects it quantitatively to a phenotype. Causal perturbation installs, prevents, repairs, removes, or rescues the state, target engagement demonstrates that an intervention changes the specified molecular species, and translational relevance adds human evidence together with an appropriate exposure and safety context. The gray stopping branches in the figure carry as much weight as the ascending pathway, since a candidate that fails localization or causality remains useful biology while falling short of a validated therapeutic target. Causal testing is constrained by the available tools, because it requires the molecular state to be installed, prevented, repaired, or removed while everything else about the protein is held constant, and almost every tool delivers the intended change together with a confounding one, so the experiment and its artifact arrive together. The common designs fail in different ways. A mutation used to block a modification may alter folding independently of the modification it removes. Overexpression introduces a young protein pool and changes stoichiometry, an effect Bido et al. made visible in microglial alpha-synuclein overexpression, where dopaminergic degeneration followed phagocytic exhaustion and not a defined aged state [112]. Global inhibition of proteostasis creates secondary damage, and Kelmer Sacramento et al. found that proteasome suppression in killifish brain reproduced loss of complex stoichiometry across many proteins at once [10]. Antibodies can alter uptake or clearance without distinguishing the proposed conformer, and Ellis et al. showed how far detection varies among nominally equivalent tau reagents [41]. Convergent designs are therefore required, combining site-specific incorporation or chemical installation, the repair-enzyme manipulation used by Qin et al. [15], selective depletion, matched structural controls, rescue, and measurement of both modified and unmodified pools, and the direction of effect must be tested within them, because accumulation can indicate a toxic species, a protective sink, a disposal intermediate, or an inert record of persistence [9,47]. Human evidence is indispensable and rarely causal by itself, since postmortem associations are affected by disease stage and selective survival, and Yoshiyama et al. found synapse loss and microglial activation preceding mature tangles in a P301S tauopathy model, which shows how far a histological endpoint can sit from the causal molecular event [113]. Induced neurons preserve some donor features and reset or distort others depending on the reprogramming route, and Chou et al. found that transdifferentiated Alzheimer neurons retain proteostatic and lysosomal repair deficits that induced pluripotent stem cell (iPSC)-derived models can lose [59]; Morrone Parfitt et al. modelled astrocyte-specific lysosomal failure in midbrain organoids, which nonetheless lack aspects of vascular, immune, and long-duration physiology [114]; and rodent and short-lived vertebrate models allow controlled labeling and perturbation while not reproducing decades of human molecular residence [47,50]. No single system is closest to human aging, and a credible case identifies what each contributes and what it leaves unresolved. Promotion therefore depends on convergence across systems at one molecular resolution, and a candidate that convinces in only one system has not cleared the pathway.

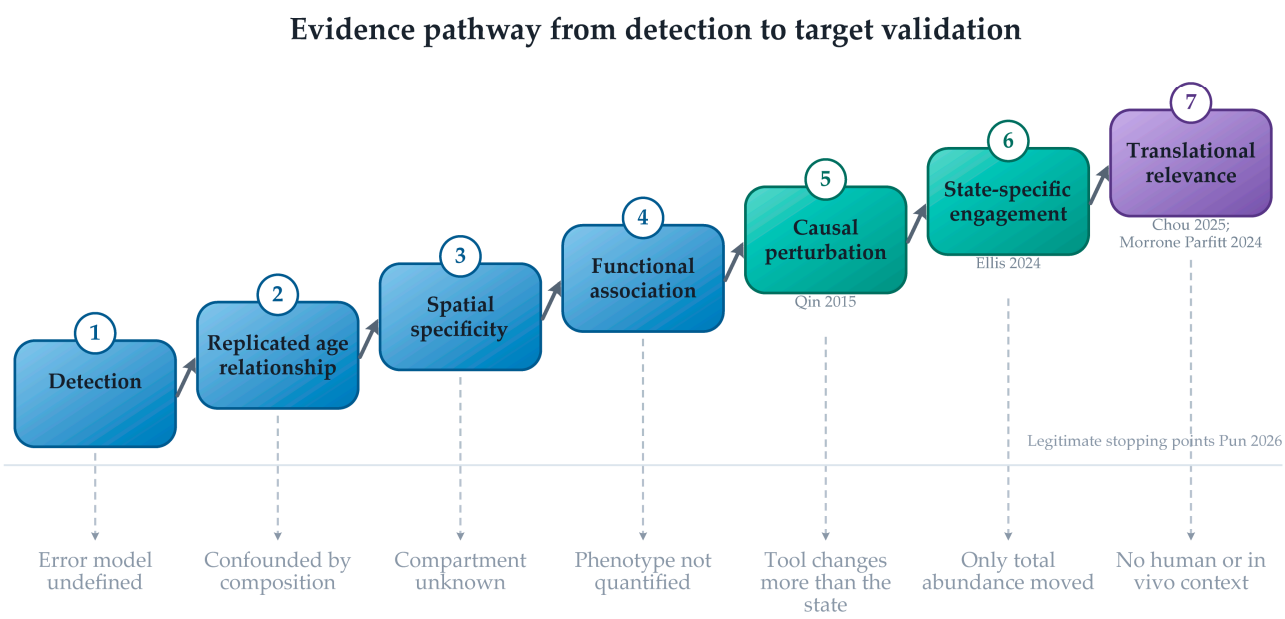


Figure 5. Evidence pathway from detection to target validation. Seven stages distinguish detection, replicated age relationship, spatial specificity, functional association, causal perturbation [15], state-specific target engagement [41], and translational relevance [59,114]. Gray branches below the pathway indicate legitimate stopping points when evidence is insufficient [22]. Association cannot skip the causal stage, and a downstream phenotype cannot replace target engagement. The final stage represents defined human or in vivo relevance and does not claim clinical efficacy.

6. Difficult Target Classes in the Aging Brain

The diseases treated later differ in their molecules, but they draw on a small number of structural situations that make a persistent protein hard to reach, and those situations are the subject of this section. The classes considered here share one property: the molecule of interest sits inside an assembly or compartment whose renewal is slow, spatially structured, or functionally essential, so that removing the protein is not equivalent to removing the state. That property has three consequences that recur in every class below. The altered population and the functional population are the same gene product, so an abundance measurement cannot separate them. The assembly, not the molecule, sets the rate at which any intervention can act, because a subunit that cannot exchange cannot be replaced however much new protein is supplied. And access is determined by the compartment, so the delivery problem differs between a nuclear scaffold, a respiratory complex, a myelin internode and a synapse even when the chemistry of the lesion is identical. Figure 6 places these classes on a common anatomical map, connecting nuclear architecture, mitochondrial complexes, compact myelin and axons, synaptic assemblies, extracellular and basement-membrane scaffolds, and neuron-microglia exchange to the neurovascular unit that controls therapeutic access to all of them.

6.1. Nuclear Architecture and Transport

Long-lived scaffold nucleoporins established that stable nuclear assemblies can retain components for exceptional periods in postmitotic brain [1]. Later work refined the picture by showing slow exchange within stable subcomplexes [2] and by describing the maintenance and surveillance mechanisms that act on pores in non-dividing cells [24]. Autophagy contributes to that surveillance under nutrient stress [115], karyopherins actively remodel the transport barrier rather than simply passing through it [116], and mitochondria make direct physical contact with the pore [117]. Pore dysfunction is now linked experimentally to

neurodegeneration through several routes [118–120]. The target is therefore not simply the nuclear pore complex. Relevant hypotheses include damaged scaffold subpopulations, altered permeability, failed subunit exchange, and interactions between pore maintenance and nuclear proteostasis. Intervening indiscriminately risks disrupting an essential transport system. The therapeutic problem is to distinguish an altered pore state from the functional majority and to measure transport consequences in the relevant neuron type. Chromatin proteins provide a related but distinct form of persistence, and histones were among the first exceptionally long-lived species identified in adult brain [1]. Histone variants, nucleosome turnover, and nuclear scaffolds integrate chemical exposure with genome maintenance. A modified or crosslinked state may change accessibility without producing a conventional ligand pocket. Replacement, repair, or controlled remodeling may be more appropriate than occupancy-driven inhibition. Direct lifetime evidence, intact-state measurements, and functional genomic readouts should be required before a chromatin-associated molecule is promoted as a molecular-age target.

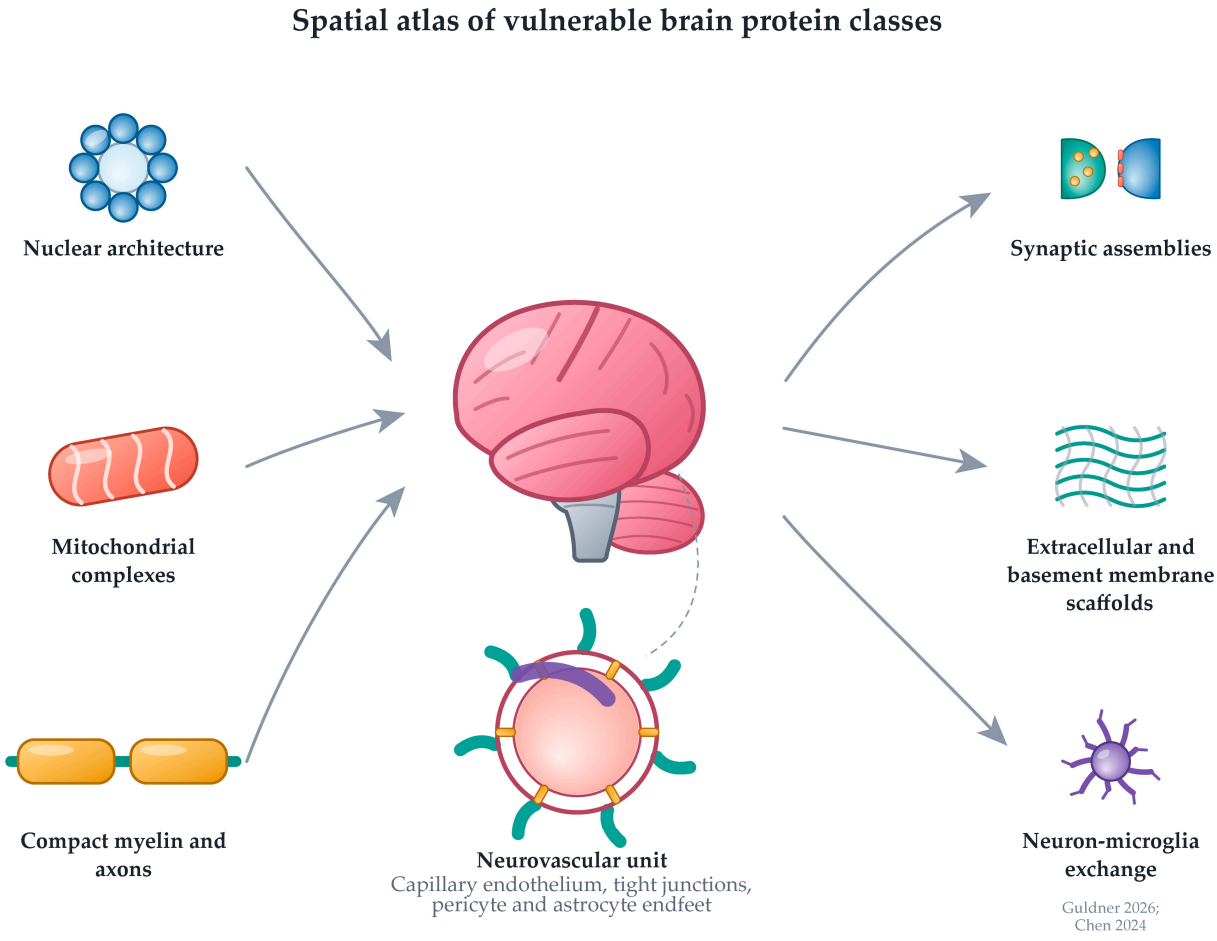


Figure 6. Spatial atlas of vulnerable brain protein classes. The central brain and neurovascular unit connect molecular-age hypotheses to nuclear architecture, mitochondrial complexes, compact myelin and axons, synaptic assemblies, extracellular and basement-membrane scaffolds, and neuron-microglia exchange [9,47]. These are target classes, not a declaration that every illustrated protein is exceptionally long-lived or pathogenic. Spatial localization is required because turnover, chemical exposure, repair, and therapeutic access differ among compartments and cell types [3,5,8].

6.2. Mitochondrial Assemblies

Respiratory-chain complexes contain subunits with different renewal rates despite physical proximity, and long-lived components have been identified within the electron transport

chain itself [4]. Persistent core components may stabilize an energetically expensive assembly, while damage to a slowly exchanging subunit could compromise electron transfer or increase reactive species; methionine sulfoxide accumulates preferentially in mitochondrial pathways of aged and Alzheimer hippocampus [70]. Whole-mitochondrion turnover does not guarantee homogeneous replacement of every complex. Conversely, altered mitochondrial dynamics and quality control can change the apparent persistence and selection of organelles [55], and alpha-synuclein interferes with those quality-control steps in Parkinson disease models [121]. Mitochondrial proteases add a further layer, since phosphorylation of a substrate can determine whether ClpXP degrades it [122]. A useful target case must connect subunit lifetime to a defined molecular lesion, assembly state, bioenergetic phenotype, and rescue, and mitochondrial targeting changes therapeutic design as well. A compound must cross the blood–brain barrier, enter the appropriate cell, cross mitochondrial membranes, and reach the relevant assembly without perturbing healthy complexes. Covalent recognition may be attractive for a unique electrophilic state but creates selectivity and safety demands. Degradation of an essential respiratory subunit may be unacceptable. Repair, stabilization, or allele and state-selective replacement could be more rational, although each requires a target-engagement assay at the subunit or proteoform level.

6.3. Myelin, Axons, and Extracellular Scaffolds

Myelin combines extreme structural persistence, high lipid content, long cellular geometry, and dependence on oligodendrocytes. A protein embedded in compact myelin experiences a chemical environment unlike a soluble neuronal enzyme. Extraction can alter recovery, and tissue-level turnover can mix internodes formed at different times. Microglial lipid handling participates directly in this economy, since loss of CLN3 in microglia impaired lipid metabolism and myelin turnover [67]. Aging white matter also acquires an immune component, with microglial CXCL10 recruiting CD8+ T cells during age-related white matter degeneration [123]. Candidate states should be localized to defined myelin compartments and related to conduction, membrane organization, or glial support. Reducing synthesis in an adult may not remove an old myelin population, while indiscriminate clearance may worsen axonal vulnerability. Axonal cytoskeletal systems and extracellular matrices present similar replacement problems. Long transport distances, local proteostasis [93], matrix crosslinking, and neurovascular interfaces create spatially heterogeneous molecular age. Microglia remodel the extracellular matrix as part of normal synaptic plasticity, so the matrix is not an inert scaffold that can be degraded without consequence [124]. Pericyte-derived fibrotic scarring is conserved across diverse central nervous system lesions, which makes scar composition a recurring rather than a disease-specific target class [125]. Extracellular targets may be more accessible to antibodies or enzymes, but diffusion through brain tissue and matrix binding can limit exposure. Crosslinks can be structural, pathological, or both [31,82]. The desired intervention may be controlled remodeling rather than maximal removal. Human regional evidence is especially important because vascular history and matrix composition differ across species and disease states, and plasma proteomic signatures of organ aging show how unevenly those compartments age within one individual [48].

6.4. Synaptic Assemblies and Intercellular Disposal

Synapses contain proteins with lifetimes that differ by molecule, fraction, and synapse type, with PSD95 lifetime spanning hours to months across the mouse brain [5]. Local translation and degradation coexist with long-lived scaffolds and receptors [53,93], and cholinergic and other synapse classes impose their own turnover constraints [126]. Aging shifts this distribution and increases insoluble or slow-degrading states [7]. Neuron-restricted labeling indicates that persistent neuronal proteins accumulate in microglia, raising hy-

potheses about transfer, phagocytosis, failed degradation, and protective disposal [9]. The presence of neuronal material in microglia does not by itself identify the route or establish toxicity, and the phagocytic system has a long-recognized capacity to redistribute material between compartments [127], so time-resolved tracing and cell-specific perturbation are required. Optineurin deficiency, which disrupts phosphorylated tau proteostasis and clusterin expression in human neurons, illustrates how a single adaptor can shift the balance between local degradation and accumulation [128]. Figure 7 compares nuclear pores, respiratory complexes, myelin and axonal proteins, and synaptic assemblies with a preserved functional pool and an altered subpopulation shown in each panel. This paired representation is central to therapeutic selectivity, because a total-protein assay collapses those pools while a state-specific assay can ask whether an intervention engages the altered population and spares necessary function. Canonical proteinopathy molecules such as tau, alpha-synuclein, amyloid beta, and TDP-43 appear in this Review mainly to illustrate proteoform and conformational-state principles, since their disease literature is already extensive and their strain and polymorph behavior is well characterized [129–132]. What unites these four classes is that the functional pool and the altered pool are the same gene product in the same compartment, so selectivity has to be demonstrated at the level of the state and cannot be inferred from the molecule. Table 6 summarizes the evidence currently available for each difficult class and the safety boundary that limits intervention.

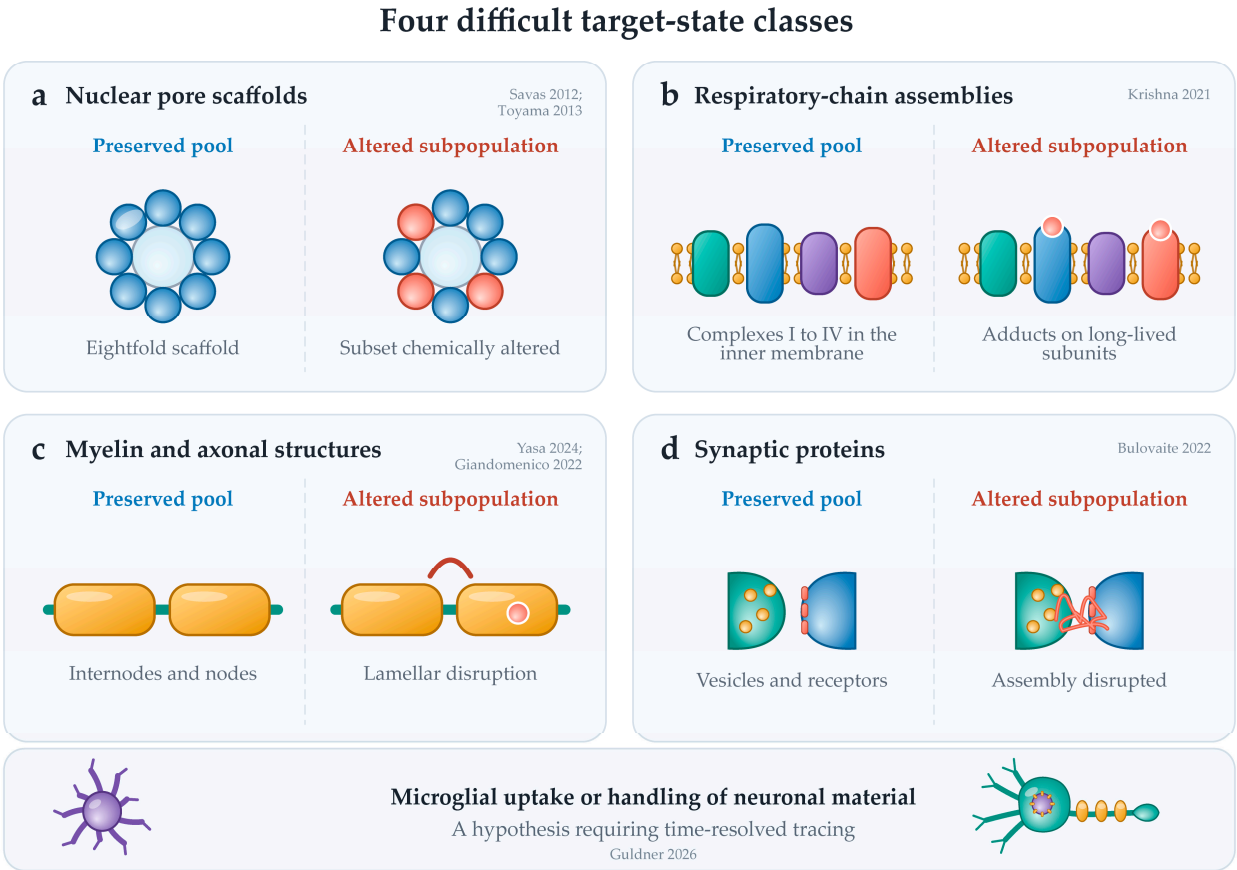


Figure 7. Four difficult target-state classes. Nuclear pore scaffolds [1,2], respiratory-chain assemblies [4], myelin and axonal structures [67,93], and synaptic proteins [5] are shown with a preserved functional pool and an altered subpopulation. This paired representation prevents total-protein depletion from being mistaken for state selectivity. The microglial vignette represents uptake or handling of neuronal material as a hypothesis that requires time-resolved tracing [9]. The panels standardize the questions of lifetime, molecular identity, function, modality, and risk.

Table 6. Difficult target classes in the aging brain. Each class is linked to the persistence or damage evidence reported for it, the target resolution a therapeutic program would need, and the function that constrains intervention.

Target Class	Reported Persistence or Damage Evidence	Required Target Resolution	Rational Modalities	Critical Safety Risk	Reference
Nuclear pore and nuclear architecture	Nucleoporins and histones identified as exceptionally long-lived in adult rat brain [1]; stable subcomplexes shown to exchange slowly [2], with maintenance and surveillance mechanisms defined in postmitotic cells [24,115]; karyopherins actively remodel the transport barrier [116]; pore dysfunction drives TDP-43 pathology in ALS [133] and aberrant pore degradation contributes to VCP disease [134]; transport failure recurs across neurodegenerative contexts [118–120]	Damaged subunit or altered permeability state within a defined neuron type	Repair, stabilization, selective replacement	Disrupted nucleocytoplasmic transport	[1,2,24,115,116, 118–120,133,134]
Mitochondrial respiratory complexes	Long-lived electron transport chain subunits identified in mouse mitochondria [4]; methionine sulfoxide enriched in mitochondrial pathways of aged and Alzheimer hippocampus [70]; mitochondrial dynamics and quality control alter apparent organelle persistence [55]; alpha-synuclein disrupts mitochondrial quality control [121]; substrate phosphorylation gates ClpXP-mediated degradation [122]	Modified subunit within an assembled complex	Stabilization, repair, selective covalent recognition	Bioenergetic failure	[4,55,70,121,122]

Table 6. *Cont.*

Target Class	Reported Persistence or Damage Evidence	Required Target Resolution	Rational Modalities	Critical Safety Risk	Reference
Myelin and axonal scaffolds	Microglial CLN3 loss impaired lipid metabolism and myelin turnover [67]; defective cholesterol clearance in aged phagocytes limited remyelination [135]; aged white matter degeneration involves microglial CXCL10-mediated CD8+ T cell recruitment [123]	Internode or axonal state with defined lineage and location	Remodeling, replacement, glial support	Demyelination or axonal transport failure	[67,123,135]
Synaptic assemblies	PSD95 lifetime ranged from hours to months across mouse synapses [5]; aged mouse neurons showed an aggregome of 1726 proteins with material detectable in microglia [9]; aging shifted insoluble-proteome behavior and proteolytic subunit turnover [7]; local translation and degradation coexist with long-lived scaffolds [53,93]; optineurin loss disrupted phosphorylated tau proteostasis in human neurons [128]	Synapse-type and assembly state, with soluble and insoluble fractions separated	Chaperone support, selective removal, state-selective binder	Loss of essential plasticity	[5,7,9,53,93,128]
Extracellular and vascular matrix	Fibronectin aggregates inhibited remyelination in multiple sclerosis lesions [136]; fibulin-2 identified as an extracellular oligodendrocyte inhibitor [137]; pericyte-derived fibrotic scarring conserved across central nervous system lesions [125]; microglia remodel matrix during normal synaptic plasticity [124]	Site or crosslink resolved in spatial context	Enzyme, antibody, controlled remodeling	Barrier and vessel instability	[124,125,136,137]

Table 6. *Cont.*

Target Class	Reported Persistence or Damage Evidence	Required Target Resolution	Rational Modalities	Critical Safety Risk	Reference
Proteinopathy proteoforms	Tau filament folds resolved from Alzheimer brain [110], with strain differences shaping disease phenotype [130]; alpha-synuclein strains discriminated between Parkinson disease and multiple system atrophy [138] and fibril polymorphism characterized structurally [131]; truncated resistant amyloid-beta proteoforms identified in human astrocytes [83]; TDP-43 and prion-like self-templating described mechanistically [129,132]; aggregation behavior of the tau isoform mixture characterized [139]	Intact proteoform and conformer	Antibody, degrader, stabilizer, synthesis modulation	Redistribution toward a more toxic state	[83,110,129–132,138,139]

7. Molecularly Aged Target States Across Neurodegenerative Diseases

The molecular-age framework becomes therapeutically useful only when it changes a decision that would otherwise be made at gene or total-protein resolution. The relevant unit may be a chemically defined proteoform, a conformational strain, a depleted functional pool, a damaged assembly, or a persistent extracellular structure, and these units are not interchangeable across diseases. Alzheimer disease and Parkinson disease provide prominent examples of conformationally heterogeneous protein assemblies, whereas amyotrophic lateral sclerosis and frontotemporal dementia expose the dual problem of cytoplasmic TDP-43 accumulation and nuclear loss of function. In Huntington disease the molecular state is defined by a measurable repeat length and a specific proteolytic event rather than by an inferred conformation. Multiple sclerosis belongs to a different class again, with molecular persistence located in myelin, debris, and lesion extracellular matrix, and not in a misfolded intracellular assembly. For each disease, target promotion requires five linked judgments: whether the state is molecularly defined, whether its relationship to age or disease stage is measured, whether perturbation supports a causal role, which modality can spare the required functional pool, and whether exposure and engagement can be demonstrated in the relevant brain compartment.

7.1. Alzheimer Disease

7.1.1. Tau Target States

Tau is not one target state, since adult human brain contains six principal tau isoforms before truncation and post-translational modification are considered, and the aggregation behavior of the resulting mixture has been studied for decades [139]. Intact-protein and human-tissue studies now resolve soluble, truncated, and disease-associated tau proteoforms [19,44], molecular profiling distinguishes pathological tau among the tauopathy dementias [43], and cryogenic electron microscopy has shown that filaments extracted from Alzheimer disease brain adopt a reproducible paired-helical and straight-filament fold [110]. Structural differences among strains propagate into distinct disease phenotypes [130]. Phosphorylation can alter phase behavior [140], acetylation acts in the opposite direction on the same process [141], GSK3-beta phosphorylation catalyzes assembly into Alzheimer-like filaments in vitro [142], and phosphorylation at a single residue blocks recognition by the E3 ligase carboxyl terminus of Hsc70-interacting protein (CHIP) [143]. Phosphorylated tau is accordingly a heterogeneous analytical category rather than one species [144]. A modification detected in diseased tissue does not become pathogenic merely because it is enriched there. The strongest target definition is therefore a bounded state such as a disease-associated filament surface, a seeding-competent soluble assembly, or a specified truncation and modification combination. Total tau depletion has a different risk profile, because soluble tau contributes to microtubule organization and other neuronal functions, and CRISPR screens in induced neurons show how many separate pathways set its steady-state level [60].

7.1.2. Amyloid-Beta Target States

Amyloid-beta is similarly heterogeneous, in that peptide length, N-terminal truncation, pyroglutamate formation, isoaspartate, oxidation, aggregation state, and cellular or extracellular location can change clearance and antibody recognition. Pyroglutamate- and isoaspartate-modified amyloid-beta species have been detected in aging and Alzheimer tissue [145], and truncated, highly resistant amyloid-beta proteoforms have been identified within human astrocytes [83]. Brain-derived amyloid-beta preparations show structural polymorphism with differing cytotoxicity [146]. Glycation modifies amyloid aggregation directly [80], and several amyloid-degrading enzymes are themselves regulated by age and oxidative state [77]. These observations support the existence of distinct molecular states, but residence time is not measured directly for most human amyloid-beta proteoforms. Chronological age, plaque maturity, and molecular age should not be treated as equivalent variables. A defensible study must establish the specific species present, its regional and cellular distribution, and whether its occupancy changes before or after clinically relevant pathology. Fluid measurements such as the plasma amyloid-beta 42/40 and phospho-tau217 ratios improve classification of amyloid status [147], but they report a population average rather than the occupancy of a defined proteoform in tissue. Causality and clinical evidence differ among these states. In tauopathy mice, synapse loss and microglial activation can precede mature tangles, which cautions against using tangle burden as the only causal or pharmacodynamic unit [113]. For extracellular amyloid-beta, randomized trials of lecanemab and donanemab provide human evidence that antibody-mediated amyloid removal can slow decline in selected patients with early symptomatic disease, while also establishing clinically consequential amyloid-related imaging abnormalities and infusion-related risks [148,149]. These trials support amyloid as a clinically modifiable disease process in defined populations. They do not show that every amyloid-beta proteoform is harmful, that plaque removal is the sole mechanism, or that a molecular-age intervention will reproduce the effect. Modality follows from the state. Extracellular aggregates or exposed filament

surfaces may be addressed by state-selective antibodies, provided that binding is compared across monomeric, oligomeric, fibrillar, truncated, and modified preparations and that the detection reagents themselves have been validated for proteoform discrimination [41]. Intracellular tau states may require brain-penetrant small molecules, intrabodies, synthesis control, or degradation. A tau-directed proteolysis-targeting chimera (PROTAC) promoted tau clearance and improved outcomes in Alzheimer-like models [150], and gene-delivered APOE2-Christchurch reduced both amyloid and tau pathology in Alzheimer mice [151], but both remain preclinical and neither establishes human brain engagement. Repair is plausible only for a defined reversible lesion with an accessible site and a controlled product. Replacement is rational only if young tau or another functional component can enter the relevant assembly. Critical experiments should measure matched-state affinity, unbound brain exposure, regional occupancy, state depletion or repair, preservation of soluble functional tau, and a proximal neuronal response before behavioral interpretation.

7.1.3. Aggregate-Directed Antibodies as the Existing Clinical Test of the Framework

Two approved therapeutics were selected on molecular state rather than on gene identity. Donanemab is directed at N-terminally truncated, pyroglutamate-modified amyloid-beta beginning at residue 3, a species generated by post-translational chemistry and found in deposited plaque rather than in the circulating peptide pool [152]; the modification is one of the spontaneous age-generated chemistries described above and has been detected in aging and Alzheimer tissue [145]. Lecanemab is directed at soluble protofibrils, which is an assembly state rather than a chemically defined proteoform [153]. In both, the therapeutic unit is a defined state of a gene product, and both reached a clinical endpoint in randomized trials [148,149]. Against the evidence ladder, these programs clear detection, replicated age association, spatial localization, and clinical evidence, and they provide the only human demonstration that modifying a defined amyloid-beta state changes a clinical trajectory. Three limits apply to these programs, and each bears on target selection. First, proximal target engagement was demonstrated at the target resolution of aggregate burden by amyloid positron emission tomography, not at the target resolution of the state that defined the antibody: no trial reports occupancy of pyroglutamate-modified amyloid-beta beginning at residue 3, or of the protofibril population, in treated human brain. The state-resolved pharmacodynamic measurement that a matched-state assay would supply is therefore absent even in this case. Second, clearance of the selected state slowed decline without establishing that the selected state was the causal one, since removing a species that is in equilibrium with others also changes the others; the trials support amyloid-beta as a modifiable disease process in defined populations rather than validating one proteoform as the causal unit [148,149]. Third, the effect sizes were modest and were obtained at the cost of amyloid-related imaging abnormalities (ARIA) and infusion reactions, which places the therapeutic window between engagement of the target state and disturbance of the vascular and functional pools surrounding it. Aducanumab is an instructive counter-case: an antibody selected on aggregate recognition, with two pivotal trials that did not agree, approved on a biomarker endpoint and subsequently withdrawn from marketing [154]. The discordance was not resolved by the biomarker, because a reduction in plaque signal is compatible with several molecular outcomes. State selection is necessary but not sufficient for this class of program, and the three antibodies differ in the precision with which the engaged state was specified and measured.

7.2. Parkinson Disease

Alpha-synuclein creates a sharp state-selectivity problem because the same protein participates in synaptic vesicle biology and can form heterogeneous pathological assemblies. Burre et al. showed a physiological role in SNARE-complex assembly [155]. Human and amplified brain-derived aggregates display conformational differences across Parkinson disease, multiple system atrophy, and experimental preparations [138,156], fibrillar polymorphs derived from distinct synucleinopathies differ in structure and biological activity [111,131], and top- and middle-down mass spectrometry has begun to resolve alpha-synuclein glycoforms [98]. Divalent and trivalent metal ions modulate aggregation in a charge-dependent manner [157], glycation is antagonized rather than reversed by DJ-1 [81], and oligomeric intermediates have their own proposed toxicity profile [158]. These findings justify a proteoform and conformer-aware target model, though not the treatment of all soluble alpha-synuclein as disposable. Age relationship and causality must be assigned separately. Parkinson disease incidence increases with age, but that epidemiological relationship does not provide a molecular clock for an individual alpha-synuclein assembly. Persistence, seed amplification, and biochemical resistance are measurable state properties, whereas chronological age is a host variable. Microglial alpha-synuclein overexpression caused phagocytic exhaustion, oxidative stress, and dopaminergic neurodegeneration in mice, supporting a causal effect of excess alpha-synuclein within that experimental context [112]. Chaperone-mediated autophagy handles alpha-synuclein directly and fails progressively with age [159,160], loss of that pathway collapses the neuronal metastable proteome [54], and alpha-synuclein in turn disrupts mitochondrial quality control [121]. Morrone Parfitt et al. showed that impaired lysosomal proteolysis in astrocytes worsened midbrain-organoid proteostasis in an early-onset Parkinson model [114]. Long-lived electron-transport-chain subunits add a parallel mitochondrial target class, but their persistence can support assembly integrity rather than indicate damage [4]. The rational intervention may therefore be selective removal of an aggregation-competent pool, restoration of lysosomal flux, stabilization of a functional synaptic state, or repair of a specified chemical lesion. Autophagy-targeting chimera (AUTOTAC)-mediated degradation of alpha-synuclein aggregates has shown activity in Parkinson disease models [161], and the underlying autophagy-targeting chimera mechanism has been described separately [162], but broad autophagy activation and selective aggregate recognition are not the same mechanism. Adeno-associated virus (AAV)-mediated expression of an alpha-synuclein-targeting intrabody improved motor outcomes in aged rats, providing in vivo proof of concept for intracellular recognition without establishing human safety, distribution, or reversibility [163]. Engineered exosome systems have delivered therapeutic cargo in Parkinson models [164,165], and mitochondria-targeted nanosystems have reached neuronal mitochondria in Alzheimer models [166], but these are platform demonstrations rather than evidence that a particular molecularly aged state was engaged. The decisive Parkinson experiments are state-resolved target engagement in dopaminergic neurons, measurement of the soluble functional pool, lysosomal and mitochondrial pharmacodynamics, and testing across patient-derived aggregate conformers instead of one recombinant fibril.

7.3. Amyotrophic Lateral Sclerosis and Frontotemporal Dementia

TDP-43 pathology combines at least two target states that require opposite therapeutic logic. Cytoplasmic, phosphorylated, truncated, or aggregated TDP-43 may support toxic gain-of-function mechanisms, and its self-templating behavior has been described in prion-like terms [129,167]. Depletion of nuclear TDP-43 disrupts RNA processing through a separate route. Human-cell and tissue studies connect TDP-43 loss of function to cryptic splice and polyadenylation events in stathmin-2 (STMN2) and unc-13 homolog A

(UNC13A) [168–170]. Sporadic ALS induced pluripotent stem cell-derived neurons also reproduce features of TDP-43 loss of function [171]. The functional pool at risk is therefore nuclear, RNA-bound TDP-43. A nonselective degrader could reduce cytoplasmic material while worsening nuclear splicing defects, and the proteostatic systems that normally counteract TDP-43 aggregates already operate at partial capacity in disease tissue [172]. Nuclear transport and pore quality control provide a linked assembly-level target. Nuclear pore dysfunction has been connected experimentally to TDP-43 pathology in ALS [133], aberrant pore degradation contributes to neurodegeneration in valosin-containing protein (VCP) disease [134], and nucleocytoplasmic transport failure recurs across several neurodegenerative contexts [118–120]. Microglial states can further modify the phenotype, as neurotoxic microglia promoted TDP-43 proteinopathy in a progranulin-deficiency model [173]. Stress granule biology adds another layer, since TIA1-mediated granules sequester HSP70 messenger RNA and promote neurodegeneration in C9orf72 mice [174]. These studies establish causal relationships within defined genetic or experimental systems. They do not show that an old nucleoporin, a TDP-43 aggregate, and a cryptic RNA event form one universal sequence in sporadic human disease. Molecular age is particularly uncertain here because postmortem abundance and insolubility rarely measure the residence time of the pathologic pool. Therapeutic design should separate removal, restoration, and downstream rescue. Conformation-selective binders or degraders would need to recognize cytoplasmic pathological TDP-43 while sparing nuclear RNA-bound protein. Nuclear import restoration may be useful only when transport failure is upstream and reversible. STMN2 splice correction provides a downstream strategy that does not require removal of TDP-43 aggregates, and mechanistic work has shown correction of TDP-43-dependent STMN2 misprocessing in experimental models [168]. UNC13A cryptic exon inclusion identifies another TDP-43-dependent consequence and a genetically stratified vulnerability [169]. These approaches remain distinct from demonstrating clinical benefit. Critical experiments should quantify nuclear and cytoplasmic TDP-43 states, cryptic exon correction, axonal function, motor-neuron exposure, and off-target RNA processing in the same model. Delivery must reach widely distributed cortical and spinal motor neurons, which raises a different anatomical requirement from focal intracerebral proof of concept.

7.4. Huntington Disease

In Huntington disease the variable that defines the state is measurable rather than inferred. An expanded CAG repeat in the first exon of HTT lengthens a polyglutamine tract in huntingtin, and repeat length is inversely related to age at onset [175]. The relevant therapeutic unit is nonetheless not the gene product. Mutant huntingtin is cleaved by caspases and calpains to N-terminal fragments that aggregate more readily, enter the nucleus, and are more toxic than the full-length protein, so proteolysis generates the pathogenic species rather than merely disposing of it [176]. A separate route produces an exon-1 fragment through incomplete splicing and aberrant polyadenylation, and that fragment is highly aggregation-prone in model systems [177]. Post-translational chemistry then modifies the behaviour of these states. Acetylation routes mutant huntingtin to autophagic degradation [178], while phosphorylation within the N-terminal region alters toxicity and also controls the cleavage events that generate the fragments [179]. Somatic expansion of the repeat during life in striatal neurons adds a molecular clock that is internal to the target and independent of chronological age [180]. The functional pool is well defined in this disease. Wild-type huntingtin is required for development and contributes to vesicular transport, autophagy, and neuronal maintenance, so lowering the total protein is not equivalent to removing the pathogenic state [181]. Non-allele-selective lowering of huntingtin by an intrathecally delivered antisense oligonucleotide did not benefit patients, and the

highest-exposure arm fared worse than placebo [182]. Because the same oligonucleotide had already been shown to lower huntingtin in cerebrospinal fluid in a dose-dependent manner [183], the intervention engaged its nominal target and still failed on state-selectivity and exposure grounds. Rational modalities therefore separate the state from the pool: allele-selective oligonucleotides directed at variants carried on the expanded allele, interference with the specific proteolytic events that generate the toxic fragments, correction of the aberrant splicing that produces the exon-1 species, and fragment-selective degradation or recognition rather than total protein lowering [184]. Delivery constraints are comparatively well characterized, since intrathecal administration reaches cortex and striatum to a measurable extent in this indication, while adeno-associated virus (AAV) approaches must cover deep grey matter. The decisive experiment is fragment-resolved rather than protein-resolved: depletion or prevention of the N-terminal and exon-1 species measured directly, with wild-type huntingtin and its transport and autophagy functions preserved in the same preparation, and with repeat-length instability monitored rather than assumed constant.

7.5. Multiple Sclerosis

Multiple sclerosis is primarily an inflammatory demyelinating disease, and its molecularly aged states differ in character from the misfolded intracellular assemblies of the other diseases considered here. The persistent structures involved, compact myelin and lesion extracellular matrix, are among the longest-lived material in the central nervous system, and they are extracellular or membrane-embedded rather than intracellular aggregates [135]. The limiting factor also differs, being the age of the clearance and repair machinery rather than the age of the target molecule. Multiple sclerosis therefore extends the framework beyond intracellular proteinopathy, and Table 7 classes it separately from the proteinopathies. Myelin is a spatially extended, lipid-rich structure whose proteins and membranes turn over unevenly. Persistent myelin components may retain function for long periods, while demyelination creates debris that inhibits repair if inflammatory clearance fails. The target state may therefore be an aged intact internode, oxidized or fragmented myelin, lipid-laden phagocytes, an aggregated extracellular-matrix component, or a remyelination-inhibitory lesion environment. These states require different interventions and should not be collapsed into total myelin protein abundance [185]. Aging directly changes repair capacity in experimental demyelination. Defective cholesterol clearance in aged phagocytes limited remyelination, linking the age of the host clearance system to persistence of myelin-derived material [135]. Activation of triggering receptor expressed on myeloid cells 2 (TREM2) promoted myelin-debris clearance and remyelination in a multiple sclerosis model, which supports a causal clearance mechanism in that setting [186]. Loss of CLN3 in microglia also impaired lipid metabolism and myelin turnover [67], and microglia-driven CXCL10 recruits CD8+ T cells during age-related white matter degeneration [123]. Such results favor interventions that restore handling of debris or lipid rather than simply increasing oligodendrocyte differentiation [187]. They also expose a safety boundary, because microglia support surveillance, synaptic remodeling, and matrix regulation [124]. Lesion extracellular matrix provides a second persistent target class. Fibronectin aggregates in multiple sclerosis lesions inhibited oligodendrocyte differentiation and remyelination [136], and fibulin-2 was identified as an extracellular inhibitor relevant to oligodendrocyte maturation [137]. Pericyte-derived fibrotic scarring is conserved across several central nervous system lesions, but conservation of a scar response does not establish that one matrix component is causal in every multiple sclerosis stage [125]. Matrix-directed enzymes, antibodies, or controlled remodeling agents therefore require spatial restriction and mechanical safety measurements. Degrading an inhibitory aggregate could facilitate repair, but broad matrix digestion could weaken vessels, basement membranes, or axonal support. Therapeutic success in multiple

sclerosis should be defined by more than immune modulation or increased myelin staining. A state-directed program should demonstrate clearance or remodeling of the specified debris or matrix pool, renewed oligodendrocyte maturation, formation of structurally competent myelin, and recovery of conduction while preserving vascular and extracellular architecture. Delivery may favor extracellular antibodies or enzymes for exposed lesion targets, small molecules for phagocyte lipid handling, and cell-targeted nucleic acids for microglial or oligodendroglial programs. Disease activity, lesion age, regional barrier permeability, and remyelination competence must be measured, because an intervention suited to an active inflammatory lesion may not act on a chronic fibrotic plaque [185,187]. Table 7 assembles these disease-specific judgments into a decision matrix rather than a ranking. Table 8 scores the same candidate states against each rung of the evidence ladder. Evidence level is assigned to the particular molecular-state claim, not to the importance of the named protein or disease. A candidate advances only when its molecular definition, functional comparator, modality, delivery route, and proximal validation experiment can be specified together. Read across the five diseases, the pattern is consistent: the molecular definition is usually the strongest element and the proximal engagement assay the weakest, so the rung that limits promotion is the same one in almost every case.

Table 7. Disease-to-target decision matrix for molecularly aged protein states. Candidate states are linked to the strongest evidence discussed in this Review, the functional pool that must be preserved, a rational modality, the principal delivery barrier, and a decisive next experiment.

Disease	Candidate Molecular State	Strongest Current Evidence	Functional Pool at Risk	Rational Modality	Delivery Barrier	Critical Validation Experiment	Reference
Alzheimer disease	Disease-associated tau filament surface or defined soluble seeding state	Cryo-EM filament folds resolved from Alzheimer brain [110]; intact tau proteoforms resolved from human cortex [19,44]; molecular features separating tauopathy dementias [43]; synapse loss preceding tangles in P301S mice [113]; preclinical tau PROTAC clearance [150]	Soluble neuronal tau	State-selective antibody, intrabody, small molecule, or selective degradation	Extracellular versus intracellular access and regional brain exposure	Matched-state engagement with preservation of soluble tau and proximal neuronal function	[19,43,44,110,113,150]
Alzheimer disease	Truncated, pyroglutamate, isoaspartate, or aggregated amyloid-beta state	Pyroglutamate and isoaspartate amyloid-beta detected in aging and Alzheimer tissue [145]; truncated resistant proteoforms in human astrocytes [83]; structural polymorphism of brain-derived extracts [146]; randomized trials of aggregate-directed antibodies [148,149]; plasma ratios improve amyloid classification [147]	Soluble amyloid precursor processing products and vascular integrity	State-selective antibody or chemistry-specific binder	Barrier transport, vascular amyloid, and target-mediated disposition	Proteoform-resolved brain occupancy linked to amyloid removal, safety, and cognition	[83,145–149]

Table 7. *Cont.*

Disease	Candidate Molecular State	Strongest Current Evidence	Functional Pool at Risk	Rational Modality	Delivery Barrier	Critical Validation Experiment	Reference
Parkinson disease	Patient-derived aggregation-competent alpha-synuclein conformer	Strain discrimination between Parkinson disease and multiple system atrophy [138]; seed amplification preserving brain-derived aggregate properties [156]; fibrillar polymorphs with distinct structure-function relationships [111]; physiological SNARE-complex role established [155]; preclinical AUTOTAC degradation [161] and AAV intrabody efficacy [163]	Soluble presynaptic alpha-synuclein required for SNARE-complex assembly	Aggregate-selective degrader, intrabody, or stabilizer	Dopaminergic-neuron exposure and intracellular expression	Engagement across patient-derived conformers with SNARE function preserved	[111,138,155,156,161,163]
Parkinson disease	Lysosomal or mitochondrial proteostasis state supporting alpha-synuclein accumulation	Astrocytic lysosomal proteolysis failure in midbrain organoids [114]; chaperone-mediated autophagy loss collapses the metastable proteome [54] and handles alpha-synuclein directly [159]; alpha-synuclein disrupts mitochondrial quality control [121]; microglial overexpression caused phagocytic exhaustion and dopaminergic loss [112]; long-lived respiratory subunits identified [4]	Basal autophagy and respiratory assemblies	Lysosomal restoration, assembly stabilization, repair, or organelle-targeted delivery	Cell-type and organelle access	Compartment-resolved pharmacodynamics with respiration, flux, and alpha-synuclein states measured together	[4,54,112,114,121,159]
ALS and frontotemporal dementia	Cytoplasmic pathological TDP-43 with nuclear depletion	Cryptic splice-polyadenylation of STMN2 on TDP-43 loss and its correction [168,170]; UNC13A mis-splicing driven by TDP-43 loss and risk variants [169]; loss-of-function hallmarks in sporadic ALS iPSC neurons [171]; nuclear pore dysfunction linked to TDP-43 pathology [133]; microglia-driven proteinopathy in progranulin deficiency [173]	Nuclear RNA-bound TDP-43	State-selective removal plus nuclear restoration or downstream splice correction	Broad cortical and spinal motor-neuron distribution	Nuclear and cytoplasmic engagement with STMN2 and UNC13A correction and axonal rescue	[133,168–171,173]

Table 7. *Cont.*

Disease	Candidate Molecular State	Strongest Current Evidence	Functional Pool at Risk	Rational Modality	Delivery Barrier	Critical Validation Experiment	Reference
Huntington disease	N-terminal proteolytic and exon-1 huntingtin fragment states carried on the expanded allele	Repeat length sets age at onset [175]; caspase and calpain cleavage generates more aggregation-prone and more toxic N-terminal fragments [176]; an exon-1 fragment arises from incomplete splicing [177]; phosphorylation and acetylation alter clearance of these species [178,179]; somatic repeat expansion continues in striatal neurons [180]	Wild-type huntingtin and its vesicular transport and autophagy functions [181]	Allele-selective oligonucleotide, correction of aberrant exon-1 splicing, interference with the generating cleavage events, or fragment-selective degradation	Intrathecal distribution with sustained striatal and cortical coverage of deep grey matter	Fragment-resolved depletion with wild-type huntingtin transport and autophagy function preserved and repeat-length instability monitored	[175–184]
Multiple sclerosis	Persistent myelin debris and lipid-loaded phagocyte state	Defective cholesterol clearance limits remyelination in aged mice [135]; TREM2 activation promoted debris clearance and remyelination [186]; microglial CLN3 loss impaired myelin turnover [67]; microglia also remodel matrix during normal plasticity [124]	Homeostatic microglial clearance and intact myelin	Clearance or lipid-handling restoration	Lesion-stage and phagocyte specificity	Debris removal linked to mature remyelination and recovered conduction	[67,124,135,186]
Multiple sclerosis	Aggregated fibronectin or inhibitory lesion matrix	Fibronectin aggregates impaired remyelination in human lesions and models [136]; fibulin-2 identified as an oligodendrocyte inhibitor [137]; pericyte-derived fibrotic scarring conserved across lesions [125]	Vascular, basement-membrane, and axonal matrix	State-selective antibody, enzyme, or controlled remodeling	Extracellular distribution and mechanical safety	Spatial target depletion with remyelination, vessel integrity, and tissue mechanics measured	[125,136,137]

Table 8. The candidate states of Table 7 scored against every rung of the evidence ladder of Section 2.4. Columns abbreviate the rungs as detection (Det.), replicated age association (Age), spatial localization (Loc.), functional association (Func.), causal perturbation (Cause), proximal target engagement (Eng.), and clinical evidence (Clin.). A plus sign indicates that the rung is supported by the evidence cited in Table 7 for that state; a plus-minus sign indicates evidence that is preclinical only, indirect, or obtained at a coarser molecular resolution than the state definition; a dash indicates that no such evidence was identified. Entries score the published claim for the specified molecular state rather than the importance of the protein or the disease, and the final column names the rung that currently limits promotion.

Candidate Target State	Det.	Age	Loc.	Func.	Cause	Eng.	Clin.	Rung That Limits Promotion
Tau disease-associated filament surface or soluble seeding state	+	±	+	±	±	–	–	Proximal engagement at the target resolution of the state

Table 8. *Cont.*

Candidate Target State	Det.	Age	Loc.	Func.	Cause	Eng.	Clin.	Rung That Limits Promotion
Truncated, pyroglutamate, isoaspartate, or aggregated amyloid-beta state	+	+	+	±	±	±	+	Causal attribution to one state, and proteoform-resolved engagement
Patient-derived aggregation-competent alpha-synuclein conformer	+	−	+	±	±	−	−	Measured age association, then human engagement
Lysosomal or mitochondrial proteostasis state supporting alpha-synuclein accumulation	±	±	+	+	±	−	−	Compositional definition of the state itself
Cytoplasmic pathological TDP-43 with nuclear depletion	+	−	+	+	+	±	−	Clinical evidence; splice correction is available as a proximal marker
Huntingtin N-terminal and exon-1 fragment states	+	±	+	+	+	±	±	Fragment-selective engagement, non-selective lowering having failed
Persistent myelin debris and lipid-loaded phagocyte state	+	+	+	+	+	−	−	Target engagement in human tissue
Aggregated fibronectin or inhibitory lesion matrix	+	−	+	+	±	−	−	Measured age association, then spatially restricted engagement

8. Therapeutic Strategies for Time-Dependent Target States

A time-dependent target changes the question from whether a protein can be inhibited to which molecular pool should be repaired, stabilized, removed, replaced, or bound. State-selective small molecules require a difference in pocket, dynamics, interface, or reactivity that is large enough to measure. Reversible covalent ligands can exploit a chemically altered environment, but kinetic selectivity and proteome-wide reactivity must be demonstrated, and large-scale chemoproteomic profiling now makes that measurable instead of assumed [188]. Molecular glues and bifunctional degraders can recruit an altered state to cellular machinery, yet brain exposure, ternary-complex cooperativity, ligase expression, and loss of the functional pool remain the principal constraints [189,190]. Rational optimization of degrader geometry and linker chemistry has been demonstrated for tractable enzyme targets [191] and for a SIRT6 degrader in hepatocellular carcinoma [192], natural-product scaffolds have been recruited into the same chemistry [193], and nanoparticle-mediated delivery of degraders has been proposed to address their exposure problem [194]. Targeted degradation is not automatically appropriate for an old protein. A stable structural component may be difficult to extract from an assembly, and degradation can create a vacancy that cannot be refilled. Ubiquitin chain architecture itself determines outcome, since K63-linked chains signal differently from degradative chains [195], and proteasome activators such as PA200 couple degradation to senescence programs [196]. Autophagic and lysosomal strategies can address aggregates or organelles but often have broad effects [160,162]. Chaperone modulation can stabilize a functional state or redirect a metastable population [197,198], although global chaperone activation changes many clients, and the decision between repair and destruction is itself made by ligase and chaperone complexes acting together [199]. SUMOylation adds a further regulatory layer linking aging to au-

tophagic capacity [200]. Enzymatic repair is mechanistically attractive when the chemistry is known and reversible [34], but delivery, substrate breadth, compartment access, cofactor demand, and product fate must be measured. Antibodies and intrabodies can recognize state-specific epitopes, with different advantages for extracellular and intracellular targets [41,163]. Failure of any of these systems can itself become pathogenic, as shown for WDR45, where disrupted endoplasmic reticulum homeostasis drives neuronal death [201].

Concrete development programs illustrate why modality and evidence level must be reported together, and Table 9 sets them side by side. Aggregate-preferring anti-amyloid antibodies have measured brain-pathology effects and randomized clinical outcomes in early Alzheimer disease [148,149], whereas tau PROTACs [150], alpha-synuclein AUTOTACs [161], and alpha-synuclein intrabodies [163] currently provide preclinical evidence only. Degrader chemistry developed against senescence and aging biology is at a comparable stage [202,203]. STMN2 splice correction addresses a downstream consequence of TDP-43 nuclear loss rather than removing TDP-43 itself [168]. Recognition of pyroglutamate, isoaspartate, truncation, oxidation, glycation, or another age-generated chemistry is a targeting hypothesis until the exact proteoform, matched-state affinity, and brain occupancy are measured. Stabilization is preferable to degradation when the functional assembly remains required and the altered state can be shifted without locking a toxic intermediate. Enzymatic repair requires direct measurement of the repaired product, and replacement requires evidence of molecular exchange. These categories should not be blended into a general statement that a platform is therapeutic. Synthesis modulation turns on timing. Lowering RNA can reduce future production but may take months to affect a persistent pool. Increasing expression can create young protein without repairing an old assembly. Replacement strategies require evidence that new molecules enter the relevant compartment and displace or dilute the aged state. Combination approaches may therefore be necessary, such as state-selective removal followed by replacement, or repair accompanied by restored quality control. Treatment duration should be derived from target turnover and pharmacodynamics rather than from a conventional short assay. Figure 8 sets eight modality classes beside a paired functional protein and altered state, and gives the capillary endothelium of the blood–brain barrier a panel of its own to indicate that selectivity is insufficient without delivery. Every program needs an assay that reports engagement of the specified proteoform or assembly in brain. Total abundance, downstream transcription, behavioral improvement, or plasma biomarker change cannot independently establish engagement. Preferred assays include state-selective mass spectrometry, occupancy measurements, conformer-specific immunoassays, complex-resolved measurements, or imaging probes whose specificity has been validated against molecular standards. Safety is inseparable from target definition, because a modification enriched with age may also occur during normal signaling or stress adaptation [32,33]. Removing microglial protein material may interfere with disposal [9,127]. Breaking extracellular crosslinks may alter vessel or matrix mechanics [31,82]. Stabilizing one conformer may trap another intermediate [158]. Dose–response, reversibility, spatial exposure, functional reserve, and recovery after withdrawal should therefore be built into target validation. The appropriate success criterion is controlled modulation of a harmful state with preserved essential function, not maximal depletion of the named protein [155].

Table 9. Reported therapeutic programs directed at defined protein states in neurodegenerative disease. Each program is listed with the state it addresses, the highest evidence level reached, and the engagement question that remains unanswered.

Agent or Strategy	Target State	System and Reported Outcome	Highest Evidence Level	Unresolved Engagement Question	Reference
Lecanemab	Aggregated extracellular amyloid-beta	Randomized trial in early Alzheimer disease; reduced amyloid burden and slowed decline, with amyloid-related imaging abnormalities and infusion reactions	Randomized clinical evidence	Which amyloid-beta proteoforms are removed, and whether removal is the sole mechanism	[148]
Donanemab	Aggregated extracellular amyloid-beta, pyroglutamate-modified epitope	Randomized trial in early symptomatic Alzheimer disease; reduced amyloid burden and slowed decline with comparable imaging risks	Randomized clinical evidence	Proteoform-resolved brain occupancy relative to plaque clearance	[149]
Small-molecule tau PROTAC	Intracellular tau	Alzheimer-like models; promoted tau clearance and improved cognitive outcomes	Preclinical in vivo	Whether soluble functional tau is preserved during degradation in brain	[150]
Alpha-synuclein AUTOTAC	Aggregated alpha-synuclein	Parkinson disease models; degradation of aggregates through the autophagy-lysosome pathway	Preclinical in vivo	Separation of selective aggregate recognition from general autophagy activation	[161,162]
AAV-delivered alpha-synuclein intrabody	Intracellular alpha-synuclein	Aged rats; improved motor function after intracerebral expression	Preclinical in vivo	Human distribution, durability, reversibility, and conformer selectivity	[163]
AAVrh.10 APOE2-Christchurch	Amyloid and tau pathology	Alzheimer disease mice; suppressed both pathologies after gene delivery	Preclinical in vivo	Whether a defined molecular state, rather than total pathology, is engaged	[151]
STMN2 splice correction	Downstream consequence of nuclear TDP-43 loss	Human neurons and mouse models; corrected cryptic splice-polyadenylation of STMN2	Preclinical mechanistic	Whether axonal rescue follows correction in sporadic disease	[168,170]
UNC13A cryptic exon targeting	Downstream consequence of nuclear TDP-43 loss	Human neurons and patient tissue; TDP-43 loss and risk variants drive mis-splicing and depletion	Human molecular association with experimental support	Whether correction is achievable and beneficial in vivo	[169]
TREM2 activation	Persistent myelin debris	Multiple sclerosis model; promoted debris clearance and remyelination	Preclinical in vivo	Whether homeostatic microglial functions are preserved	[186]
Chaperone-mediated autophagy restoration	Metastable neuronal proteome including alpha-synuclein	Mouse neurons; loss of the pathway collapsed the metastable proteome	Preclinical mechanistic	Whether selective substrate handling can be restored without broad proteostatic change	[54,159,160]

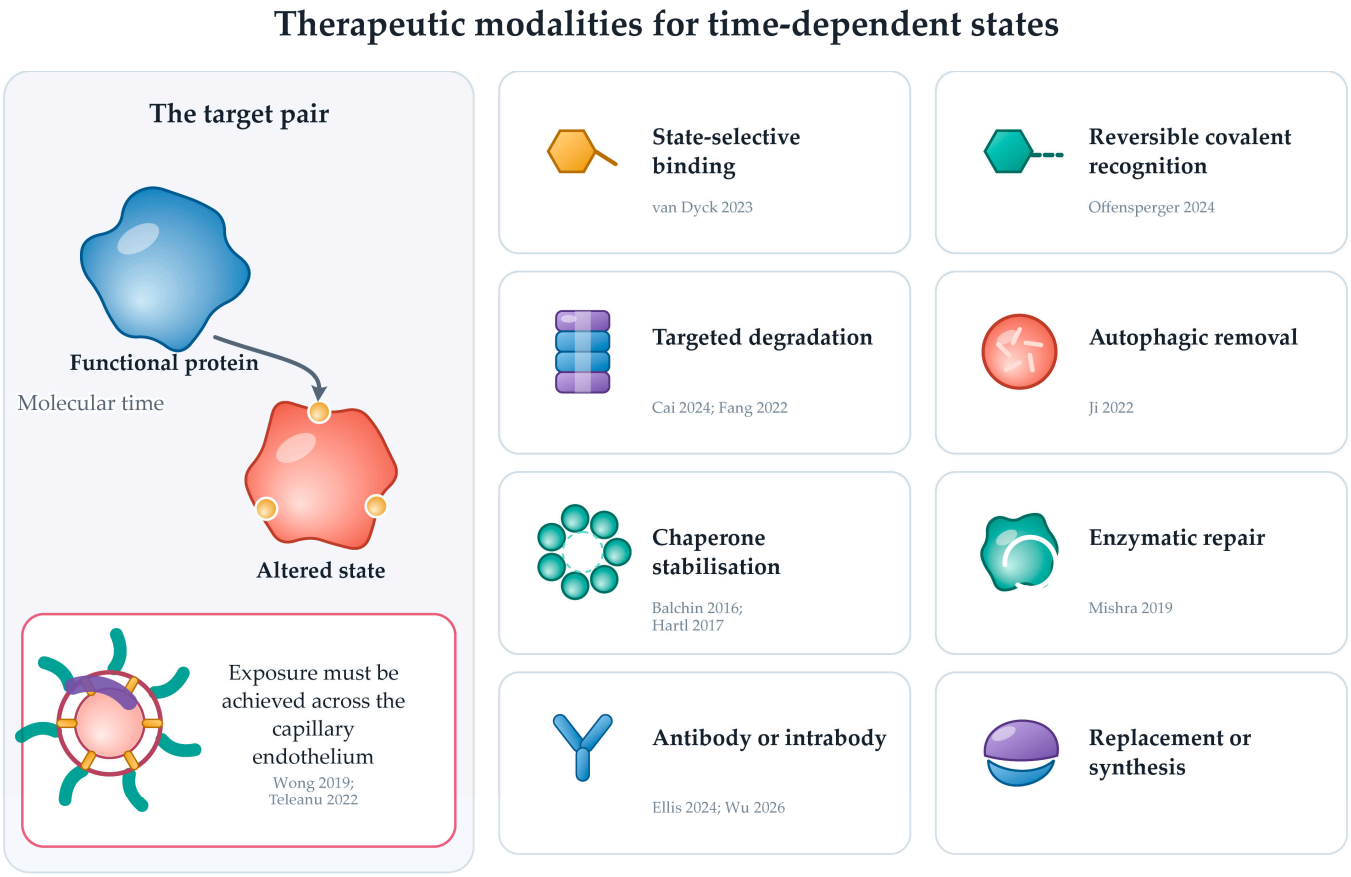


Figure 8. Therapeutic modalities for time-dependent states. The paired panel separates a functional protein from an altered state. Eight modality classes represent state-selective binding [148], reversible covalent recognition [188], targeted degradation [189,190], autophagic removal [162], chaperone stabilization [197,198], enzymatic repair [34], antibody or intrabody recognition [41,163], and replacement or synthesis modulation. Exposure across the capillary endothelium of the blood–brain barrier [204,205] must be achieved in addition to cellular selectivity. Arrows denote intended mechanisms, not demonstrated efficacy for a particular target.

9. Delivery and Pharmacology in an Aged Neurovascular System

9.1. Access to a Target State as a Conditional Sequence

A state can be defined, dated and shown to be causal and still be unreachable, which is the problem this section addresses. Brain delivery is not a binary property, and for a molecularly aged target exposure is a sequence of conditional steps: the active species must remain intact in plasma or cerebrospinal fluid, reach brain interstitial space, enter the relevant cell when necessary, access the correct organelle or extracellular structure, encounter the defined state, and remain long enough to produce a proximal pharmacodynamic change. Efflux, plasma binding, endothelial sequestration, lysosomal trapping, membrane partitioning, metabolism, and target-mediated disposition can interrupt this sequence, and the strategies developed to overcome them have been reviewed for Alzheimer disease specifically [204] and for central nervous system delivery generally [205]. Aging and neurodegeneration alter vascular integrity and transport heterogeneously across regions and patients. Barrier leakage is therefore neither a reproducible delivery mechanism nor evidence that a therapeutic reaches the cellular target. Small molecules offer the clearest route to intracellular target states when their unbound brain exposure is sufficient. Design must balance permeability, polar surface area, efflux liability, metabolic stability, solubility, and nonspecific tissue binding, and predictive models for barrier permeability remain useful for triage rather than for

decision [206]. A compound optimized against soluble recombinant tau can partition into membranes without reaching cytosolic tau. A ligand for alpha-synuclein can bind abundant monomer before encountering a rarer aggregate. Reactive recognition of an oxidized, glycated, or otherwise modified residue adds another constraint, because the warhead must survive distribution while retaining kinetic selectivity, which is why proteome-wide reactivity profiling belongs in the design cycle rather than at its end [188]. Bifunctional degraders introduce molecular size, conformational, efflux, and ligase-expression requirements [189,190]. Their success criterion is not total brain concentration but formation of the productive ternary complex and depletion of the intended state in the relevant neuron. Antibody delivery requires separate consideration of endothelial transport and parenchymal target access. Lower-affinity transferrin-receptor engagement increased brain uptake of a therapeutic antibody in mice [207], and engineered Fc transport vehicles delivered proteins across the blood–brain barrier in mice and nonhuman primates [208]. These studies establish receptor-mediated transcytosis as an experimentally tractable transport mechanism. They do not guarantee uniform parenchymal distribution, neuronal uptake, or engagement of an intracellular proteoform. Receptor affinity, valency, endothelial retention, peripheral target sinks, species differences, receptor occupancy, and safety must be optimized together. For extracellular amyloid-beta or exposed lesion matrix, an antibody can act without entering neurons, as the amyloid trials indicate [148,149]. For tau, alpha-synuclein, or TDP-43 states inside cells, a transported antibody still needs a validated uptake and endosomal-escape mechanism. Intrabodies and gene delivery can create recognition capacity within the target cell. AAV expression of an alpha-synuclein-targeting intrabody improved motor function in aged rats [163], and AAV-mediated APOE2-Christchurch delivery reduced amyloid and tau pathology in Alzheimer mice [151]. These are preclinical interventions with different mechanisms, not evidence of a common platform effect. Vector tropism, dose, cellular mosaicism, expression durability, immune responses, genomic persistence, and limited reversibility become part of the pharmacology. An intrabody must retain affinity in the reducing intracellular environment and avoid stabilizing a harmful intermediate. Expression of a repair enzyme or replacement protein requires control of stoichiometry and compartment targeting. For ALS and frontotemporal dementia, delivery must cover cortical and spinal motor-neuron territories and not a single injection field.

9.2. Mapping the Class of Target State to Its Delivery Constraint

The taxonomy of target states determines the delivery problem before any platform is considered, because the classes of target state do not share an access route. An extracellular-matrix or compact-myelin state requires distribution within a dense, poorly perfused extracellular compartment and no cell entry at all, and its principal risk is mechanical rather than cytotoxic [125]. An intracellular soluble or aggregated protein requires transport across the endothelium, across the plasma membrane, and into the cytosol, and then requires the active species to find a rare state among an abundant canonical pool. A mitochondrial respiratory-chain assembly adds a third and fourth address, since the species must accumulate in the organelle and then reach a membrane-embedded complex [4]. A nuclear-pore scaffold presents the hardest version of the problem, because exchange of the persistent subunits is so slow that a delivered replacement may never be incorporated on a therapeutic timescale [2]. These are four different problems, and a platform validated for one does not transfer to the others. Table 10 therefore maps each class of target state to the constraint it imposes, the platform for which a precedent exists, the exposure measurement that the claim requires, and the question that the precedent leaves open.

Table 10. Classes of molecularly aged target state mapped to their delivery constraints and platforms. Each class is paired with the access problem it imposes, a platform for which an experimental precedent is cited in this Review, the exposure measurement that a claim of engagement requires, and the question that the available precedent leaves unanswered.

Class of Target State	Example in This Review	Principal Access Problem	Platform with Reported Precedent	Exposure Measurement Required	What the Precedent Does Not Establish
Extracellular matrix or compact myelin	Aggregated fibronectin and inhibitory lesion matrix; aged intact internode	Distribution within a dense, poorly perfused extracellular compartment; no cell entry needed; mechanical risk on remodeling	Systemically delivered antibody or enzyme with spatial restriction; focused ultrasound to raise regional access; intrathecal delivery for surface lesions [136]	Interstitial concentration, spatial extent of target depletion, and tissue mechanical and vascular integrity	That remodeling can be confined to the lesion, or that vessel and basement-membrane architecture is preserved
Extracellular parenchymal aggregate	Plaque-associated truncated and pyroglutamate amyloid-beta	Endothelial transport is the limiting step; the target is reachable without entering neurons	Antibody, including receptor-mediated transcytosis and engineered transport vehicles; clinical precedent exists for this class [148,149,207,208]	Plasma and cerebrospinal-fluid profiles, free and target-bound antibody, regional aggregate change, and vascular safety monitoring	Occupancy of the defined proteoform rather than of total aggregate burden
Intracellular soluble or aggregated protein	Tau seeding states; alpha-synuclein conformers; cytoplasmic TDP-43; huntingtin fragments	Three sequential barriers followed by discrimination of a rare state against an abundant functional pool	Brain-penetrant small molecule; bifunctional degrader [189,190]; gene-delivered intrabody [163]; intrathecal oligonucleotide for synthesis control	Unbound brain concentration, productive ternary-complex formation or state depletion in the relevant neuron, and preservation of the canonical pool	That total brain concentration predicts engagement of the state, or that selectivity measured in vitro survives in cells
Mitochondrial assembly	Long-lived respiratory-chain subunits and their damaged states	Four sequential compartments, ending at a membrane-embedded complex within a charged organelle	Organelle-targeted nanocarrier or biomimetic system; ligand-directed carriers [166]	Mitochondrial accumulation quantified against cytosolic, lysosomal, and membrane compartments, with respiration and organelle stress measured in parallel	That colocalization at the optical resolution used corresponds to access to the complex

Table 10. *Cont.*

Class of Target State	Example in This Review	Principal Access Problem	Platform with Reported Precedent	Exposure Measurement Required	What the Precedent Does Not Establish
Nuclear scaffold and transport machinery	Persistent nucleoporin scaffold states	Nuclear-envelope access combined with exchange rates so slow that replacement may be kinetically unavailable	Gene-delivered replacement subunit or repair activity; small molecules directed at transport function [151]	Measured subunit exchange after intervention together with a transport or permeability readout	That expression of a replacement subunit results in incorporation into the existing assembly
Synaptic assembly	Postsynaptic density states with lifetimes spanning hours to months	A spatially distributed target with local turnover and strong heterogeneity between synapse classes	Small molecule with broad parenchymal distribution; cell-type-directed nucleic acid to the relevant neuronal population [5]	Exposure in the synaptic fraction and local turnover of the state, reported by synapse class rather than averaged	That bulk tissue exposure represents exposure at the synapse, or that one synapse class is representative
Clearance and repair machinery of a non-neuronal cell	Lipid-laden phagocyte state and defective cholesterol clearance	Cell-type-selective delivery, where the therapeutic goal is to restore a cellular process rather than to bind a molecule	Small molecules directed at phagocyte lipid handling; microglia-directed carriers [186]	Exposure in the target cell type relative to others, with homeostatic phagocytic and synaptic functions measured	Selectivity over homeostatic microglial functions throughout the brain

Nanoparticles and lipid carriers should be selected for a target-state requirement, not added as a generic catalogue [209]. Peptide-functionalized lipid nanoparticles have achieved systemic messenger RNA delivery to the mouse brain [210], and biomimetic nanosystems have delivered curcumin to neuronal mitochondria in Alzheimer models [166]. These data support platform feasibility in defined models. They do not establish disease-state selectivity, human blood–brain barrier transport, or therapeutic benefit. Particle size, composition, protein corona, complement activation, uptake by liver and spleen, endothelial transfection, cell-type tropism, cargo release, and repeat-dose tolerability need direct measurement, and computational design tools can prioritize but not substitute for those measurements [211]. Organelle-targeted designs add a second address after cell entry. Mitochondrial localization should therefore be quantified against cytosolic, lysosomal, and membrane compartments, with respiratory function and off-target organelle stress measured in parallel. Extracellular vesicles offer endogenous membrane architecture and potential cell-targeting features, but their identity and dose are difficult to standardize. Systemically administered targeted exosomes delivered siRNA to mouse brain [212], and engineered exosome systems delivered catalase or genetically encoded cargo in Parkinson models [164,165]. These studies are proof of delivery and preclinical activity. They do not show that extracellular vesicles preferentially recognize a molecularly aged target. Source-cell heterogeneity, cargo loading, co-isolated material, vesicle number, biodistribution, uptake mechanism, endosomal escape, immunogenicity, and manufacturing consistency must be resolved before comparing them with synthetic carriers, and transport across the barrier is itself modulated by inflammation [213]. Enrichment methods developed for plasma vesicle proteomics can help standardize the input material [214]. A vesicle study should report the molecular cargo

that reaches the target cell, not only fluorescence associated with brain tissue. Intranasal administration may reduce systemic exposure or exploit olfactory and trigeminal pathways, but deposition in the nasal cavity is not equivalent to delivery to a disease-relevant brain compartment. Formulation residence time, mucociliary clearance, enzymatic degradation, dosing volume, device, species anatomy, regional distribution, and the fraction entering blood all influence interpretation, as illustrated by pharmacokinetic characterization of a nose-to-brain peptide candidate [215]. For a molecularly aged state, intranasal delivery is justified only when the route produces reproducible unbound exposure and proximal engagement in the required region and cell type. A behavioral effect after intranasal dosing without a brain concentration profile and state-resolved pharmacodynamics remains insufficient evidence of target engagement. Cell-specific and organelle-specific delivery should be treated as quantitative selectivity. Microglial delivery may be rational for myelin-debris clearance [186] but could alter homeostatic phagocytosis throughout the brain [124]. Oligodendrocyte targeting may support remyelination but will not remove extracellular fibronectin aggregates [136]. Dopaminergic-neuron delivery is relevant to intracellular alpha-synuclein, whereas broad lysosomal activation may affect neurons and glia differently [114]. Mitochondrial, lysosomal, nuclear, synaptic, and extracellular targets each require a compartment marker, a delivered active species, and a target-state assay. Co-localization microscopy alone can overestimate organelle access when optical resolution is insufficient or fluorophores separate from their cargo. Table 11 summarizes what each delivery platform has actually been shown to achieve.

Table 11. Brain delivery platforms and the outcomes reported for them. Each platform is listed with the experimental system, the measured delivery result, and the target-state question that the study did not address.

Platform	Experimental System	Reported Delivery Outcome	Question Left Open for a Molecularly Aged Target	Reference
Reduced-affinity transferrin receptor antibody	Mouse	Lower receptor affinity increased brain uptake of a therapeutic antibody	Whether parenchymal distribution reaches the cell type holding the target state	[207]
Engineered Fc transport vehicle	Mouse and nonhuman primate	Protein cargo delivered across the blood–brain barrier	Whether intracellular proteoforms can be engaged after transcytosis	[208]
Aggregate-directed IgG (lecanemab, donanemab)	Human, randomized trials	Reduced brain amyloid burden with slowed clinical decline and defined imaging risks	Which amyloid-beta proteoforms are cleared and in what order	[148,149]
AAV-delivered intrabody or gene product	Aged rat; Alzheimer mouse	Intracerebral intrabody expression improved motor function; APOE2-Christchurch suppressed amyloid and tau pathology	Durability, reversibility, and coverage of distributed neuronal populations	[151,163]

Table 11. *Cont.*

Platform	Experimental System	Reported Delivery Outcome	Question Left Open for a Molecularly Aged Target	Reference
Peptide-functionalized lipid nanoparticles	Mouse	Systemic messenger RNA delivery to brain	Cell-type tropism and repeat-dose tolerability in aged animals	[210]
Biomimetic mitochondria-targeted nanosystem	Alzheimer mouse	Curcumin delivered to neuronal mitochondria	Quantitative organelle selectivity against cytosolic and lysosomal compartments	[166]
Engineered and targeted exosomes	Mouse; Parkinson models	siRNA delivered to brain after systemic injection; catalase and encoded cargo delivered intracerebrally	Standardization of vesicle identity, dose, and cargo reaching the target cell	[164,165,212,213]
Intranasal peptide formulation	Rodent pharmacokinetics	Nose-to-brain delivery characterized with stability and exposure parameters	Reproducible unbound regional exposure and proximal engagement	[215]

9.3. Exposure Requirements Implied by State Selectivity

State selectivity changes the exposure question, because instead of asking whether a compound enters the brain, the framework asks what fraction of a defined pool must be engaged, for how long, to shift a state that accumulated over years, and the answer differs by therapeutic direction. For an intervention that prevents formation of the state, the pool declines with a time constant set by the loss rate of the pool itself, so the speed of the effect is a property of the target and not of the drug: complete blockade of formation in a population whose half-life is months still requires something like three to five half-lives for the pool to approach its new steady state, and partial blockade sustained over that period gives a proportionally smaller reduction rather than a slower one [216]. For an intervention that removes the state, the therapeutic adds a clearance term, net decline requires that added clearance to exceed the rate at which the state is formed, and the reduction reached at steady state is approximately the added clearance divided by total clearance. This is the arithmetic that makes intermittent dosing rational against a slowly accumulating target, because what matters is the clearance integrated across the dosing interval rather than the concentration at any instant, and it is consistent with the monthly and fortnightly schedules used by the aggregate-directed antibodies [148,149]. For repair, the limit is not exposure at all. The accessible fraction of modified sites bounds the achievable effect, so once accessible sites are saturated, further exposure repairs nothing and a buried population remains unchanged [34]. A program should therefore state which of these three regimes it is in before selecting a dose, because they imply different relationships between exposure and effect.

Two practical consequences follow for dosing interval and for pharmacodynamic biomarker selection. The dosing interval should be set against the half-life of the target pool rather than that of the drug: when the pool half-life greatly exceeds the interval, exposure can be fractionated without loss of effect and trough engagement matters more than peak concentration, whereas a pool that turns over within days leaves no such latitude. Complete occupancy is also not the objective, since raising occupancy toward saturation recruits the canonical population and

erases the selectivity that defined the program, so the exposure target is a window bounded below by the clearance needed to exceed formation and above by engagement of the functional pool, which is a different design problem from maximizing tolerated exposure. Biomarker selection follows from the same mismatch of timescales, and a single marker cannot serve. An early marker must be state-resolved and must be read within one dosing interval, which means occupancy of a defined epitope, a flux measurement, or a splicing or enzymatic consequence of engagement [168,170]; a late marker reports the size of the pool and can only move on the time constant of the pool itself. A program that measures only the pool will classify an active intervention as inactive at early time points, and a program that measures only occupancy can show engagement without ever showing that the accumulated state moved. Withdrawal and washout separate persistent modulation from continuing exposure, and the recovery rate after withdrawal is itself an estimate of the formation rate. None of these schedules can currently be anchored in human tissue, because human residence times for the candidate states are unmeasured and durations are extrapolated from rodent kinetics [3,6,8,9]. A human lifetime estimate for even one candidate state would constrain the dosing duration of every program directed at it.

9.4. Pharmacokinetic and Pharmacodynamic Reporting

Pharmacokinetic reporting should include plasma and cerebrospinal-fluid profiles when relevant, total and unbound brain concentrations, regional distribution, cell or compartment exposure where feasible, active metabolites, and time relative to dosing. Total brain concentration can be misleading for lipophilic compounds sequestered in myelin or membranes. Antibodies require free and target-bound measurements, while carriers require intact-cargo and released-cargo measurements. Pharmacodynamic reporting should remain proximal to the state: occupancy of a defined epitope, disappearance or repair of a proteoform, correction of TDP-43-dependent splicing [168], restoration of lysosomal flux [114], remodeling of a specified matrix aggregate [136], or exchange within a respiratory assembly [4]. Downstream transcriptomics, imaging, electrophysiology, and behavior then test consequence rather than substitute for engagement. Turnover sets the exposure–response schedule. A synthesis-lowering intervention can reduce RNA immediately while a persistent protein pool changes over months [3,9]. A repair strategy may act rapidly on accessible sites but leave a buried assembly unchanged. Degradation may show a threshold when a state becomes extractable. Replacement may require natural turnover or active subunit exchange [2]. Hysteresis between exposure and engagement can therefore be mechanistically informative. Sampling times should be derived from the measured lifetime distribution and modality mechanism, with washout used to distinguish persistent target modulation from continuing exposure. Dose selection must preserve the functional pool, since increasing a state-selective binder can erase selectivity through occupation of the canonical population. High degrader exposure can recruit weak off-target ternary complexes [190]. Excess repair-enzyme activity can consume cofactors or alter unrelated substrates [14,34]. Broad matrix remodeling can weaken vessels or axonal support [125]. Matched-state engagement curves, functional reserve, recovery after withdrawal, and chronic safety should be measured across dose and time. Renal and hepatic clearance, immune activity, vascular disease, polypharmacy, and metabolic reserve also change in older patients. The desired therapeutic window is differential state modulation with an acceptable functional and systemic cost, not the highest tolerated total exposure.

10. Machine Learning and Deep Learning Across the Discovery Chain

10.1. Proteoform Identification and Quantitative Uncertainty

Computation enters this framework at four points, and the first is the measurement itself. Machine learning improves spectrum prediction, peptide scoring, retention-time and

ion-mobility modeling, open-search prioritization, and modification localization [94,217], and deep models recover identifications from precursor information that conventional scoring discards [95]. The limiting problem is label validity, since training spectra are enriched for analytes that existing workflows already identify, while rare, modified, long, hydrophobic, crosslinked, and intact species are underrepresented, and search-space expansion can raise apparent discovery while weakening localization and false-discovery control [28]. Evaluation therefore requires independently characterized standards, external laboratories, unfamiliar modification classes, and retained negatives, with cell-resolved imaging proteomics supplying the histological context that a spectral library cannot [108]. Proteoform calling is a layered inference in which peptide-spectrum match, site localization, intact mass, and combinatorial assignment carry different uncertainty [18], so collapsing them into one confidence score hides the weakest link. Probabilities should be calibrated at each level, models permitted to abstain, and decoys built to reflect the expanded chemistry rather than sequence permutation alone. Sensitivity without chemical validity enlarges a false target space, and products of alternate decoding that are absent from the reference database are misassigned whatever the model capacity [109].

10.2. Multimodal Target Prioritization

Target prioritization can combine turnover trajectories, proteoform occupancy, spatial localization, insolubility, structural features, genetic perturbation, and human disease data [22]. Representation learning and knowledge graphs expose relationships that no single assay captures, supported by proteome-scale localization and interaction resources [218] and by models trained across tissue contexts [105,219]. Predicted interaction networks are now large enough to screen systematically [220–222], although curated subsets exist precisely because many predicted complexes do not form [223], and fluid proteomics adds a further modality in cerebrospinal fluid [224] and serum [225]. The resulting score remains an association until perturbation establishes dependence. Models should expose which evidence domain drives a ranking and how it changes when one modality is withheld, because donor, laboratory, disease-stage, and protein-family leakage generate internal performance that fails prospectively [226]. Causal claims need explicit assumptions, since age covaries with medication, comorbidity, cell composition, survival, and collection, and a causal graph clarifies the proposed relationships without removing unmeasured confounding. Perturbational data help when the intervention is specific and read at the intended molecular level; tau-directed CRISPR screens in induced neurons show both the value and the target-resolution limit of altering gene dosage rather than a proteoform [60]. Chemical probes carry off-target effects that only proteome-wide profiling detects [188], and image-based phenotypic screening supplies a mechanism-agnostic readout [227]. A useful learning loop selects experiments that discriminate between mechanistic hypotheses rather than experiments expected to improve a benchmark score.

10.3. Modified-State Structure and Molecular Design

Canonical structure prediction provides a starting scaffold, not a ground-truth aged state. Proteome-scale prediction has made canonical models routine [228], and design methods generate soluble analogues of membrane proteins [229] and de novo functional proteins [230], yet deamidation, stereochemical inversion, truncation, crosslinking, oxidation, and complex remodeling alter local energy landscapes in ways these models were not trained to represent. Modification-aware modeling must therefore define chemical topology, protonation, stereochemistry, force-field support, and experimental restraints, prefer ensembles for disordered or cryptic targets, and raise reported uncertainty outside training experience. Ligand models face the same target-state problem, and learned scoring and geo-

metric deep learning have improved structure-based design [231–234], contrastive learning supports genome-scale screening [235], and generative models have produced candidates that were synthesized and tested in antibacterial [236,237], transcriptional-phenotype [238], and oncology and natural-product settings [239–242]. Training data nevertheless rarely contain matched affinities for aged and unmodified proteoforms, so a model can optimize canonical binding while missing state selectivity; prospective assays should test both states, related modifications, family members, and relevant complexes, and docking scores remain prioritization signals rather than affinities [46,243,244]. Transfer learning extends small datasets [226,245] and safety classifiers support triage [246], but proteoform-specific assays are costly enough that active learning, including the selection of perturbations rather than compounds [247], sets how far these methods reach. Figure 9 represents the resulting loop, in which task-specific models rather than one universal network receive spectra, turnover curves, spatial measurements, proteoforms, structural ensembles, perturbations, and chemistry, and experimental results including rejected hypotheses return as training evidence. The figure does not imply that an algorithm can infer causality or druggability from observational multi-omics alone.

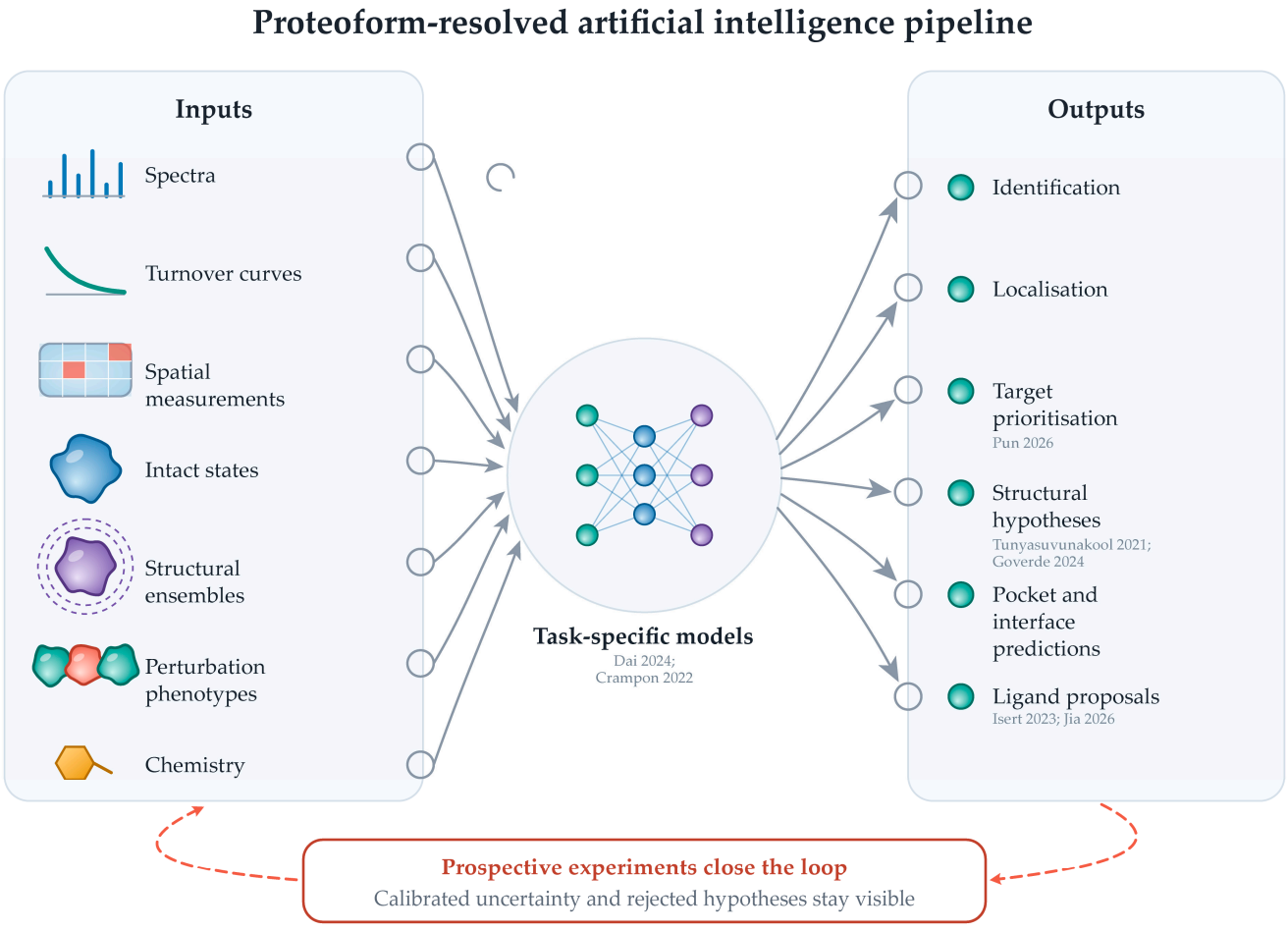


Figure 9. Proteoform-resolved artificial intelligence pipeline. Spectra, turnover curves, spatial measurements, intact states, structural ensembles, perturbation phenotypes, and chemistry data enter task-specific models [95,231]. Outputs include identification, localization, target prioritization [22], structural hypotheses [228,229], pocket or interface predictions, and ligand proposals [234,235]. Calibrated uncertainty and rejected hypotheses remain visible. Prospective experiments close the loop. The central network is not a universal black box and does not replace causal or pharmacological validation.

10.4. Classical Quantum Chemistry for Bounded Molecular-Age Questions

Classical quantum chemistry is already relevant to molecular-age questions. Density-functional theory, correlated wave-function methods, semiempirical approaches, and combined quantum mechanics and molecular mechanics can address succinimide formation, deamidation, racemization, oxidation, electrophile adduction, and covalent recognition, while end-point free-energy methods such as MM/PBSA and MM/GBSA remain widely used for binding estimates and carry approximations that must be stated and not assumed away [248]. Machine-learned corrections to quantum-level calculations have been applied to neuroactive small molecules including levodopa [249], delta-learning combines low-level and high-level electronic structure in medicinal chemistry workflows [250], and integrated platforms couple quantum-mechanical descriptors to predictive models with explicit explainability requirements [251]. The decisive variable is the chemical model rather than the method. Residue context, protonation, solvent, dielectric environment, catalytic groups, and conformational sampling must be specified [252,253], because a high-level calculation on an unrealistic geometry is not a mechanistic result. Reaction energies, barriers, and binding contributions should be tested for sensitivity to model size and method and then connected to experiment, a standard that industrial applications have made explicit [254], and related in silico design fields such as radiopharmaceutical chemistry show the same dependence on a defined chemical model [255].

10.5. Quantum Computing as an Exploratory Implementation

Quantum computing is a possible implementation for selected electronic-structure, kernel, or optimization tasks [23,256]. It is not a synonym for quantum chemistry, it does not make a whole modified protein computable, and it has no current application to the target-state problem. Near-term devices are limited by qubit number, connectivity, gate error, circuit depth, sampling cost, and state preparation, so a defensible study starts from a chemically defined active region and a strong classical comparator [257] and reports the Hamiltonian, basis, active space, mapping, algorithm, mitigation, shot budget, hardware, cost, and uncertainty, stating whether any claimed advantage is empirical, asymptotic, projected, or absent. Quantum machine learning is held to the same standard, since small proteoform datasets are vulnerable to leakage and classical kernels are strong baselines [246], and encoding, measurement, and tuning costs belong in the comparison, as quantum kernel models for ADME-Tox prediction show, where the classical comparator determines whether a gain exists [258]. Negative results are therefore informative, and benchmark datasets, error characterization, and resource estimates remain useful outcomes where no advantage is observed. Figure 10 enforces this boundary: the quantum path receives only a compact active region, outputs are compared against the same classical baselines and experimental data, and the crossed whole-protein path indicates that biological scale is not a reason to skip problem reduction. Across all four computational layers the constraint is the same, in that each inherits the molecular resolution of the evidence it is given, and none of them can supply a target state that the experiments never resolved.

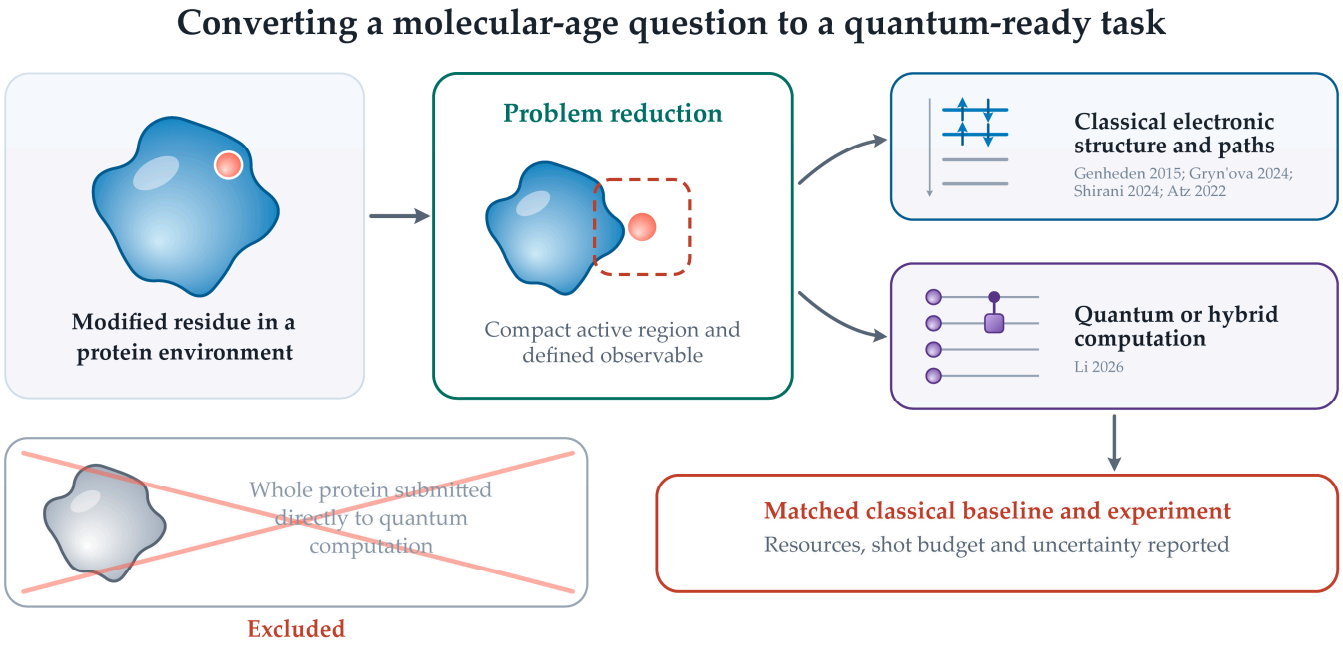


Figure 10. Converting molecular-age questions to quantum-ready tasks. A modified residue within a protein environment is first analyzed with classical sampling, electronic-structure methods [248,252], reaction-path calculations [249,250], and benchmark data. Only a compact active region or fixed representation proceeds to quantum or hybrid computation [23]. Outputs are compared with matched classical calculations and experiments. The excluded whole-protein path emphasizes that quantum readiness requires problem reduction, explicit resources, and a chemically defined observable rather than scale-based rhetoric.

11. Benchmarks, Evidence Cards, and Matched-State Assays

11.1. Benchmark Architecture and Leakage Barriers

Claims about molecular age are only comparable between laboratories if the unit of evaluation, meaning the entity that one row of the dataset represents, the evidence summary and the assay are standardized, and this section sets out all three. Figure 11 shows a benchmark organized around the unit of evaluation rather than random rows, with donors, laboratories, brain regions, cell types, protein families, peptides, proteoforms, spectra, turnover curves, and negative experiments represented explicitly. The choice of split is the substantive decision: a peptide-level random split leaks nearly identical spectra, a protein-level split still leaks homologous families as predicted-structure resources expand the pool of related training examples [220–222], a donor split retains laboratory artifacts, and a laboratory split retains shared reference materials, so the split should follow the intended use and be declared before tuning. Minimum evaluation includes a simple baseline, calibration, uncertainty, ablation, external data, and prospective testing, with false-discovery and localization control for identification [28], precision among testable top candidates rather than a global curve for ranking, subgroup-calibrated error distributions for regression [246], and synthesis, identity confirmation, matched state-selectivity assays, and reported failures for generative design [236–238]. Missingness and negative outcomes should be retained rather than excluded, and the benchmark should release accessions, processing parameters, databases, decoy procedures, tissue metadata, kinetic models, structure provenance, code, environment versions, model weights where permissible, and a model card, adding qubits, circuit depth, shots, noise, mitigation, and resource estimates for quantum work [23,258]. A result is reproducible when another group can reconstruct the unit of evaluation and the endpoint, not merely rerun an architecture.

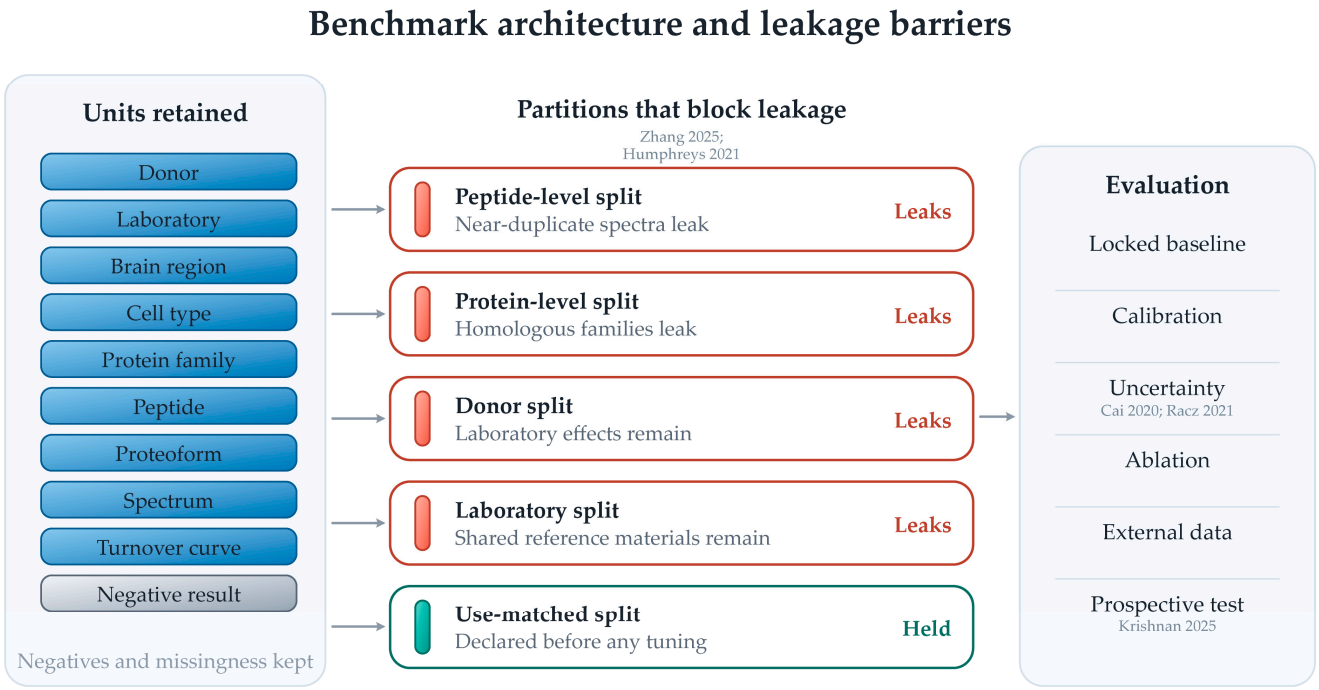


Figure 11. Benchmark architecture and leakage barriers. Donor, laboratory, brain-region, cell-type, protein-family, peptide, proteoform, spectrum, turnover, and negative-result units are retained in the dataset design. Peptide-, protein-, donor- and laboratory-level splits are each shown to leak, through near-duplicate spectra, homologous families, residual laboratory effects and shared reference materials, and only a use-matched split declared before any tuning holds [220,221]. Evaluation includes calibration and uncertainty [226,246], ablation, locked baselines, external data, and prospective experiments [236]. A result is reproducible when another group can reconstruct the unit of evaluation and the endpoint, not when they can rerun the architecture. The conceptual panels contain no study data.

11.2. Standardized Evidence Cards for Target-State Comparison

A review of difficult targets becomes uninformative when each candidate is described in a different evidential vocabulary, so we propose a standardized evidence card that begins with the molecular unit and states whether the candidate is a gene product, peptide, modification site, intact proteoform, conformation, complex, insoluble fraction, or spatially defined assembly [16,17]. Lifetime evidence is recorded next, with species, age, brain region, cell type, labeling design, kinetic model, and uncertainty [3,8], and chemical identity is recorded separately, because a persistent population can be chemically uncharacterized [1] while an age-associated modification can sit on a protein of ordinary turnover [70]. The causal fields follow: detection method and confidence, age relationship, spatial localization, functional phenotype, perturbation type, rescue, and the highest evidence level reached. The card records the known weaknesses of each perturbation class rather than only its result, since a residue substitution is not a clean causal test unless the replacement preserves folding, localization, expression, and interaction, repair-enzyme manipulation carries its substrate scope [15,34], and degradation or antibody experiments must measure both the proposed harmful state and the functional pool [150,161]; where an intervention changes only total abundance, engagement is recorded as unresolved. Therapeutic direction is then written as a verb bound to the state, such as repair an isoaspartyl site, stabilize a functional assembly, remove a toxic fragment, block formation of a crosslink, replace a nonexchangeable component, or bind a conformer selectively, and never as target the protein. Assay feasibility, brain delivery, exposure, reversibility, and safety are scored on separate axes [204,205], because a candidate can be biologically compelling but pharma-

cologically immature, or ligandable but biologically unsupported, and keeping the axes apart prevents a pocket prediction from outweighing a weak causal record. Four worked cards show what the format changes. For the nuclear pore, lifetime evidence supports persistence of scaffold components in adult brain [1] and slow exchange refines that interpretation [2,24]; the productive question is not whether nucleoporins are druggable as a family but whether a defined aged subpopulation acquires a lesion that alters transport in a particular neuronal context, as pore dysfunction in ALS and VCP disease models suggests [133,134], so the decisive experiment pairs cell-selective age tracing with intact-state analysis, single-cell transport measurement [116], controlled subunit replacement, and rescue. The mitochondrial card starts from subunit-resolved persistence within respiratory assemblies [4], lists oxidation [70], adduction, truncation, altered interaction, and failed exchange as candidate lesions, and requires rescue to distinguish direct correction from global stimulation of biogenesis [55]; pharmacology adds four separate exposure boundaries, since brain entry, cell uptake, mitochondrial accumulation, and access to the membrane complex are distinct requirements [166]. Myelin and synaptic cards require spatial history, because internodes form at different times and synapse types maintain different proteome dynamics [5], so a whole-brain average can define a target that exists in no single compartment: a myelin candidate specifies lineage, internode location, membrane fraction, and relation to conduction [67,135], and a synaptic candidate specifies location, synapse class, solubility, local turnover [53,93], and whether microglial material represents transfer, phagocytosis, or failed degradation [9]. A compound that improves respiration, or increases myelin staining, without measuring the proposed state remains a phenotypic modulator.

11.3. Matched-State Assays as the Central Pharmacological Requirement

The decisive assay for this field compares the aged state with the relevant functional comparator under conditions that preserve their molecular differences. Recombinant canonical protein is insufficient when the hypothesis concerns a modification, truncation, conformational ensemble, membrane context, or complex, as the structural differences among patient-derived alpha-synuclein polymorphs show [111,138]. The comparator should differ from the test material only in the state under study, and site-specific synthesis, semisynthesis, enzymatic installation, genetic-code expansion, controlled aging, native purification, and cell-derived preparations each solve part of that problem while adding their own artifact, so identity and occupancy need orthogonal confirmation including intact-mass measurement of the final material [18,99]. Binding studies measure affinity, kinetics, stoichiometry, and competition against both states, because a selectivity ratio without absolute affinity misleads when one preparation contains inactive material; immobilization can expose cryptic surfaces, tags can alter disordered proteins, and thermal-shift assays can fail for heterogeneous targets, so two biophysical principles should agree and integrity should be confirmed before and after. Where covalency is proposed, time-dependent occupancy, reversibility, site identity, and proteome-wide selectivity are required [188]. Functional assays must preserve the context that creates the state: a respiratory-chain subunit needs a membrane and assembly partners [4], a nuclear-pore state needs transport readouts [116], myelin states need membrane organization or conduction [185], synaptic states need vesicle cycling or plasticity rather than viability [155], and extracellular crosslinks need mechanical or permeability measurements [125]. Engagement in cells and brain should be proximal, measured by state-specific targeted mass spectrometry, intact-proteoform methods that preserve combinations peptide assays lose [19,40], conformation-selective reagents tested against related assemblies [41], chemical proteomics for covalent engagement, or imaging once tracer identity, affinity, nonspecific binding, metabolism, and partial-volume effects

are established [107]. Time enters the pharmacodynamic model as an explicit variable rather than as a sampling convenience, because the interval between engaging a state and any measurable change in its pool is set by the kinetics of the pool and differs by modality. A synthesis-lowering intervention can reduce messenger RNA within hours while the protein population changes over months [3]; repair can act rapidly at accessible sites and leave a buried population unchanged [34]; degradation can appear only as a threshold once an assembly becomes extractable [7]; and replacement can require natural turnover or active subunit exchange [2]. Sampling schedules must therefore be derived from the measured lifetime distribution and the modality mechanism, since short exposure can classify an active synthesis strategy as inactive while long exposure can hide transient off-target stress behind adaptation. Matched-state assays also define informative negative results, because a compound can bind both states equally, fail to reach the compartment, engage the target without changing function, or change function without measurable engagement, and each rejects a different hypothesis. Preserving those distinctions prevents failed compounds from collapsing into one inactive class and allows loss of function in the comparator pool to be measured directly rather than inferred once toxicity appears.

11.4. Human Tissue and Experimental Models Across Molecular Timescales

Human brain tissue provides the longest relevant exposure history but is usually cross-sectional and postmortem. It can establish that a state exists in the target organ, define regional and cellular localization, quantify heterogeneity, and relate the state to neuropathology, as shown for tau proteoforms [19,44] and amyloid-beta species in astrocytes [83], but it cannot determine whether the state preceded disease, followed terminal physiology, or caused dysfunction. Cohorts should therefore record postmortem interval, agonal state, tissue pH, fixation, storage, dissection, comorbidity, medication, sex, ancestry, pathology stage, and cause of death, with batches balanced across these variables and extraction recovery tested against standards. Longitudinal animal labeling supplies the kinetic and perturbational detail that human tissue cannot: rodents permit isotope schedules, cell-selective labeling, region sampling, genetic manipulation, and pharmacokinetics [3,6,8,9], short-lived fish compress turnover, translation, and proteostasis change into a brief lifespan [10,47,50], and invertebrate systems permit large causal screens [52]. None recreates decades of human residence time, so conservation must be evaluated at the level of protein, site, chemical environment, assembly, cell type, and phenotype, because a conserved sequence with a different lifetime or compartment is not a conserved molecular-age state. Engineered human systems trade age for control: induced pluripotent stem cell models give genotype-defined cells but can erase age features during reprogramming, whereas direct conversion retains more donor-age signature, as transdifferentiated Alzheimer neurons preserving lysosomal repair deficits show [59], and some states survive reprogramming, since sporadic ALS iPSC-derived neurons reproduce TDP-43 loss-of-function hallmarks [171]. Organoids add multicellular organization while lacking vascular, immune, and systemic physiology, though astrocytic lysosomal failure has been modeled in them [114], and ex vivo human slices preserve native states briefly and allow engagement measurement without a claim of efficacy. The model should be chosen for a defined evidence step rather than ranked as globally closest to human aging: human tissue establishes existence and context, longitudinal models establish kinetics, engineered systems install or prevent the state, reconstitution tests mechanism, and in vivo pharmacology measures exposure, engagement, function, and safety. Discordance between them is informative rather than noise, since it can reveal species differences, stage dependence, protective adaptation, or an incorrect target definition.

Fluid biomarkers raise a separate problem, because cerebrospinal-fluid and plasma proteomics have identified candidate Alzheimer disease markers and organ-aging signatures [48,224], and the plasma amyloid-beta 42/40 and phospho-tau217 ratios improve classification of amyloid status [147], but a fluid measurement reports a population average generated by production, drainage, barrier function, peripheral sources, and peptidase activity, and it does not report occupancy of a defined proteoform in a defined brain cell. A program selected on a target state will usually be monitored on a biomarker that cannot resolve that state, so a successful state-selective intervention and an unsuccessful one can produce the same fluid readout, and the biomarker then cannot adjudicate a failed trial: it is uninformative about whether the state was engaged, whether the wrong state was chosen, or whether exposure was inadequate. Three bottlenecks stand between current assays and a proteoform-resolved readout. Analytically, the modified species of interest is often a minor fraction of a low-abundance analyte, and immunoassays for predefined epitopes may not discriminate neighbouring or combinatorial states [41], so targeted or intact-state mass spectrometry is required at concentrations near its limits [19,40]. Biologically, the relationship between a brain proteoform and its fluid counterpart is unknown for every candidate state discussed here, and a modification that changes clearance or drainage will distort that relationship in the same direction as the disease process. Operationally, assays that resolve proteoforms are not yet standardized across laboratories, which is the same reference-material problem that limits benchmarking itself [20]. Until these are addressed, programs should pair an accessible fluid marker with a state-resolved measurement in tissue or an ex vivo preparation, and should report which of the two carries the pharmacodynamic claim.

12. Open Questions and Interpretive Boundaries

Unresolved Questions That Define the 2026 Need

Six questions remain open, and together they define what the field would have to measure for the framework to become routine. The first is distribution, since no human brain atlas yet resolves protein lifetime, intact proteoforms, site-specific spontaneous chemistry, cell type, region, and functional state together. Existing datasets illuminate components of this space but use different species, labeling designs, extraction methods, and molecular units [3,8,11,19]. Shared reference materials and harmonized metadata are required before studies can be integrated without erasing their assumptions [20]. The second question is directionality, since longer lifetime can be adaptation or failure [4,6]. Aggregation can sequester harmful intermediates or reflect failed disposal [47]. Microglial uptake can protect neurons or propagate inflammation [9,173]. A modification can decrease or increase function depending on site and occupancy [143]. The field needs perturbations that change the state while preserving sequence, abundance, and context as far as possible. Rescue should restore the molecular state and phenotype in the same experiment. The third question is target granularity, because bottom-up evidence may identify a site without the intact combination. Structural methods may resolve a conformation without chemical identity [110]. Antibodies may recognize an epitope shared across several states [41]. Drug discovery needs a target resolution that is specific enough for selectivity but measurable enough for pharmacology. In some cases the target will be one intact proteoform; in others it will be a bounded ensemble or assembly state [45]. Explicit uncertainty is preferable to an artificially precise label. The fourth question is replacement, since persistent assemblies may not accept new subunits even when synthesis increases [2]. Selective removal may create a structural deficit, and repair may not reach buried sites. Longitudinal experiments should measure exchange after intervention and identify whether function returns through repair, dilution, remodeling, or compensation. This matters most for nuclear

scaffolds, myelin, extracellular matrices, and mitochondrial complexes [1,4,125,135]. The fifth question is computational ground truth, because models inherit the chemical and biological detail of their labels [22]. Quantum calculations inherit the realism of their molecular model [252]. Better architectures cannot recover a missing aged state, and a more accurate energy cannot validate an irrelevant active region. Benchmarks should therefore reward calibrated abstention, external validity, and prospective experimental value rather than only internal accuracy. Negative datasets and failed state-selectivity assays are essential training evidence. The final question is clinical tractability, where human relevance requires more than detection in diseased tissue. The state should be present at an actionable stage, measurable with a pharmacodynamic assay, accessible to a modality, and separable from essential function. Exposure and engagement must be achievable in the aged brain at an acceptable chronic dose [204,205]. These constraints will eliminate many candidates. That attrition is a sign of a rigorous target field, not a failure of the molecular-age concept.

13. Roadmap and Conclusions

Figure 12 sets out a roadmap that begins with human tissue and longitudinal model systems, then moves through a proteoform-resolved atlas, causal perturbation, state-specific assays, modality selection, computation, delivery, and target engagement, with failure branches returning information to the atlas. The roadmap is an iterative program and not a linear promise of translation, and in it many candidates should stop when chemistry, localization, causality, selectivity, or exposure cannot be demonstrated. Near-term priorities follow from the gaps identified above. Reference materials for modified sites and shared intact-proteoform standards are prerequisites for comparing laboratories at all [20]. Region and cell-type-resolved turnover maps extend what current rodent atlases provide toward human tissue [8,9]. Perturbation systems that install or repair defined states remain the limiting reagent for causal work [15]. The next layer requires assays that compare aged and functional pools directly, together with pharmacodynamic measurements in the brain. Machine learning should be evaluated prospectively under leakage-resistant splits [22], and quantum work should focus on small molecular tasks with chemical-accuracy targets and published resource estimates [23]. These milestones are measurable and remain useful even if a therapeutic program fails. The conclusion they support is narrow but consequential: a long-lived or age-associated protein is not automatically a drug target. The target becomes credible when a specific molecular state is detected, localized, connected causally to dysfunction, selectively engaged, and modulated without unacceptable loss of function. Molecular time therefore changes target identity before it changes modality. Machine learning can help resolve and prioritize that identity. Classical quantum chemistry can interrogate selected mechanisms, and quantum computing may eventually contribute to carefully reduced tasks. None of these methods can replace the experimental evidence that defines which old protein state should be changed, in which cell, at what stage, and in which direction.

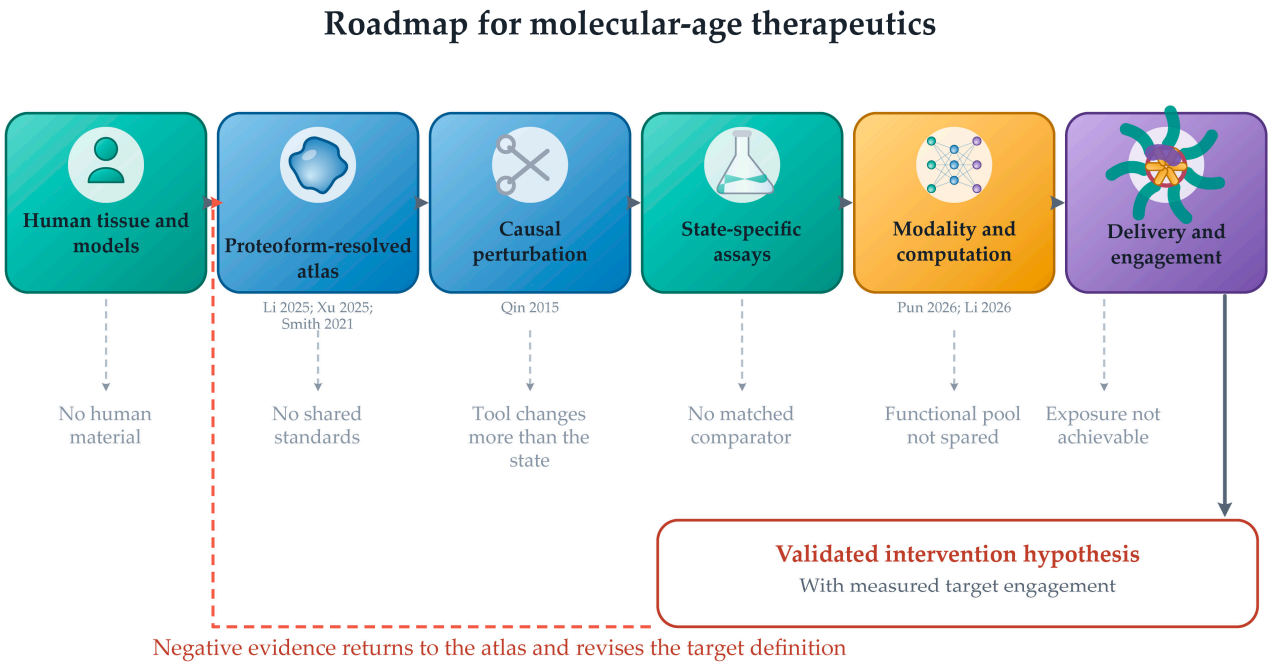


Figure 12. Roadmap for molecular-age therapeutics. Human tissue and longitudinal model systems feed a proteoform-resolved atlas [8,19,20], causal perturbation [15], state-specific assays, modality selection, computation [22,23], delivery, and brain target engagement. Feedback arrows and stopped branches preserve negative evidence and allow target definitions to be revised. The endpoint is a validated intervention hypothesis with measured engagement, not a predicted cure or a fixed clinical timeline.

Author Contributions: Conceptualization, R.A. and K.S.A.; literature search and screening, R.A., S.A.A. and A.A.A.; evidence synthesis and interpretation, R.A., M.A., W.A.A. and M.A.K.; writing—original draft preparation, R.A.; writing—review and editing, K.S.A., M.A.K., A.K., M.A., W.A.A., S.A.A. and A.A.A.; visualization, A.A.A., W.A.A. and A.K.; supervision, K.S.A.; project administration, R.A. and K.S.A.; funding acquisition, K.S.A. All authors have read and agreed to the published version of the manuscript.

Funding: This research received no external funding. The article processing charge (APC) was funded by the Deanship of Graduate Studies and Scientific Research, Qassim University, under grant number QU-APC-2026.

Institutional Review Board Statement: Not applicable.

Informed Consent Statement: Not applicable.

Data Availability Statement: No new data were created or analysed in this study. All data discussed are available in the cited published articles. The atomic coordinates used to draw the structural inset in Figure 3 are available from the Protein Data Bank under accession 2WJ7. Data sharing is therefore not applicable to this article.

Acknowledgments: The Researchers would like to thank the Deanship of Graduate Studies and Scientific Research at Qassim University (https://www.qu.edu.sa) for financial support (QU-APC-2026). Nano Banana Pro (Gemini 3 Pro Image; Google, Mountain View, CA, USA) was used to generate illustrative icons for the graphical abstract. Figures 1–12 were created by the authors without generative AI. The authors reviewed all AI-generated icons and take full responsibility for the scientific accuracy and integrity of the manuscript.

Conflicts of Interest: The authors declare no conflicts of interest.

References

1. Savas, J.N.; Toyama, B.H.; Xu, T.; Yates, J.R., 3rd; Hetzer, M.W. Extremely long-lived nuclear pore proteins in the rat brain. *Science* **2012**, *335*, 942. [CrossRef] [PubMed]
2. Toyama, B.H.; Savas, J.N.; Park, S.K.; Harris, M.S.; Ingolia, N.T.; Yates, J.R., 3rd; Hetzer, M.W. Identification of long-lived proteins reveals exceptional stability of essential cellular structures. *Cell* **2013**, *154*, 971–982. [CrossRef] [PubMed]
3. Fornasiero, E.F.; Mandad, S.; Wildhagen, H.; Alevra, M.; Rammner, B.; Keihani, S.; Opazo, F.; Urban, I.; Ischebeck, T.; Sakib, M.S.; et al. Precisely measured protein lifetimes in the mouse brain reveal differences across tissues and subcellular fractions. *Nat. Commun.* **2018**, *9*, 4230. [CrossRef] [PubMed]
4. Krishna, S.; Arrojo, E.D.R.; Capitanio, J.S.; Ramachandra, R.; Ellisman, M.; Hetzer, M.W. Identification of long-lived proteins in the mitochondria reveals increased stability of the electron transport chain. *Dev. Cell* **2021**, *56*, 2952–2965.e9. [CrossRef] [PubMed]
5. Bulovaite, E.; Qiu, Z.; Kratschke, M.; Zgraj, A.; Fricker, D.G.; Tuck, E.J.; Gokhale, R.; Koniaris, B.; Jami, S.A.; Merino-Serrais, P.; et al. A brain atlas of synapse protein lifetime across the mouse lifespan. *Neuron* **2022**, *110*, 4057–4073.e8. [CrossRef] [PubMed]
6. Kluever, V.; Russo, B.; Mandad, S.; Kumar, N.H.; Alevra, M.; Ori, A.; Rizzoli, S.O.; Urlaub, H.; Schneider, A.; Fornasiero, E.F. Protein lifetimes in aged brains reveal a proteostatic adaptation linking physiological aging to neurodegeneration. *Sci. Adv.* **2022**, *8*, eabn4437. [CrossRef] [PubMed]
7. Rao, N.R.; Upadhyay, A.; Savas, J.N. Derailed protein turnover in the aging mammalian brain. *Mol. Syst. Biol.* **2024**, *20*, 120–139. [CrossRef] [PubMed]
8. Li, W.; Dasgupta, A.; Yang, K.; Wang, S.; Hemandhar-Kumar, N.; Chepyala, S.R.; Yarbro, J.M.; Hu, Z.; Salovska, B.; Fornasiero, E.F.; et al. Turnover atlas of proteome and phosphoproteome across mouse tissues and brain regions. *Cell* **2025**, *188*, 2267–2287.e21. [CrossRef] [PubMed]
9. Guldner, I.H.; Wagner, V.P.; Moran-Losada, P.; Shi, S.M.; Golub, S.W.; Hevler, J.F.; Chen, K.; Meese, B.T.; Ghoochani, A.; Pulido, E.; et al. Ageing promotes microglial accumulation of slow-degrading synaptic proteins. *Nature* **2026**, *650*, 930–941. [CrossRef] [PubMed]
10. Kelmer Sacramento, E.; Kirkpatrick, J.M.; Mazzetto, M.; Baumgart, M.; Bartolome, A.; Di Sanzo, S.; Caterino, C.; Sanguanini, M.; Papaevgeniou, N.; Lefaki, M.; et al. Reduced proteasome activity in the aging brain results in ribosome stoichiometry loss and aggregation. *Mol. Syst. Biol.* **2020**, *16*, e9596. [CrossRef] [PubMed]
11. Ding, Y.; Zuo, Y.; Zhang, B.; Fan, Y.; Xu, G.; Cheng, Z.; Ma, S.; Fang, S.; Tian, A.; Gao, D.; et al. Comprehensive human proteome profiles across a 50-year lifespan reveal aging trajectories and signatures. *Cell* **2025**, *188*, 5763–5784.e26. [CrossRef] [PubMed]
12. Baldensperger, T.; Preissler, M.; Becker, C.F.W. Non-enzymatic posttranslational protein modifications in protein aggregation and neurodegenerative diseases. *RSC Chem. Biol.* **2025**, *6*, 129–149. [CrossRef] [PubMed]
13. Reissner, K.J.; Aswad, D.W. Deamidation and isoaspartate formation in proteins: Unwanted alterations or surreptitious signals? *Cell Mol. Life Sci.* **2003**, *60*, 1281–1295. [CrossRef] [PubMed]
14. Shimizu, T.; Matsuoka, Y.; Shirasawa, T. Biological significance of isoaspartate and its repair system. *Biol. Pharm. Bull.* **2005**, *28*, 1590–1596. [CrossRef] [PubMed]
15. Qin, Z.; Dimitrijevic, A.; Aswad, D.W. Accelerated protein damage in brains of PIMT+/− mice; a possible model for the variability of cognitive decline in human aging. *Neurobiol. Aging* **2015**, *36*, 1029–1036. [CrossRef] [PubMed]
16. Smith, L.M.; Kelleher, N.L. The Consortium for Top Down Proteomics. Proteoform: A single term describing protein complexity. *Nat. Methods* **2013**, *10*, 186–187. [CrossRef] [PubMed]
17. Aebersold, R.; Agar, J.N.; Amster, I.J.; Baker, M.S.; Bertozzi, C.R.; Boja, E.S.; Costello, C.E.; Cravatt, B.F.; Fenselau, C.; Garcia, B.A.; et al. How many human proteoforms are there? *Nat. Chem. Biol.* **2018**, *14*, 206–214. [CrossRef] [PubMed]
18. Schaffer, L.V.; Millikin, R.J.; Miller, R.M.; Anderson, L.C.; Fellers, R.T.; Ge, Y.; Kelleher, N.L.; LeDuc, R.D.; Liu, X.; Payne, S.H.; et al. Identification and Quantification of Proteoforms by Mass Spectrometry. *Proteomics* **2019**, *19*, e1800361. [CrossRef] [PubMed]
19. Xu, T.; Su, T.; Soye, B.J.D.; Kandi, S.; Huang, C.F.; Wilkins, J.T.; Castellani, R.J.; Kafader, J.O.; Patrie, S.M.; Vassar, R.; et al. The Proteoform Landscape of Tau from the Human Brain. *J. Proteome Res.* **2025**, *24*, 2916–2925. [CrossRef] [PubMed]
20. Smith, L.M.; Agar, J.N.; Chamot-Rooke, J.; Danis, P.O.; Ge, Y.; Loo, J.A.; Pasa-Tolic, L.; Tsybin, Y.O.; Kelleher, N.L. The Consortium for Top Down Proteomics. The Human Proteoform Project: Defining the human proteome. *Sci. Adv.* **2021**, *7*, eabk0734. [CrossRef] [PubMed]
21. Sun, Y.; A, J.; Liu, Z.; Sun, R.; Qian, L.; Payne, S.H.; Bittremieux, W.; Ralser, M.; Li, C.; Chen, Y.; et al. AI proteomics: From protein identification to virtual cells. *Nat. Methods* **2026**, *23*, 1697–1709. [CrossRef] [PubMed]
22. Pun, F.W.; Podolskiy, D.; Izumchenko, E.; Mortlock, A.; Oprea, T.I.; Scheibye-Knudsen, M.; Fortney, K.; Morgen, E.; Ren, F.; Zhavoronkov, A. Target identification and assessment in the era of AI. *Nat. Rev. Drug Discov.* **2026**, *25*, 534–552. [CrossRef] [PubMed]
23. Li, J.; Wei, L.; Tong, H.H.Y.; Zou, Q. Quantum computing applications in drug discovery. *Brief. Bioinform.* **2026**, *27*, bbag274. [CrossRef] [PubMed]

24. Liu, J.; Hetzer, M.W. Nuclear pore complex maintenance and implications for age-related diseases. *Trends Cell Biol.* **2022**, *32*, 216–227. [CrossRef] [PubMed]
25. Jiang, S.; Srikanth, M.; Serpe, R.; Yavari, S.; Gaur, P.; Collins, G.A.; Soni, R.; Menon, V.; Myeku, N. Early proteasome downregulation and dysfunction drive proteostasis failure in Alzheimer's disease. *Brain* **2025**, *148*, 4372–4388. [CrossRef] [PubMed]
26. Stavoe, A.K.H.; Holzbaur, E.L.F. Autophagy in Neurons. *Annu. Rev. Cell Dev. Biol.* **2019**, *35*, 477–500. [CrossRef] [PubMed]
27. Polidori, M.C. Embracing complexity of (brain) aging. *FEBS Lett.* **2024**, *598*, 2067–2073. [CrossRef] [PubMed]
28. Hawkins, C.L.; Davies, M.J. Detection, identification, and quantification of oxidative protein modifications. *J. Biol. Chem.* **2019**, *294*, 19683–19708. [CrossRef] [PubMed]
29. Ott, C.; Jacobs, K.; Haucke, E.; Navarrete Santos, A.; Grune, T.; Simm, A. Role of advanced glycation end products in cellular signaling. *Redox Biol.* **2014**, *2*, 411–429. [CrossRef] [PubMed]
30. Yamashima, T. Can 'calpain-cathepsin hypothesis' explain Alzheimer neuronal death? *Ageing Res. Rev.* **2016**, *32*, 169–179. [CrossRef] [PubMed]
31. Fuentes-Lemus, E.; Hagglund, P.; Lopez-Alarcon, C.; Davies, M.J. Oxidative Crosslinking of Peptides and Proteins: Mechanisms of Formation, Detection, Characterization and Quantification. *Molecules* **2021**, *27*, 15. [CrossRef] [PubMed]
32. Akan, I.; Olivier-Van Stichelen, S.; Bond, M.R.; Hanover, J.A. Nutrient-driven O-GlcNAc in proteostasis and neurodegeneration. *J. Neurochem.* **2018**, *144*, 7–34. [CrossRef] [PubMed]
33. Lee, B.E.; Suh, P.G.; Kim, J.I. O-GlcNAcylation in health and neurodegenerative diseases. *Exp. Mol. Med.* **2021**, *53*, 1674–1682. [CrossRef] [PubMed]
34. Mishra, P.K.K.; Mahawar, M. PIMT-Mediated Protein Repair: Mechanism and Implications. *Biochemistry* **2019**, *84*, 453–463. [CrossRef] [PubMed]
35. Chatterjee, T.; Das, G.; Chatterjee, B.K.; Dhar, J.; Ghosh, S.; Chakrabarti, P. The role of isoaspartate in fibrillation and its prevention by Protein-L-isoaspartyl methyltransferase. *Biochim. Biophys. Acta Gen. Subj.* **2020**, *1864*, 129500. [CrossRef] [PubMed]
36. Wang, J.; Mukherjee, S.; Zubarev, R.A. Isoaspartate and neurodegeneration. *Aging* **2022**, *14*, 8882–8883. [CrossRef] [PubMed]
37. Wang, J.; Guo, C.; Meng, Z.; Zwan, M.D.; Chen, X.; Seelow, S.; Lundstrom, S.L.; Rodin, S.; Teunissen, C.E.; Zubarev, R.A. Testing the link between isoaspartate and Alzheimer's disease etiology. *Alzheimer's Dement.* **2023**, *19*, 1491–1502. [CrossRef] [PubMed]
38. Deol, K.K.; Strieter, E.R. The ubiquitin proteoform problem. *Curr. Opin. Chem. Biol.* **2021**, *63*, 95–104. [CrossRef] [PubMed]
39. Zhou, H.; Ning, Z.; Starr, A.E.; Abu-Farha, M.; Figeys, D. Advancements in top-down proteomics. *Anal. Chem.* **2012**, *84*, 720–734. [CrossRef] [PubMed]
40. Kaulich, P.T.; Tholey, A. Top-Down Proteomics: Why and When? *Proteomics* **2025**, *25*, 6–12. [CrossRef] [PubMed]
41. Ellis, M.J.; Lekka, C.; Holden, K.L.; Tulmin, H.; Seedat, F.; O'Brien, D.P.; Dhayal, S.; Zeissler, M.L.; Knudsen, J.G.; Kessler, B.M.; et al. Identification of high-performing antibodies for the reliable detection of Tau proteoforms by Western blotting and immunohistochemistry. *Acta Neuropathol.* **2024**, *147*, 87. [CrossRef] [PubMed]
42. Zhu, K.F.; Yuan, C.; Du, Y.M.; Sun, K.L.; Zhang, X.K.; Vogel, H.; Jia, X.D.; Gao, Y.Z.; Zhang, Q.F.; Wang, D.P.; et al. Applications and prospects of cryo-EM in drug discovery. *Mil. Med. Res.* **2023**, *10*, 10. [CrossRef] [PubMed]
43. Kumar, M.; Schlaffner, C.N.; Tang, S.; Beuvink, M.A.; Viode, A.; Mair, W.; Jha, M.; Uncu, C.; Wesseling, H.; Wang, T.; et al. Molecular features of human pathological tau distinguish tauopathy-associated dementias. *Cell* **2026**, *189*, 956–968.e13. [CrossRef] [PubMed]
44. Lantero-Rodriguez, J.; Camporesi, E.; Montoliu-Gaya, L.; Gobom, J.; Piotrowska, D.; Olsson, M.; Burmann, I.M.; Becker, B.; Brinkmalm, A.; Burmann, B.M.; et al. Tau protein profiling in tauopathies: A human brain study. *Mol. Neurodegener.* **2024**, *19*, 54. [CrossRef] [PubMed]
45. Noor, A.; Zafar, S.; Zerr, I. Neurodegenerative Proteinopathies in the Proteoform Spectrum-Tools and Challenges. *Int. J. Mol. Sci.* **2021**, *22*, 1085. [CrossRef] [PubMed]
46. Sulimov, V.B.; Kutov, D.C.; Sulimov, A.V. Advances in Docking. *Curr. Med. Chem.* **2019**, *26*, 7555–7580. [CrossRef] [PubMed]
47. Chen, Y.R.; Harel, I.; Singh, P.P.; Ziv, I.; Moses, E.; Goshtchevsky, U.; Machado, B.E.; Brunet, A.; Jarosz, D.F. Tissue-specific landscape of protein aggregation and quality control in an aging vertebrate. *Dev. Cell* **2024**, *59*, 1892–1911.e13. [CrossRef] [PubMed]
48. Oh, H.S.; Rutledge, J.; Nachun, D.; Palovics, R.; Abiose, O.; Moran-Losada, P.; Channappa, D.; Urey, D.Y.; Kim, K.; Sung, Y.J.; et al. Organ aging signatures in the plasma proteome track health and disease. *Nature* **2023**, *624*, 164–172. [CrossRef] [PubMed]
49. Alecki, C.; Rizwan, J.; Le, P.; Jacob-Tomas, S.; Comaduran, M.F.; Verbrugghe, M.; Xu, J.M.S.; Minotti, S.; Lynch, J.; Biswas, J.; et al. Localized molecular chaperone synthesis maintains neuronal dendrite proteostasis. *Nat. Commun.* **2024**, *15*, 10796. [CrossRef] [PubMed]
50. Di Fraia, D.; Marino, A.; Lee, J.H.; Kelmer Sacramento, E.; Baumgart, M.; Bagnoli, S.; Balla, T.; Schalk, F.; Kamrad, S.; Guan, R.; et al. Altered translation elongation contributes to key hallmarks of aging in the killifish brain. *Science* **2025**, *389*, eadk3079. [CrossRef] [PubMed]
51. Dionne, O.; Laurent, B. Translational traffic jam in aging brains. *Science* **2025**, *389*, 457–458. [CrossRef] [PubMed]

52. Lee, J.; Lee, B.; Lee, H.; Kim, E.J.E.; Kim, S.S.; Kwon, H.C.; Lee, H.; Lee, G.Y.; Hong, W.; Ham, S.; et al. Pelota-mediated ribosome-associated quality control counteracts aging and age-associated pathologies across species. *Proc. Natl. Acad. Sci. USA* **2025**, *122*, e2505217122. [CrossRef] [PubMed]
53. Karpova, A.; Hiesinger, P.R.; Kuijpers, M.; Albrecht, A.; Kirstein, J.; Andres-Alonso, M.; Biermeier, A.; Eickholt, B.J.; Mikhaylova, M.; Maglione, M.; et al. Neuronal autophagy in the control of synapse function. *Neuron* **2025**, *113*, 974–990. [CrossRef] [PubMed]
54. Bourdenx, M.; Martin-Segura, A.; Scrivo, A.; Rodriguez-Navarro, J.A.; Kaushik, S.; Tasset, I.; Diaz, A.; Storm, N.J.; Xin, Q.; Juste, Y.R.; et al. Chaperone-mediated autophagy prevents collapse of the neuronal metastable proteome. *Cell* **2021**, *184*, 2696–2714.e25. [CrossRef] [PubMed]
55. Fogo, G.M.; Raghunayakula, S.; Emaus, K.J.; Torres Torres, F.J.; Shangguan, G.; Wider, J.M.; Huttemann, M.; Sanderson, T.H. Mitochondrial dynamics and quality control regulate proteostasis in neuronal ischemia-reperfusion. *Autophagy* **2025**, *21*, 1492–1506. [CrossRef] [PubMed]
56. Antal, B.B.; van Nieuwenhuizen, H.; Chesebro, A.G.; Strey, H.H.; Jones, D.T.; Clarke, K.; Weistuch, C.; Ratai, E.M.; Dill, K.A.; Mujica-Parodi, L.R. Brain aging shows nonlinear transitions, suggesting a midlife "critical window" for metabolic intervention. *Proc. Natl. Acad. Sci. USA* **2025**, *122*, e2416433122. [CrossRef] [PubMed]
57. Cozachenco, D.; Ribeiro, F.C.; Ferreira, S.T. Defective proteostasis in Alzheimer's disease. *Ageing Res. Rev.* **2023**, *85*, 101862. [CrossRef] [PubMed]
58. Kurtishi, A.; Rosen, B.; Patil, K.S.; Alves, G.W.; Moller, S.G. Cellular Proteostasis in Neurodegeneration. *Mol. Neurobiol.* **2019**, *56*, 3676–3689. [CrossRef] [PubMed]
59. Chou, C.C.; Vest, R.; Prado, M.A.; Wilson-Grady, J.; Paulo, J.A.; Shibuya, Y.; Moran-Losada, P.; Lee, T.T.; Luo, J.; Gygi, S.P.; et al. Proteostasis and lysosomal repair deficits in transdifferentiated neurons of Alzheimer's disease. *Nat. Cell Biol.* **2025**, *27*, 619–632. [CrossRef] [PubMed]
60. Samelson, A.J.; Ariqat, N.; McKetney, J.; Rohanitazangi, G.; Parra Bravo, C.; Bose, R.S.; Travaglini, K.J.; Lam, V.L.; Goodness, D.; Ta, T.; et al. CRISPR screens in iPSC-derived neurons reveal principles of tau proteostasis. *Cell* **2026**, *189*, 1517–1534.e19. [CrossRef] [PubMed]
61. Fernandes, V.; Choudhary, M.; Kumar, A.; Singh, S.B. Proteotoxicity and mitochondrial dynamics in aging diabetic brain. *Pharmacol. Res.* **2020**, *159*, 104948. [CrossRef] [PubMed]
62. Mackiewicz, M.M.; Overk, C.; Achim, C.L.; Masliah, E. Pathogenesis of age-related HIV neurodegeneration. *J. Neurovirol.* **2019**, *25*, 622–633. [CrossRef] [PubMed]
63. Akbar, M.; Toppo, P.; Nazir, A. Ageing, proteostasis, and the gut: Insights into neurological health and disease. *Ageing Res. Rev.* **2024**, *101*, 102504. [CrossRef] [PubMed]
64. Zullo, J.M.; Drake, D.; Aron, L.; O'Hern, P.; Dhamne, S.C.; Davidsohn, N.; Mao, C.A.; Klein, W.H.; Rotenberg, A.; Bennett, D.A.; et al. Regulation of lifespan by neural excitation and REST. *Nature* **2019**, *574*, 359–364. [CrossRef] [PubMed]
65. Lu, T.; Aron, L.; Zullo, J.; Pan, Y.; Kim, H.; Chen, Y.; Yang, T.H.; Kim, H.M.; Drake, D.; Liu, X.S.; et al. REST and stress resistance in ageing and Alzheimer's disease. *Nature* **2014**, *507*, 448–454. [CrossRef] [PubMed]
66. Ai, R.; Fang, E.F. NAD^+ restores proteostasis through splicing-dependent autophagy. *Autophagy* **2026**, *22*, 436–438. [CrossRef] [PubMed]
67. Yasa, S.; Butz, E.S.; Colombo, A.; Chandrachud, U.; Montore, L.; Tschirner, S.; Prestel, M.; Sheridan, S.D.; Muller, S.A.; Groh, J.; et al. Loss of CLN3 in microglia leads to impaired lipid metabolism and myelin turnover. *Commun. Biol.* **2024**, *7*, 1373. [CrossRef] [PubMed]
68. Stadtman, E.R. Protein oxidation in aging and age-related diseases. *Ann. N. Y. Acad. Sci.* **2001**, *928*, 22–38. [CrossRef] [PubMed]
69. Stadtman, E.R.; Berlett, B.S. Reactive oxygen-mediated protein oxidation in aging and disease. *Drug Metab. Rev.* **1998**, *30*, 225–243. [CrossRef] [PubMed]
70. Lopes, F.; Schlatzer, D.; Li, M.; Yilmaz, S.; Wang, R.; Qi, X.; Ayati, M.; Koyuturk, M.; Chance, M.R. Methionine Sulfoxide Speciation in Mouse Hippocampus Revealed by Global Proteomics Exhibits Age- and Alzheimer's Disease-Dependent Changes Targeted to Mitochondrial and Glycolytic Pathways. *Int. J. Mol. Sci.* **2024**, *25*, 6516. [CrossRef] [PubMed]
71. Iskusnykh, I.Y.; Zakharova, A.A.; Pathak, D. Glutathione in Brain Disorders and Aging. *Molecules* **2022**, *27*, 324. [CrossRef] [PubMed]
72. Feeney, M.B.; Schoneich, C. Tyrosine modifications in aging. *Antioxid. Redox Signal.* **2012**, *17*, 1571–1579. [CrossRef] [PubMed]
73. Frazzini, V.; Rockabrand, E.; Mocchegiani, E.; Sensi, S.L. Oxidative stress and brain aging: Is zinc the link? *Biogerontology* **2006**, *7*, 307–314. [CrossRef] [PubMed]
74. Perluigi, M.; Swomley, A.M.; Butterfield, D.A. Redox proteomics and the dynamic molecular landscape of the aging brain. *Ageing Res. Rev.* **2014**, *13*, 75–89. [CrossRef] [PubMed]
75. Sultana, R.; Butterfield, D.A. Protein Oxidation in Aging and Alzheimer's Disease Brain. *Antioxidants* **2024**, *13*, 574. [CrossRef] [PubMed]

76. Malorny, N.; Chausse, B.; Khodaie, B.; Elgez, A.; Soder, L.; Lewen, A.; Egorov, A.V.; Kann, O. TNF-alpha and IFN-gamma impair neural oscillations and induce neurodegeneration by microglial nitric oxide, metabolic and oxidative stress. *J. Neuroinflamm.* **2026**, *23*, 160. [CrossRef] [PubMed]
77. Nalivaeva, N.N.; Turner, A.J. Role of Ageing and Oxidative Stress in Regulation of Amyloid-Degrading Enzymes and Development of Neurodegeneration. *Curr. Aging Sci.* **2017**, *10*, 32–40. [CrossRef] [PubMed]
78. Zhang, S.; Rocourt, C.; Cheng, W.H. Selenoproteins and the aging brain. *Mech. Ageing Dev.* **2010**, *131*, 253–260. [CrossRef] [PubMed]
79. van Boekel, M.A. The role of glycation in aging and diabetes mellitus. *Mol. Biol. Rep.* **1991**, *15*, 57–64. [CrossRef] [PubMed]
80. Sirangelo, I.; Iannuzzi, C. Understanding the Role of Protein Glycation in the Amyloid Aggregation Process. *Int. J. Mol. Sci.* **2021**, *22*, 6609. [CrossRef] [PubMed]
81. Gao, Q.; Jacob-Dolan, J.W.; Scheck, R.A. Parkinsonism-Associated Protein DJ-1 Is an Antagonist, Not an Eraser, for Protein Glycation. *Biochemistry* **2023**, *62*, 1181–1190. [CrossRef] [PubMed]
82. Griffin, M.; Casadio, R.; Bergamini, C.M. Transglutaminases: Nature's biological glues. *Biochem. J.* **2002**, *368*, 377–396. [CrossRef] [PubMed]
83. Beretta, C.; Svensson, E.; Dakhel, A.; Zysk, M.; Hanrieder, J.; Sehlin, D.; Michno, W.; Erlandsson, A. Amyloid-beta deposits in human astrocytes contain truncated and highly resistant proteoforms. *Mol. Cell. Neurosci.* **2024**, *128*, 103916. [CrossRef] [PubMed]
84. Chen, D.; Geis-Asteggiante, L.; Gomes, F.P.; Ostrand-Rosenberg, S.; Fenselau, C. Top-Down Proteomic Characterization of Truncated Proteoforms. *J. Proteome Res.* **2019**, *18*, 4013–4019. [CrossRef] [PubMed]
85. Bassnett, S. On the mechanism of organelle degradation in the vertebrate lens. *Exp. Eye Res.* **2009**, *88*, 133–139. [CrossRef] [PubMed]
86. Lynnerup, N.; Kjeldsen, H.; Heegaard, S.; Jacobsen, C.; Heinemeier, J. Radiocarbon dating of the human eye lens crystallines reveal proteins without carbon turnover throughout life. *PLoS ONE* **2008**, *3*, e1529. [CrossRef] [PubMed]
87. Masters, P.M.; Bada, J.L.; Zigler, J.S., Jr. Aspartic acid racemisation in the human lens during ageing and in cataract formation. *Nature* **1977**, *268*, 71–73. [CrossRef] [PubMed]
88. Wilmarth, P.A.; Tanner, S.; Dasari, S.; Nagalla, S.R.; Riviere, M.A.; Bafna, V.; Pevzner, P.A.; David, L.L. Age-related changes in human crystallins determined from comparative analysis of post-translational modifications in young and aged lens: Does deamidation contribute to crystallin insolubility? *J. Proteome Res.* **2006**, *5*, 2554–2566. [CrossRef] [PubMed]
89. Truscott, R.J.W.; Friedrich, M.G. Molecular Processes Implicated in Human Age-Related Nuclear Cataract. *Investig. Ophthalmol. Vis. Sci.* **2019**, *60*, 5007–5021. [CrossRef] [PubMed]
90. Lampi, K.J.; Wilmarth, P.A.; Murray, M.R.; David, L.L. Lens beta-crystallins: The role of deamidation and related modifications in aging and cataract. *Prog. Biophys. Mol. Biol.* **2014**, *115*, 21–31. [CrossRef] [PubMed]
91. Gupta, R.; Srivastava, O.P. Effect of deamidation of asparagine 146 on functional and structural properties of human lens alphaB-crystallin. *Investig. Ophthalmol. Vis. Sci.* **2004**, *45*, 206–214. [CrossRef] [PubMed]
92. Benedek, G.B. Theory of transparency of the eye. *Appl. Opt.* **1971**, *10*, 459–473. [CrossRef] [PubMed]
93. Giandomenico, S.L.; Alvarez-Castelao, B.; Schuman, E.M. Proteostatic regulation in neuronal compartments. *Trends Neurosci.* **2022**, *45*, 41–52. [CrossRef] [PubMed]
94. Wen, B.; Zeng, W.F.; Liao, Y.; Shi, Z.; Savage, S.R.; Jiang, W.; Zhang, B. Deep Learning in Proteomics. *Proteomics* **2020**, *20*, e1900335. [CrossRef] [PubMed]
95. Dai, Y.; Yang, Y.; Wu, E.; Shen, C.; Qiao, L. Deep Learning Powers Protein Identification from Precursor MS Information. *J. Proteome Res.* **2024**, *23*, 3837–3846. [CrossRef] [PubMed]
96. Nickerson, J.L.; Baghalabadi, V.; Rajendran, S.; Jakubec, P.J.; Said, H.; McMillen, T.S.; Dang, Z.; Doucette, A.A. Recent advances in top-down proteome sample processing ahead of MS analysis. *Mass Spectrom. Rev.* **2023**, *42*, 457–495. [CrossRef] [PubMed]
97. Cupp-Sutton, K.A.; Wu, S. High-throughput quantitative top-down proteomics. *Mol. Omics* **2020**, *16*, 91–99. [CrossRef] [PubMed]
98. Miller, S.A.; Jeanne Dit Fouque, K.; Hard, E.R.; Balana, A.T.; Kaplan, D.; Voinov, V.G.; Ridgeway, M.E.; Park, M.A.; Anderson, G.A.; Pratt, M.R.; et al. Top/Middle-Down Characterization of alpha-Synuclein Glycoforms. *Anal. Chem.* **2023**, *95*, 18039–18045. [CrossRef] [PubMed]
99. Bennett, J.L.; El-Baba, T.J.; Zouboulis, K.C.; Kirschbaum, C.; Song, H.; Butroid, F.I.; Benesch, J.L.P.; Lutomski, C.A.; Robinson, C.V. Uncovering hidden protein modifications with native top-down mass spectrometry. *Nat. Methods* **2025**, *22*, 2127–2137. [CrossRef] [PubMed]
100. de Souza, N.; Picotti, P. Mass spectrometry analysis of the structural proteome. *Curr. Opin. Struct. Biol.* **2020**, *60*, 57–65. [CrossRef] [PubMed]
101. Su, P.; Hollas, M.A.R.; Butun, F.A.; Kanchustambham, V.L.; Rubakhin, S.; Ramani, N.; Greer, J.B.; Early, B.P.; Fellers, R.T.; Caldwell, M.A.; et al. Single Cell Analysis of Proteoforms. *J. Proteome Res.* **2024**, *23*, 1883–1893. [CrossRef] [PubMed]

102. Rossetti, D.V.; Inserra, I.; Nestico, A.; Vincenzoni, F.; Iavarone, F.; Messana, I.; Castagnola, M.; Massimi, L.; Tamburrini, G.; Caldarelli, M.; et al. Pediatric Brain Tumors: Signatures from the Intact Proteome. *Int. J. Mol. Sci.* **2022**, *23*, 3196. [CrossRef] [PubMed]
103. Lundberg, E.; Borner, G.H.H. Spatial proteomics: A powerful discovery tool for cell biology. *Nat. Rev. Mol. Cell Biol.* **2019**, *20*, 285–302. [CrossRef] [PubMed]
104. Mund, A.; Brunner, A.D.; Mann, M. Unbiased spatial proteomics with single-cell resolution in tissues. *Mol. Cell* **2022**, *82*, 2335–2349. [CrossRef] [PubMed]
105. Hu, B.; He, R.; Pang, K.; Wang, G.; Wang, N.; Zhu, W.; Sui, X.; Teng, H.; Liu, T.; Zhu, J.; et al. High-resolution spatially resolved proteomics of complex tissues based on microfluidics and transfer learning. *Cell* **2025**, *188*, 734–748.e22. [CrossRef] [PubMed]
106. Bhatia, H.S.; Brunner, A.D.; Ozturk, F.; Kapoor, S.; Rong, Z.; Mai, H.; Thielert, M.; Ali, M.; Al-Maskari, R.; Paetzold, J.C.; et al. Spatial proteomics in three-dimensional intact specimens. *Cell* **2022**, *185*, 5040–5058.e19. [CrossRef] [PubMed]
107. Yang, M.; Hu, H.; Su, P.; Thomas, P.M.; Camarillo, J.M.; Greer, J.B.; Early, B.P.; Fellers, R.T.; Kelleher, N.L.; Laskin, J. Proteoform-Selective Imaging of Tissues Using Mass Spectrometry. *Angew. Chem. Int. Ed. Engl.* **2022**, *61*, e202200721. [CrossRef] [PubMed]
108. Rosenberger, F.A.; Madler, S.C.; Thorhauge, K.H.; Steigerwald, S.; Fromme, M.; Lebedev, M.; Weiss, C.A.M.; Oeller, M.; Wahle, M.; Metousis, A.; et al. Deep Visual Proteomics maps proteotoxicity in a genetic liver disease. *Nature* **2025**, *642*, 484–491. [CrossRef] [PubMed]
109. Tsour, S.; Machne, R.; Leduc, A.; Widmer, S.; Koo, E.; Guez, J.; Karczewski, K.J.; Slavov, N. Alternate RNA decoding results in stable and abundant proteins in mammals. *Nature* **2026**, *656*, 506–515. [CrossRef] [PubMed]
110. Fitzpatrick, A.W.P.; Falcon, B.; He, S.; Murzin, A.G.; Murshudov, G.; Garringer, H.J.; Crowther, R.A.; Ghetti, B.; Goedert, M.; Scheres, S.H.W. Cryo-EM structures of tau filaments from Alzheimer's disease. *Nature* **2017**, *547*, 185–190. [CrossRef] [PubMed]
111. Serdiuk, T.; Redeker, V.; Savistchenko, J.; Neupane, S.; Haenseler, W.; Fleischmann, Y.; Reber, V.; Keller, S.; Tiberi, C.; Bachmann-Gagescu, R.; et al. Structure-function relationship of alpha-synuclein fibrillar polymorphs derived from distinct synucleinopathies. *Mol. Syst. Biol.* **2026**, *22*, 868–901. [CrossRef] [PubMed]
112. Bido, S.; Muggeo, S.; Massimino, L.; Marzi, M.J.; Giannelli, S.G.; Melacini, E.; Nannoni, M.; Gambare, D.; Bellini, E.; Ordazzo, G.; et al. Microglia-specific overexpression of alpha-synuclein leads to severe dopaminergic neurodegeneration by phagocytic exhaustion and oxidative toxicity. *Nat. Commun.* **2021**, *12*, 6237. [CrossRef] [PubMed]
113. Yoshiyama, Y.; Higuchi, M.; Zhang, B.; Huang, S.M.; Iwata, N.; Saido, T.C.; Maeda, J.; Suhara, T.; Trojanowski, J.Q.; Lee, V.M. Synapse loss and microglial activation precede tangles in a P301S tauopathy mouse model. *Neuron* **2007**, *53*, 337–351. [CrossRef] [PubMed]
114. Morrone Parfitt, G.; Coccia, E.; Goldman, C.; Whitney, K.; Reyes, R.; Sarrafha, L.; Nam, K.H.; Sohail, S.; Jones, D.R.; Crary, J.F.; et al. Disruption of lysosomal proteolysis in astrocytes facilitates midbrain organoid proteostasis failure in an early-onset Parkinson's disease model. *Nat. Commun.* **2024**, *15*, 447. [CrossRef] [PubMed]
115. Gross, A.S.; Graef, M. Stress eating: Autophagy targets nuclear pore complexes. *J. Cell Biol.* **2020**, *219*, e202006007. [CrossRef] [PubMed]
116. Kozai, T.; Fernandez-Martinez, J.; Kapinos, L.E.; Gallardo, P.; van Eeuwen, T.; Saladin, M.; Eliasian, R.; Mazur, A.; Zhang, W.; Tempkin, J.; et al. Karyopherins remodel the dynamic organization of the nuclear pore complex transport barrier. *Nat. Cell Biol.* **2025**, *27*, 2089–2101. [CrossRef] [PubMed]
117. Menendez-Montes, I.; Marin-Vicente, C.; Mukherjee, S.; Ahmed, M.S.; Gomez, M.J.; Anene-Nzelu, C.G.; Lee, C.J.M.; Koslowski, S.; Solmonson, A.; Tassin, T.; et al. Mitochondria directly interact with the nuclear pore complex. *Nature* **2026**, *654*, 786–797. [CrossRef] [PubMed]
118. Coyne, A.N.; Rothstein, J.D. Nuclear pore complexes—A doorway to neural injury in neurodegeneration. *Nat. Rev. Neurol.* **2022**, *18*, 348–362. [CrossRef] [PubMed]
119. Fare, C.M.; Rothstein, J.D. Nuclear pore dysfunction and disease: A complex opportunity. *Nucleus* **2024**, *15*, 2314297. [CrossRef] [PubMed]
120. Cristi, A.C.; Rapuri, S.; Coyne, A.N. Nuclear pore complex and nucleocytoplasmic transport disruption in neurodegeneration. *FEBS Lett.* **2023**, *597*, 2546–2566. [CrossRef] [PubMed]
121. Shen, L.; Dettmer, U. Alpha-Synuclein Effects on Mitochondrial Quality Control in Parkinson's Disease. *Biomolecules* **2024**, *14*, 1649. [CrossRef] [PubMed]
122. Feng, Y.; Goncalves, M.M.; Jitkova, Y.; Keszei, A.F.A.; Yan, Y.; Sarathy, C.; St-Germain, J.; Kenney, T.M.G.; Tcheng, M.; Trudel, V.; et al. Serine phosphorylation facilitates protein degradation by the human mitochondrial ClpXP protease. *Proc. Natl. Acad. Sci. USA* **2025**, *122*, e2422447122. [CrossRef] [PubMed]
123. Groh, J.; Feng, R.; Yuan, X.; Liu, L.; Klein, D.; Hutahaean, G.; Butz, E.; Wang, Z.; Steinbrecher, L.; Neher, J.; et al. Microglia activation orchestrates CXCL10-mediated $CD8^+$ T cell recruitment to promote aging-related white matter degeneration. *Nat. Neurosci.* **2025**, *28*, 1160–1173. [CrossRef] [PubMed]

124. Nguyen, P.T.; Dorman, L.C.; Pan, S.; Vainchtein, I.D.; Han, R.T.; Nakao-Inoue, H.; Taloma, S.E.; Barron, J.J.; Molofsky, A.B.; Kheirbek, M.A.; et al. Microglial Remodeling of the Extracellular Matrix Promotes Synapse Plasticity. *Cell* **2020**, *182*, 388–403.e15. [CrossRef] [PubMed]
125. Dias, D.O.; Kalkitsas, J.; Kelahmetoglu, Y.; Estrada, C.P.; Tatarishvili, J.; Holl, D.; Jansson, L.; Banitalebi, S.; Amiry-Moghaddam, M.; Ernst, A.; et al. Pericyte-derived fibrotic scarring is conserved across diverse central nervous system lesions. *Nat. Commun.* **2021**, *12*, 5501. [CrossRef] [PubMed]
126. Klein, J. The Central Cholinergic Synapse: A Primer. *Int. J. Mol. Sci.* **2025**, *26*, 9670. [CrossRef] [PubMed]
127. Lasser, A. The mononuclear phagocytic system: A review. *Hum. Pathol.* **1983**, *14*, 108–126. [CrossRef] [PubMed]
128. Augur, Z.M.; Fogo, G.M.; Arbery, M.R.; Stern, A.M.; Benoit, C.R.; Hsieh, Y.C.; Young-Pearse, T.L. Optineurin deficiency disrupts phosphorylated tau proteostasis and clusterin expression in human neurons. *Acta Neuropathol. Commun.* **2025**, *13*, 188. [CrossRef] [PubMed]
129. Nonaka, T.; Hasegawa, M. TDP-43 Prions. *Cold Spring Harb. Perspect. Med.* **2018**, *8*, a024463. [CrossRef] [PubMed]
130. Vaquer-Alicea, J.; Diamond, M.I.; Joachimiak, L.A. Tau strains shape disease. *Acta Neuropathol.* **2021**, *142*, 57–71. [CrossRef] [PubMed]
131. Mehra, S.; Gadhe, L.; Bera, R.; Sawner, A.S.; Maji, S.K. Structural and Functional Insights into alpha-Synuclein Fibril Polymorphism. *Biomolecules* **2021**, *11*, 1419. [CrossRef] [PubMed]
132. Carta, M.; Aguzzi, A. Molecular foundations of prion strain diversity. *Curr. Opin. Neurobiol.* **2022**, *72*, 22–31. [CrossRef] [PubMed]
133. Ramirez-Nunez, O.; Rico-Rios, S.; Torres, P.; Ayala, V.; Fernandez-Bernal, A.; Ceron-Codorniu, M.; Andres-Benito, P.; Vinyals, A.; Maqsood, S.; Ferrer, I.; et al. Nuclear pore complex dysfunction drives TDP-43 pathology in ALS. *Redox Biol.* **2025**, *86*, 103824. [CrossRef] [PubMed]
134. Dubey, S.K.; Chaubey, D.; Ikenaga, C.; Lin, W.W.; Bellen, H.J.; Lloyd, T.E. Aberrant nuclear pore complex degradation contributes to neurodegeneration in VCP disease. *Neuron* **2026**, *114*, 850–867.e8. [CrossRef] [PubMed]
135. Cantuti-Castelvetri, L.; Fitzner, D.; Bosch-Queralt, M.; Weil, M.T.; Su, M.; Sen, P.; Ruhwedel, T.; Mitkovski, M.; Trendelenburg, G.; Lutjohann, D.; et al. Defective cholesterol clearance limits remyelination in the aged central nervous system. *Science* **2018**, *359*, 684–688. [CrossRef] [PubMed]
136. Stoffels, J.M.; de Jonge, J.C.; Stancic, M.; Nomden, A.; van Strien, M.E.; Ma, D.; Siskova, Z.; Maier, O.; Ffrench-Constant, C.; Franklin, R.J.; et al. Fibronectin aggregation in multiple sclerosis lesions impairs remyelination. *Brain* **2013**, *136*, 116–131. [CrossRef] [PubMed]
137. Ghorbani, S.; Li, C.; Lozinski, B.M.; Moezzi, D.; D'Mello, C.; Dong, Y.; Visser, F.; Li, H.; Silva, C.; Khakpour, M.; et al. Fibulin-2 is an extracellular matrix inhibitor of oligodendrocytes relevant to multiple sclerosis. *J. Clin. Invest.* **2024**, *134*, e176910. [CrossRef] [PubMed]
138. Shahnawaz, M.; Mukherjee, A.; Pritzkow, S.; Mendez, N.; Rabadia, P.; Liu, X.; Hu, B.; Schmeichel, A.; Singer, W.; Wu, G.; et al. Discriminating alpha-synuclein strains in Parkinson's disease and multiple system atrophy. *Nature* **2020**, *578*, 273–277. [CrossRef] [PubMed]
139. Nizynski, B.; Dzwolak, W.; Nieznanski, K. Amyloidogenesis of Tau protein. *Protein Sci.* **2017**, *26*, 2126–2150. [CrossRef] [PubMed]
140. Powell, W.C.; Nahum, M.; Pankratz, K.; Herlory, M.; Greenwood, J.; Poliyenko, D.; Holland, P.; Jing, R.; Biggerstaff, L.; Stowell, M.H.B.; et al. Post-Translational Modifications Control Phase Transitions of Tau. *ACS Cent. Sci.* **2024**, *10*, 2145–2161. [CrossRef] [PubMed]
141. Ferreon, J.C.; Jain, A.; Choi, K.J.; Tsoi, P.S.; MacKenzie, K.R.; Jung, S.Y.; Ferreon, A.C. Acetylation Disfavors Tau Phase Separation. *Int. J. Mol. Sci.* **2018**, *19*, 1360. [CrossRef] [PubMed]
142. Chakraborty, P.; Ibanez de Opakua, A.; Purslow, J.A.; Fromm, S.A.; Chatterjee, D.; Zachrdla, M.; Zhuang, S.; Puri, S.; Wolozin, B.; Zweckstetter, M. GSK3beta phosphorylation catalyzes the aggregation of tau into Alzheimer's disease-like filaments. *Proc. Natl. Acad. Sci. USA* **2024**, *121*, e2414176121. [CrossRef] [PubMed]
143. Nadel, C.M.; Pokhrel, S.; Wucherer, K.; Oehler, A.; Thwin, A.C.; Basu, K.; Callahan, M.D.; Southworth, D.R.; Mordes, D.A.; Craik, C.S.; et al. Phosphorylation of tau at a single residue inhibits binding to the E3 ubiquitin ligase, CHIP. *Nat. Commun.* **2024**, *15*, 7972. [CrossRef] [PubMed]
144. Rawat, P.; Sehar, U.; Bisht, J.; Selman, A.; Culberson, J.; Reddy, P.H. Phosphorylated Tau in Alzheimer's Disease and Other Tauopathies. *Int. J. Mol. Sci.* **2022**, *23*, 12841. [CrossRef] [PubMed]
145. Moro, M.L.; Phillips, A.S.; Gaimster, K.; Paul, C.; Mudher, A.; Nicoll, J.A.R.; Boche, D. Pyroglutamate and Isoaspartate modified Amyloid-Beta in ageing and Alzheimer's disease. *Acta Neuropathol. Commun.* **2018**, *6*, 3. [CrossRef] [PubMed]
146. Al Adem, K.; Lee, S. Structural polymorphism and cytotoxicity of brain-derived beta-amyloid extracts. *Protein Sci.* **2023**, *32*, e4639. [CrossRef] [PubMed]
147. Rissman, R.A.; Langford, O.; Raman, R.; Donohue, M.C.; Abdel-Latif, S.; Meyer, M.R.; Wente-Roth, T.; Kirmess, K.M.; Ngolab, J.; Winston, C.N.; et al. Plasma Abeta42/Abeta40 and phospho-tau217 concentration ratios increase the accuracy of amyloid PET classification in preclinical Alzheimer's disease. *Alzheimer's Dement.* **2024**, *20*, 1214–1224. [CrossRef] [PubMed]

148. van Dyck, C.H.; Swanson, C.J.; Aisen, P.; Bateman, R.J.; Chen, C.; Gee, M.; Kanekiyo, M.; Li, D.; Reyderman, L.; Cohen, S.; et al. Lecanemab in Early Alzheimer's Disease. *N. Engl. J. Med.* **2023**, *388*, 9–21. [CrossRef] [PubMed]
149. Sims, J.R.; Zimmer, J.A.; Evans, C.D.; Lu, M.; Ardayfio, P.; Sparks, J.; Wessels, A.M.; Shcherbinin, S.; Wang, H.; Monkul Nery, E.S.; et al. Donanemab in Early Symptomatic Alzheimer Disease: The TRAILBLAZER-ALZ 2 Randomized Clinical Trial. *JAMA* **2023**, *330*, 512–527. [CrossRef] [PubMed]
150. Wang, W.; Zhou, Q.; Jiang, T.; Li, S.; Ye, J.; Zheng, J.; Wang, X.; Liu, Y.; Deng, M.; Ke, D.; et al. A novel small-molecule PROTAC selectively promotes tau clearance to improve cognitive functions in Alzheimer-like models. *Theranostics* **2021**, *11*, 5279–5295. [CrossRef] [PubMed]
151. Gunaydin, C.; Sondhi, D.; Kaminsky, S.M.; Lephart, H.C.; Leopold, P.L.; Hackett, N.R.; Khanna, R.; Crystal, R.G. AAVrh.10 delivery of novel APOE2-Christchurch variant suppresses amyloid and Tau pathology in Alzheimer's disease mice. *Mol. Ther.* **2024**, *32*, 4303–4318. [CrossRef] [PubMed]
152. DeMattos, R.B.; Lu, J.; Tang, Y.; Racke, M.M.; DeLong, C.A.; Tzaferis, J.A.; Hole, J.T.; Forster, B.M.; McDonnell, P.C.; Liu, F.; et al. A plaque-specific antibody clears existing beta-amyloid plaques in Alzheimer's disease mice. *Neuron* **2012**, *76*, 908–920. [CrossRef] [PubMed]
153. Tucker, S.; Möller, C.; Tegerstedt, K.; Lord, A.; Laudon, H.; Sjödahl, J.; Söderberg, L.; Spens, E.; Sahlin, C.; Waara, E.R.; et al. The murine version of BAN2401 (mAb158) selectively reduces amyloid-beta protofibrils in brain and cerebrospinal fluid of tg-ArcSwe mice. *J. Alzheimer's Dis.* **2015**, *43*, 575–588. [CrossRef] [PubMed]
154. Budd Haeberlein, S.; Aisen, P.S.; Barkhof, F.; Chalkias, S.; Chen, T.; Cohen, S.; Dent, G.; Hansson, O.; Harrison, K.; von Hehn, C.; et al. Two Randomized Phase 3 Studies of Aducanumab in Early Alzheimer's Disease. *J. Prev. Alzheimer's Dis.* **2022**, *9*, 197–210. [CrossRef] [PubMed]
155. Burre, J.; Sharma, M.; Tsetsenis, T.; Buchman, V.; Etherton, M.R.; Sudhof, T.C. Alpha-synuclein promotes SNARE-complex assembly in vivo and in vitro. *Science* **2010**, *329*, 1663–1667. [CrossRef] [PubMed]
156. Wang, F.; Banerjee, V.; Barria, C.; Ramirez, S.; Allison, T.; Gorski, D.; Evans, H.; Nguyen, Q.; Harrison, D.; Al-Lahham, R.; et al. Seed amplification of MSA alpha-synuclein aggregates preserves the biological and structural properties of brain-derived aggregates. *Nat. Commun.* **2025**, *16*, 11266. [CrossRef] [PubMed]
157. Graves, N.J.; Jaafar, A.K.; Gambin, Y.; Sierecki, E. Divalent and Trivalent Metallic Ions Differentially Affect Alpha-Synuclein Aggregation. *ACS Chem. Neurosci.* **2025**, *16*, 3497–3512. [CrossRef] [PubMed]
158. Du, X.Y.; Xie, X.X.; Liu, R.T. The Role of alpha-Synuclein Oligomers in Parkinson's Disease. *Int. J. Mol. Sci.* **2020**, *21*, 8645. [CrossRef] [PubMed]
159. Bandyopadhyay, U.; Cuervo, A.M. Chaperone-mediated autophagy in aging and neurodegeneration: Lessons from alpha-synuclein. *Exp. Gerontol.* **2007**, *42*, 120–128. [CrossRef] [PubMed]
160. Cuervo, A.M.; Wong, E. Chaperone-mediated autophagy: Roles in disease and aging. *Cell Res.* **2014**, *24*, 92–104. [CrossRef] [PubMed]
161. Lee, J.; Sung, K.W.; Bae, E.J.; Yoon, D.; Kim, D.; Lee, J.S.; Park, D.H.; Park, D.Y.; Mun, S.R.; Kwon, S.C.; et al. Targeted degradation of □-synuclein aggregates in Parkinson's disease using the AUTOTAC technology. *Mol. Neurodegener.* **2023**, *18*, 41. [CrossRef] [PubMed]
162. Ji, C.H.; Lee, M.J.; Kim, H.Y.; Heo, A.J.; Park, D.Y.; Kim, Y.K.; Kim, B.Y.; Kwon, Y.T. Targeted protein degradation via the autophagy-lysosome system: AUTOTAC (AUTOphagy-TArgeting Chimera). *Autophagy* **2022**, *18*, 2259–2262. [CrossRef] [PubMed]
163. Wu, K.J.; Chiu, Y.S.; Yu, S.J.; Wang, Y.S.; Chen, C.T.; Peng, Y.C.; Chuang, Y.M.; Chu, C.Y.; Li, Y.C.; Wang, K.L.; et al. AAV-mediated intracerebral expression of an alpha-synuclein-targeting intrabody improves motor functions in aged rats. *Sci. Rep.* **2026**, *16*, 4632. [CrossRef] [PubMed]
164. Haney, M.J.; Klyachko, N.L.; Zhao, Y.; Gupta, R.; Plotnikova, E.G.; He, Z.; Patel, T.; Piroyan, A.; Sokolsky, M.; Kabanov, A.V.; et al. Exosomes as drug delivery vehicles for Parkinson's disease therapy. *J. Control. Release* **2015**, *207*, 18–30. [CrossRef] [PubMed]
165. Kojima, R.; Bojar, D.; Rizzi, G.; Hamri, G.C.; El-Baba, M.D.; Saxena, P.; Auslander, S.; Tan, K.R.; Fussenegger, M. Designer exosomes produced by implanted cells intracerebrally deliver therapeutic cargo for Parkinson's disease treatment. *Nat. Commun.* **2018**, *9*, 1305. [CrossRef] [PubMed]
166. Gao, C.; Wang, Y.; Sun, J.; Han, Y.; Gong, W.; Li, Y.; Feng, Y.; Wang, H.; Yang, M.; Li, Z.; et al. Neuronal mitochondria-targeted delivery of curcumin by biomimetic engineered nanosystems in Alzheimer's disease mice. *Acta Biomater.* **2020**, *108*, 285–299. [CrossRef] [PubMed]
167. Wood, A.; Gurfinkel, Y.; Polain, N.; Lamont, W.; Lyn Rea, S. Molecular Mechanisms Underlying TDP-43 Pathology in Cellular and Animal Models of ALS and FTLD. *Int. J. Mol. Sci.* **2021**, *22*, 4705. [CrossRef] [PubMed]
168. Baughn, M.W.; Melamed, Z.; Lopez-Erauskin, J.; Beccari, M.S.; Ling, K.; Zuberi, A.; Presa, M.; Gonzalo-Gil, E.; Maimon, R.; Vazquez-Sanchez, S.; et al. Mechanism of STMN2 cryptic splice-polyadenylation and its correction for TDP-43 proteinopathies. *Science* **2023**, *379*, 1140–1149. [CrossRef] [PubMed]

169. Brown, A.L.; Wilkins, O.G.; Keuss, M.J.; Kargbo-Hill, S.E.; Zanovello, M.; Lee, W.C.; Bampton, A.; Lee, F.C.Y.; Masino, L.; Qi, Y.A.; et al. TDP-43 loss and ALS-risk SNPs drive mis-splicing and depletion of UNC13A. *Nature* **2022**, *603*, 131–137. [CrossRef] [PubMed]
170. Klim, J.R.; Williams, L.A.; Limone, F.; Guerra San Juan, I.; Davis-Dusenbery, B.N.; Mordes, D.A.; Burberry, A.; Steinbaugh, M.J.; Gamage, K.K.; Kirchner, R.; et al. ALS-implicated protein TDP-43 sustains levels of STMN2, a mediator of motor neuron growth and repair. *Nat. Neurosci.* **2019**, *22*, 167–179. [CrossRef] [PubMed]
171. Rothstein, J.D.; Keeley, O.; Warlick, C.; Miller, T.M.; Ly, C.V.; Glass, J.D.; Coyne, A.N. Sporadic ALS induced pluripotent stem cell derived neurons reveal hallmarks of TDP-43 loss of function. *Nat. Commun.* **2025**, *16*, 7092. [CrossRef] [PubMed]
172. Cascella, R.; Fani, G.; Bigi, A.; Chiti, F.; Cecchi, C. Partial Failure of Proteostasis Systems Counteracting TDP-43 Aggregates in Neurodegenerative Diseases. *Int. J. Mol. Sci.* **2019**, *20*, 3685. [CrossRef] [PubMed]
173. Zhang, J.; Velmeshev, D.; Hashimoto, K.; Huang, Y.H.; Hofmann, J.W.; Shi, X.; Chen, J.; Leidal, A.M.; Dishart, J.G.; Cahill, M.K.; et al. Neurotoxic microglia promote TDP-43 proteinopathy in progranulin deficiency. *Nature* **2020**, *588*, 459–465. [CrossRef] [PubMed]
174. Wei, Y.; Li, D.; Yang, R.; Liu, Y.; Luo, X.; Zhao, W.; Yang, H.; Chen, Z.; Shen, C.; Wang, Y.; et al. TIA1-mediated stress granules promote neurodegeneration by sequestering HSP70 mRNA in C9orf72 mice. *Brain* **2025**, *148*, 4482–4494. [CrossRef] [PubMed]
175. MacDonald, M.E.; Ambrose, C.M.; Duyao, M.P.; Myers, R.H.; Lin, C.; Srinidhi, L.; Barnes, G.; Taylor, A.; James, M.; Groot, N.; et al. A novel gene containing a trinucleotide repeat that is expanded and unstable on Huntington's disease chromosomes. *Cell* **1993**, *72*, 971–983. [CrossRef] [PubMed]
176. Graham, R.K.; Deng, Y.; Slow, E.J.; Haigh, B.; Bissada, N.; Lu, G.; Pearson, J.; Shehadeh, J.; Bertram, L.; Murphy, Z.; et al. Cleavage at the caspase-6 site is required for neuronal dysfunction and degeneration due to mutant huntingtin. *Cell* **2006**, *125*, 1179–1191. [CrossRef] [PubMed]
177. Sathasivam, K.; Neueder, A.; Gipson, T.A.; Landles, C.; Benjamin, A.C.; Bondulich, M.K.; Smith, D.L.; Faull, R.L.; Roos, R.A.; Howland, D.; et al. Aberrant splicing of HTT generates the pathogenic exon 1 protein in Huntington disease. *Proc. Natl. Acad. Sci. USA* **2013**, *110*, 2366–2370. [CrossRef] [PubMed]
178. Jeong, H.; Then, F.; Melia, T.J., Jr.; Mazzulli, J.R.; Cui, L.; Savas, J.N.; Voisine, C.; Paganetti, P.; Tanese, N.; Hart, A.C.; et al. Acetylation targets mutant huntingtin to autophagosomes for degradation. *Cell* **2009**, *137*, 60–72. [CrossRef] [PubMed]
179. Schilling, B.; Gafni, J.; Torcassi, C.; Cong, X.; Row, R.H.; LaFevre-Bernt, M.A.; Cusack, M.P.; Ratovitski, T.; Hirschhorn, R.; Ross, C.A.; et al. Huntingtin phosphorylation sites mapped by mass spectrometry. Modulation of cleavage and toxicity. *J. Biol. Chem.* **2006**, *281*, 23686–23697. [CrossRef] [PubMed]
180. Handsaker, R.E.; Kashin, S.; Reed, N.M.; Tan, S.; Lee, W.S.; McDonald, T.M.; Morris, K.; Kamitaki, N.; Mullally, C.D.; Morakabati, N.R.; et al. Long somatic DNA-repeat expansion drives neurodegeneration in Huntington's disease. *Cell* **2025**, *188*, 623–639.e619. [CrossRef] [PubMed]
181. Saudou, F.; Humbert, S. The Biology of Huntingtin. *Neuron* **2016**, *89*, 910–926. [CrossRef] [PubMed]
182. McColgan, P.; Thobhani, A.; Boak, L.; Schobel, S.A.; Nicotra, A.; Palermo, G.; Trundell, D.; Zhou, J.; Schlegel, V.; Sanwald Ducray, P.; et al. Tominersen in Adults with Manifest Huntington's Disease. *N. Engl. J. Med.* **2023**, *389*, 2203–2205. [CrossRef] [PubMed]
183. Tabrizi, S.J.; Leavitt, B.R.; Landwehrmeyer, G.B.; Wild, E.J.; Saft, C.; Barker, R.A.; Blair, N.F.; Craufurd, D.; Priller, J.; Rickards, H.; et al. Targeting Huntingtin Expression in Patients with Huntington's Disease. *N. Engl. J. Med.* **2019**, *380*, 2307–2316. [CrossRef] [PubMed]
184. Tabrizi, S.J.; Estevez-Fraga, C.; van Roon-Mom, W.M.C.; Flower, M.D.; Scahill, R.I.; Wild, E.J.; Muñoz-Sanjuan, I.; Sampaio, C.; Rosser, A.E.; Leavitt, B.R. Potential disease-modifying therapies for Huntington's disease: Lessons learned and future opportunities. *Lancet Neurol.* **2022**, *21*, 645–658. [CrossRef] [PubMed]
185. Zhao, X.; Jacob, C. Mechanisms of Demyelination and Remyelination Strategies for Multiple Sclerosis. *Int. J. Mol. Sci.* **2023**, *24*, 6373. [CrossRef] [PubMed]
186. Cignarella, F.; Filipello, F.; Bollman, B.; Cantoni, C.; Locca, A.; Mikesell, R.; Manis, M.; Ibrahim, A.; Deng, L.; Benitez, B.A.; et al. TREM2 activation on microglia promotes myelin debris clearance and remyelination in a model of multiple sclerosis. *Acta Neuropathol.* **2020**, *140*, 513–534. [CrossRef] [PubMed]
187. Al Jaf, A.I.A.; Peria, S.; Fabiano, T.; Ragnini-Wilson, A. Remyelinating Drugs at a Crossroad: How to Improve Clinical Efficacy and Drug Screenings. *Cells* **2024**, *13*, 1326. [CrossRef] [PubMed]
188. Offensperger, F.; Tin, G.; Duran-Frigola, M.; Hahn, E.; Dobner, S.; Ende, C.W.A.; Strohbach, J.W.; Rukavina, A.; Brennsteiner, V.; Ogilvie, K.; et al. Large-scale chemoproteomics expedites ligand discovery and predicts ligand behavior in cells. *Science* **2024**, *384*, eadk5864. [CrossRef] [PubMed]
189. Cai, Z.; Yang, Z.; Li, H.; Fang, Y. Research progress of PROTACs for neurodegenerative diseases therapy. *Bioorg. Chem.* **2024**, *147*, 107386. [CrossRef] [PubMed]
190. Fang, Y.; Wang, J.; Zhao, M.; Zheng, Q.; Ren, C.; Wang, Y.; Zhang, J. Progress and Challenges in Targeted Protein Degradation for Neurodegenerative Disease Therapy. *J. Med. Chem.* **2022**, *65*, 11454–11477. [CrossRef] [PubMed]

191. Monsen, P.J.; Bommi, P.V.; Grigorescu, A.A.; Lauing, K.L.; Mao, Y.; Berardi, P.; Zhai, L.; Ojo, O.; Penco-Campillo, M.; Koch, T.; et al. Rational Design and Optimization of a Potent IDO1 Proteolysis Targeting Chimera (PROTAC). *J. Med. Chem.* **2025**, *68*, 4961–4987. [CrossRef] [PubMed]
192. Huang, J.; Su, J.; Wang, H.; Chen, J.; Tian, Y.; Zhang, J.; Feng, T.; Di, L.; Lu, X.; Sheng, H.; et al. Discovery of Novel PROTAC SIRT6 Degraders with Potent Efficacy against Hepatocellular Carcinoma. *J. Med. Chem.* **2024**, *67*, 17319–17349. [CrossRef] [PubMed]
193. Liu, M.; Martyn, A.P.; Quinn, R.J. Natural product-based PROteolysis TArgeting Chimeras (PROTACs). *Nat. Prod. Rep.* **2022**, *39*, 2292–2307. [CrossRef] [PubMed]
194. Baker, A.G.; Ho, A.P.T.; Itzhaki, L.S.; Fruk, L. Nanoparticle-Mediated Targeted Protein Degradation: An Emerging Therapeutics Technology. *Angew. Chem. Int. Ed. Engl.* **2025**, *64*, e202503958. [CrossRef]
195. Lim, K.L.; Lim, G.G. K63-linked ubiquitination and neurodegeneration. *Neurobiol. Dis.* **2011**, *43*, 9–16. [CrossRef] [PubMed]
196. Wen, P.; Sun, Y.; Jiang, T.X.; Qiu, X.B. PA200-Mediated Proteasomal Protein Degradation and Regulation of Cellular Senescence. *Int. J. Mol. Sci.* **2024**, *25*, 5637. [CrossRef] [PubMed]
197. Balchin, D.; Hayer-Hartl, M.; Hartl, F.U. In vivo aspects of protein folding and quality control. *Science* **2016**, *353*, aac4354. [CrossRef] [PubMed]
198. Hartl, F.U. Protein Misfolding Diseases. *Annu. Rev. Biochem.* **2017**, *86*, 21–26. [CrossRef] [PubMed]
199. Kevei, E.; Pokrzywa, W.; Hoppe, T. Repair or destruction-an intimate liaison between ubiquitin ligases and molecular chaperones in proteostasis. *FEBS Lett.* **2017**, *591*, 2616–2635. [CrossRef] [PubMed]
200. Vijayakumaran, S.; Pountney, D.L. SUMOylation, aging and autophagy in neurodegeneration. *Neurotoxicology* **2018**, *66*, 53–57. [CrossRef] [PubMed]
201. Wan, H.; Wang, Q.; Chen, X.; Zeng, Q.; Shao, Y.; Fang, H.; Liao, X.; Li, H.S.; Liu, M.G.; Xu, T.L.; et al. WDR45 contributes to neurodegeneration through regulation of ER homeostasis and neuronal death. *Autophagy* **2020**, *16*, 531–547. [CrossRef] [PubMed]
202. Sun, Y.; Liu, S.; Chen, L.; Zhou, Z.; Yin, X.; Shi, Y.; Li, H.; Li, J.; Lu, Y.; Jiang, W.; et al. AI-driven discovery of dual antiaging and anti-AD therapeutics via PROTAC target deconvolution of a super-enhancer-regulated axis. *Sci. Adv.* **2025**, *11*, eadz9283. [CrossRef] [PubMed]
203. Fan, G.; Zhang, Q.; Guo, W.; Liu, M.; Tan, D.; Tang, Z.; Yang, J. Proteolysis-targeting chimera (PROTAC): A promising senolytic strategy. *Ageing Res. Rev.* **2026**, *115*, 103027. [CrossRef] [PubMed]
204. Wong, K.H.; Riaz, M.K.; Xie, Y.; Zhang, X.; Liu, Q.; Chen, H.; Bian, Z.; Chen, X.; Lu, A.; Yang, Z. Review of Current Strategies for Delivering Alzheimer's Disease Drugs across the Blood-Brain Barrier. *Int. J. Mol. Sci.* **2019**, *20*, 381. [CrossRef] [PubMed]
205. Teleanu, R.I.; Preda, M.D.; Niculescu, A.G.; Vladacenco, O.; Radu, C.I.; Grumezescu, A.M.; Teleanu, D.M. Current Strategies to Enhance Delivery of Drugs across the Blood-Brain Barrier. *Pharmaceutics* **2022**, *14*, 987. [CrossRef] [PubMed]
206. Suenderhauf, C.; Hammann, F.; Huwyler, J. Computational prediction of blood-brain barrier permeability using decision tree induction. *Molecules* **2012**, *17*, 10429–10445. [CrossRef] [PubMed]
207. Yu, Y.J.; Zhang, Y.; Kenrick, M.; Hoyte, K.; Luk, W.; Lu, Y.; Atwal, J.; Elliott, J.M.; Prabhu, S.; Watts, R.J.; et al. Boosting brain uptake of a therapeutic antibody by reducing its affinity for a transcytosis target. *Sci. Transl. Med.* **2011**, *3*, 84ra44. [CrossRef] [PubMed]
208. Kariolis, M.S.; Wells, R.C.; Getz, J.A.; Kwan, W.; Mahon, C.S.; Tong, R.; Kim, D.J.; Srivastava, A.; Bedard, C.; Henne, K.R.; et al. Brain delivery of therapeutic proteins using an Fc fragment blood-brain barrier transport vehicle in mice and monkeys. *Sci. Transl. Med.* **2020**, *12*, eaay1359. [CrossRef] [PubMed]
209. Pinheiro, R.G.R.; Coutinho, A.J.; Pinheiro, M.; Neves, A.R. Nanoparticles for Targeted Brain Drug Delivery: What Do We Know? *Int. J. Mol. Sci.* **2021**, *22*, 11654. [CrossRef] [PubMed]
210. Han, E.L.; Tang, S.; Kim, D.; Murray, A.M.; Swingle, K.L.; Hamilton, A.G.; Mrksich, K.; Padilla, M.S.; Palanki, R.; Li, J.J.; et al. Peptide-Functionalized Lipid Nanoparticles for Targeted Systemic mRNA Delivery to the Brain. *Nano Lett.* **2025**, *25*, 800–810. [CrossRef] [PubMed]
211. Vora, L.K.; Gholap, A.D.; Jetha, K.; Thakur, R.R.S.; Solanki, H.K.; Chavda, V.P. Artificial Intelligence in Pharmaceutical Technology and Drug Delivery Design. *Pharmaceutics* **2023**, *15*, 1916. [CrossRef] [PubMed]
212. Alvarez-Erviti, L.; Seow, Y.; Yin, H.; Betts, C.; Lakhal, S.; Wood, M.J. Delivery of siRNA to the mouse brain by systemic injection of targeted exosomes. *Nat. Biotechnol.* **2011**, *29*, 341–345. [CrossRef] [PubMed]
213. Banks, W.A.; Sharma, P.; Bullock, K.M.; Hansen, K.M.; Ludwig, N.; Whiteside, T.L. Transport of Extracellular Vesicles across the Blood-Brain Barrier: Brain Pharmacokinetics and Effects of Inflammation. *Int. J. Mol. Sci.* **2020**, *21*, 4407. [CrossRef] [PubMed]
214. Wu, C.C.; Tsantilas, K.A.; Park, J.; Plubell, D.; Sanders, J.A.; Naicker, P.; Govender, I.; Buthelezi, S.; Stoychev, S.; Jordaan, J.; et al. Enrichment of extracellular vesicles using Mag-Net for the analysis of the plasma proteome. *Nat. Commun.* **2025**, *16*, 5447. [CrossRef] [PubMed]
215. Di Scala, C.; Armstrong, N.; Chahinian, H.; Chabriere, E.; Fantini, J.; Yahi, N. AmyP53, a Therapeutic Peptide Candidate for the Treatment of Alzheimer's and Parkinson's Disease: Safety, Stability, Pharmacokinetics Parameters and Nose-to Brain Delivery. *Int. J. Mol. Sci.* **2022**, *23*, 13383. [CrossRef] [PubMed]

216. Dayneka, N.L.; Garg, V.; Jusko, W.J. Comparison of four basic models of indirect pharmacodynamic responses. *J. Pharmacokinet. Biopharm.* **1993**, *21*, 457–478. [CrossRef] [PubMed]
217. Patel, L.; Shukla, T.; Huang, X.; Ussery, D.W.; Wang, S. Machine Learning Methods in Drug Discovery. *Molecules* **2020**, *25*, 5277. [CrossRef] [PubMed]
218. Cho, N.H.; Cheveralls, K.C.; Brunner, A.D.; Kim, K.; Michaelis, A.C.; Raghavan, P.; Kobayashi, H.; Savy, L.; Li, J.Y.; Canaj, H.; et al. OpenCell: Endogenous tagging for the cartography of human cellular organization. *Science* **2022**, *375*, eabi6983. [CrossRef] [PubMed]
219. Wang, B.; Zhang, X.; Xu, C.; Han, X.; Wang, Y.; Situ, C.; Li, Y.; Guo, X. DeepSP: A Deep Learning Framework for Spatial Proteomics. *J. Proteome Res.* **2023**, *22*, 2186–2198. [CrossRef] [PubMed]
220. Zhang, J.; Humphreys, I.R.; Pei, J.; Kim, J.; Choi, C.; Yuan, R.; Durham, J.; Liu, S.; Choi, H.J.; Baek, M.; et al. Predicting protein-protein interactions in the human proteome. *Science* **2025**, *390*, eadt1630. [CrossRef] [PubMed]
221. Humphreys, I.R.; Pei, J.; Baek, M.; Krishnakumar, A.; Anishchenko, I.; Ovchinnikov, S.; Zhang, J.; Ness, T.J.; Banjade, S.; Bagde, S.R.; et al. Computed structures of core eukaryotic protein complexes. *Science* **2021**, *374*, eabm4805. [CrossRef] [PubMed]
222. Humphreys, I.R.; Zhang, J.; Baek, M.; Wang, Y.; Krishnakumar, A.; Pei, J.; Anishchenko, I.; Tower, C.A.; Jackson, B.A.; Warrier, T.; et al. Protein interactions in human pathogens revealed through deep learning. *Nat. Microbiol.* **2024**, *9*, 2642–2652. [CrossRef] [PubMed]
223. Schmid, E.W.; Walter, J.C. Predictomes, a classifier-curated database of AlphaFold-modeled protein-protein interactions. *Mol. Cell* **2025**, *85*, 1216–1232.e5. [CrossRef] [PubMed]
224. Bader, J.M.; Geyer, P.E.; Muller, J.B.; Strauss, M.T.; Koch, M.; Leypoldt, F.; Koertvelyessy, P.; Bittner, D.; Schipke, C.G.; Incesoy, E.I.; et al. Proteome profiling in cerebrospinal fluid reveals novel biomarkers of Alzheimer's disease. *Mol. Syst. Biol.* **2020**, *16*, e9356. [CrossRef] [PubMed]
225. Cai, X.; Xue, Z.; Zeng, F.F.; Tang, J.; Yue, L.; Wang, B.; Ge, W.; Xie, Y.; Miao, Z.; Gou, W.; et al. Population serum proteomics uncovers a prognostic protein classifier for metabolic syndrome. *Cell Rep. Med.* **2023**, *4*, 101172. [CrossRef] [PubMed]
226. Cai, C.; Wang, S.; Xu, Y.; Zhang, W.; Tang, K.; Ouyang, Q.; Lai, L.; Pei, J. Transfer Learning for Drug Discovery. *J. Med. Chem.* **2020**, *63*, 8683–8694. [CrossRef] [PubMed]
227. Krentzel, D.; Shorte, S.L.; Zimmer, C. Deep learning in image-based phenotypic drug discovery. *Trends Cell Biol.* **2023**, *33*, 538–554. [CrossRef] [PubMed]
228. Tunyasuvunakool, K.; Adler, J.; Wu, Z.; Green, T.; Zielinski, M.; Zidek, A.; Bridgland, A.; Cowie, A.; Meyer, C.; Laydon, A.; et al. Highly accurate protein structure prediction for the human proteome. *Nature* **2021**, *596*, 590–596. [CrossRef] [PubMed]
229. Goverde, C.A.; Pacesa, M.; Goldbach, N.; Dornfeld, L.J.; Balbi, P.E.M.; Georgeon, S.; Rosset, S.; Kapoor, S.; Choudhury, J.; Dauparas, J.; et al. Computational design of soluble and functional membrane protein analogues. *Nature* **2024**, *631*, 449–458. [CrossRef] [PubMed]
230. Zhu, J.; Liang, M.; Sun, K.; Wei, Y.; Guo, R.; Zhang, L.; Shi, J.; Ma, D.; Hu, Q.; Huang, G.; et al. De novo design of transmembrane fluorescence-activating proteins. *Nature* **2025**, *640*, 249–257. [CrossRef] [PubMed]
231. Crampon, K.; Giorkallos, A.; Deldossi, M.; Baud, S.; Steffenel, L.A. Machine-learning methods for ligand-protein molecular docking. *Drug Discov. Today* **2022**, *27*, 151–164. [CrossRef] [PubMed]
232. Yang, C.; Chen, E.A.; Zhang, Y. Protein-Ligand Docking in the Machine-Learning Era. *Molecules* **2022**, *27*, 4568. [CrossRef] [PubMed]
233. Ozcelik, R.; van Tilborg, D.; Jimenez-Luna, J.; Grisoni, F. Structure-Based Drug Discovery with Deep Learning. *ChemBioChem* **2023**, *24*, e202200776. [CrossRef] [PubMed]
234. Isert, C.; Atz, K.; Schneider, G. Structure-based drug design with geometric deep learning. *Curr. Opin. Struct. Biol.* **2023**, *79*, 102548. [CrossRef] [PubMed]
235. Jia, Y.; Gao, B.; Tan, J.; Zheng, J.; Hong, X.; Zhu, W.; Tan, H.; Xiao, Y.; Tan, L.; Cai, H.; et al. Deep contrastive learning enables genome-wide virtual screening. *Science* **2026**, *391*, eads9530. [CrossRef] [PubMed]
236. Krishnan, A.; Anahtar, M.N.; Valeri, J.A.; Jin, W.; Donghia, N.M.; Sieben, L.; Luttens, A.; Zhang, Y.; Modaresi, S.M.; Hennes, A.; et al. A generative deep learning approach to de novo antibiotic design. *Cell* **2025**, *188*, 5962–5979.e22. [CrossRef] [PubMed]
237. Wan, F.; Torres, M.D.T.; Peng, J.; de la Fuente-Nunez, C. Deep-learning-enabled antibiotic discovery through molecular de-extinction. *Nat. Biomed. Eng.* **2024**, *8*, 854–871. [CrossRef] [PubMed]
238. Xing, J.; Tan, M.; Leshchiner, D.; Sun, M.; Abdelgied, M.; Huang, L.; Paithankar, S.; Uhl, K.; Shankar, R.; Lisabeth, E.; et al. Deep-learning-based de novo discovery and design of therapeutics that reverse disease-associated transcriptional phenotypes. *Cell* **2026**, *189*, 2556–2572.e19. [CrossRef] [PubMed]
239. Duo, L.; Liu, Y.; Ren, J.; Tang, B.; Hirst, J.D. Artificial intelligence for small molecule anticancer drug discovery. *Expert Opin. Drug Discov.* **2024**, *19*, 933–948. [CrossRef] [PubMed]
240. Gupta, R.; Srivastava, D.; Sahu, M.; Tiwari, S.; Ambasta, R.K.; Kumar, P. Artificial intelligence to deep learning: Machine intelligence approach for drug discovery. *Mol. Divers.* **2021**, *25*, 1315–1360. [CrossRef] [PubMed]

241. Sarvepalli, S.; Vadarevu, S. Role of artificial intelligence in cancer drug discovery and development. *Cancer Lett.* **2025**, *627*, 217821. [CrossRef] [PubMed]
242. Yuan, X.; Yang, X.; Pan, Q.; Luo, C.; Luan, X.; Zhang, H. Artificial intelligence in natural products research. *Chin. J. Nat. Med.* **2025**, *23*, 1342–1357. [CrossRef] [PubMed]
243. Batool, M.; Ahmad, B.; Choi, S. A Structure-Based Drug Discovery Paradigm. *Int. J. Mol. Sci.* **2019**, *20*, 2783. [CrossRef] [PubMed]
244. Kimber, T.B.; Chen, Y.; Volkamer, A. Deep Learning in Virtual Screening: Recent Applications and Developments. *Int. J. Mol. Sci.* **2021**, *22*, 4435. [CrossRef] [PubMed]
245. Tropsha, A.; Isayev, O.; Varnek, A.; Schneider, G.; Cherkasov, A. Integrating QSAR modelling and deep learning in drug discovery: The emergence of deep QSAR. *Nat. Rev. Drug Discov.* **2024**, *23*, 141–155. [CrossRef] [PubMed]
246. Racz, A.; Bajusz, D.; Miranda-Quintana, R.A.; Heberger, K. Machine learning models for classification tasks related to drug safety. *Mol. Divers.* **2021**, *25*, 1409–1424. [CrossRef] [PubMed]
247. Zheng, Y.; Schupp, J.C.; Adams, T.; Clair, G.; Justet, A.; Ahangari, F.; Yan, X.; Hansen, P.; Carlon, M.; Cortesi, E.; et al. A deep generative model for deciphering cellular dynamics and in silico drug discovery in complex diseases. *Nat. Biomed. Eng.* **2025**, *9*, 2155–2180. [CrossRef] [PubMed]
248. Genheden, S.; Ryde, U. The MM/PBSA and MM/GBSA methods to estimate ligand-binding affinities. *Expert Opin. Drug Discov.* **2015**, *10*, 449–461. [CrossRef] [PubMed]
249. Shirani, H.; Hashemianzadeh, S.M. Quantum-level machine learning calculations of Levodopa. *Comput. Biol. Chem.* **2024**, *112*, 108146. [CrossRef] [PubMed]
250. Atz, K.; Isert, C.; Bocker, M.N.A.; Jimenez-Luna, J.; Schneider, G. Delta-Quantum machine-learning for medicinal chemistry. *Phys. Chem. Chem. Phys.* **2022**, *24*, 10775–10783. [CrossRef] [PubMed]
251. Madushanka, A.; Laird, E.; Clark, C.; Kraka, E. SmartCADD: AI-QM Empowered Drug Discovery Platform with Explainability. *J. Chem. Inf. Model.* **2024**, *64*, 6799–6813. [CrossRef] [PubMed]
252. Gryn'ova, G.; Bereau, T.; Muller, C.; Friederich, P.; Wade, R.C.; Nunes-Alves, A.; Soares, T.A.; Merz, K., Jr. EDITORIAL: Chemical Compound Space Exploration by Multiscale High-Throughput Screening and Machine Learning. *J. Chem. Inf. Model.* **2024**, *64*, 5737–5738. [CrossRef] [PubMed]
253. Mater, A.C.; Coote, M.L. Deep Learning in Chemistry. *J. Chem. Inf. Model.* **2019**, *59*, 2545–2559. [CrossRef] [PubMed]
254. Goller, A.H. Editorial special issue on "Quantum Mechanics in Industry". *J. Comput. Aided Mol. Des.* **2021**, *35*, 397–398. [CrossRef] [PubMed]
255. Salahinejad, M.; Winkler, D.A.; Shiri, F. Discovery and Design of Radiopharmaceuticals by In silico Methods. *Curr. Radiopharm.* **2022**, *15*, 271–319. [CrossRef] [PubMed]
256. Chow, J.C.L. Quantum Computing in Medicine. *Med. Sci.* **2024**, *12*, 67. [CrossRef] [PubMed]
257. Velmurugan, D.; Pachaiappan, R.; Ramakrishnan, C. Recent Trends in Drug Design and Discovery. *Curr. Top. Med. Chem.* **2020**, *20*, 1761–1770. [CrossRef] [PubMed]
258. Bhatia, A.S.; Saggi, M.K.; Kais, S. Quantum Machine Learning Predicting ADME-Tox Properties in Drug Discovery. *J. Chem. Inf. Model.* **2023**, *63*, 6476–6486. [CrossRef] [PubMed]

Disclaimer/Publisher's Note: The statements, opinions and data contained in all publications are solely those of the individual author(s) and contributor(s) and not of MDPI and/or the editor(s). MDPI and/or the editor(s) disclaim responsibility for any injury to people or property resulting from any ideas, methods, instructions or products referred to in the content.